Report
No. FAA-RD-70-13

THEORETICAL CONSIDERATIONS FOR DESCRIBING THE STATE OF SKY THROUGH AUTOMATIC TECHNIQUES

R.O. Duda, R.L. Mancuso, R.H. Blackmer, Jr.
Stanford Research Institute
Menlo Park, California 94025

MAY 1970

FINAL REPORT

PREPARED FOR

ENVIRONMENTAL SCIENCE SERVICES ADMINISTRATION
Weather Bureau
Silver Spring, Maryland 20910

U.S. FEDERAL AVIATION ADMINISTRATION
Systems Research & Development Service
Washington, D.C. 20590

Essa Contract No. E-203-69(N)

TECHNICAL REPORT STANDARD TITLE PAGE

1. Report No.	2. Government Accession No.	3. Recipient's Catalog No.
FAA-RD-70-13		AD No.

4. Title and Subtitle	5. Report Date
Theoretical Considerations for Describing the State of the Sky Through Automatic Techniques	May 1970
	6. Performing Organization Code

7. Author(s)	8. Performing Organization Report No.
R. O. Duda, R. L. Mancuso and R. H. Blackmer, Jr.	

9. Performing Organization Name and Address	10. Work Unit No.
Standford Research Institute Menlo Park, California 94025	450-402-17E
	11. Contract or Grant No.
	FA65WAI-96
	13. Type of Report and Period Covered
12. Sponsoring Agency Name and Address Department of Transportation Federal Aviation Administration, Washington, D.C. 20590 Department of Commerce ESSA/Weather Bureau, Silver Spring, Md. 20910	Final Report
	14. Sponsoring Agency Code

15. Supplementary Notes

16. Abstract

This report describes a computer model for the simulation of optical and radar ceilometers. The model has two components, a statistical cloud model that describes a sky composed of multiple layers of random clouds, and an instrument model that permits the calculation of the responses of ceilometers. The digital computer program based on this model is described, and program flowcharts, listings, and sample printout are given.

17. Key Words	18. Distribution Statement
Cloud cover Cloud height indicators Ceiling	Availability is unlimited. Document may be released to the clearinghouse for Federal Scientific and Technical Information, Springfield, Va. 22151 for sale to the public.

19. Security Classif. (of this report)	20. Security Classif. (of this page)	21. No. of Pages	22. Price
Unclassified	Unclassified	182	$3.00

Form DOT F 1700.7 (8-69)

PREFACE

This research was supported jointly by the Federal Aviation Administration, Department of Transportation, and the Environmental Science Services Administration/Weather Bureau, Department of Commerce. The assistance of Sidney M. Serebreny and Edward E. Uthe in this effort is gratefully acknowledged.

CONTENTS

ILLUSTRATIONS

TABLES

SYMBOLS

a	Base line for optical ceilometer	(m)
a_d	Drop radius	(m)
A	Atmospheric attenuation rate	(db/1000 ft)
A_r	Receiver area	(m^2)
A_t	Target area	(m^2)
c	Speed of light	(m/s)
c_a	Cloud amount	(tenths)
C	Radar constant	(watts·m^3)
d	Base-height correlation distance	(m)
d_i	Drop diameter	(m)
D	Cloud diameter	(m)
E	Illuminance	(lumens/m^2)
F	Luminous flux	(lumens)
F_{max}	Maximum received luminous flux	(lumens)
F_r	Received luminous flux	(lumens)
F_T	Transmitted luminous flux	(lumens)
G	Antenna gain	(-)
h	Cloud height	(m)
$\bar{h}$	Average cloud height	(m)
I	Luminous intensity	(lumens/ster)
I_T	Transmitted luminous intensity	(lumens/ster)
K	Scale factor for exponential distribution transmission factor	(/m^2)

ℓ	Cloud length	(m)
ℓ_c	Length of cross section of common volume	(m)
ℓ_m	Mean cloud length	(m)
m	Complex refractive index	(-)
n	Number density of clouds per unit surface area	($/m^2$)
n_i	Number of drops per unit volume of diameter d_i	($/m^3$)
N	Number density of showers	(/m)
N_0	Scale factor for exponential distribution	(/m)
p	Probability density	(---)
P_r	Average received power	(watts)
P_T	Transmitted power	(watts)
Q	Angular scattering efficiency of the sphere	(/ster)
r	Distance from rotating beam to volume element	(m)
r	Radar range	(m)
r_{min}	Minimum radar range	(m)
r_s	Radius of shower	(m)
$\hat{r}$	Range to top of cloud	(m)
R	Precipitation rate	(mm/hr)
s	Distance from fixed beam to volume element	(m)
t	Time	(s)
t_b	Layer beginning time	(s)
t_e	Layer ending time	(s)
$\bar{t}$	Mean cloud-layer thickness	(m)
u	Random disturbance in cloud height	(m)
v	Cloud speed	(m/s)

V	Scattering volume	(m^3)
w	Width of cross section of common volume	(m)
W	Liquid water content	(gm/m^3)
x	Coordinate pointing east	(m)
y	Coordinate pointing north	(m)
z	Deviation of cloud base from mean	(m)
$\bar{z}$	Mean deviation	(m)
Z	Radar reflectivity factor	(mmf/m^3)
α	Fixed-beam half-angle for optical ceilometers	(rad)
α_a	Atmospheric attenuation rate	(/m)
α_d	Decay rate for exponential distribution	(/m)
β	Angular volume scattering coefficient	(/m-ster)
β_d	Decay rate for exponential distribution	(/m)
γ	Rotating-beam half-angle for optical ceilometer	(rad)
Δx	Spatial sampling interval	(m)
η	Radar reflectivity per unit volume	(/m)
θ	Inclination angle for optical ceilometer	(rad)
θ	Decay factor in ceiling-height equations	(-)
θ_b	Horizontal beam angle for radar ceilometer	(rad)
θ_{min}	Inclination angle for initial response	(rad)
θ_{max}	Inclination angle for maximum response	(rad)
θ_{decay}	Angular change for 1/e flux decay	(rad)
λ	Wavelength	(m)
ζ	Correlation shift	(m)
ρ	Aspect ratio	(-)
σ	Volume scattering coefficient	(/m)

σ_b	Base-height standard deviation	(m)
σ_i	Backscattering cross section per unit volume	(/m)
τ	Pulse duration	(sec)
φ	Polar scattering angle	(rad)
φ_b	Vertical beam angle for radar ceilometer	(rad)
ψ	Angle between scattered light and receiver	(rad)
ψ_c	Cloud direction	(rad)
ω	Solid angle	(ster)
ω_r	Solid angle for receiver	(ster)
ω_T	Solid angle for transmitter	(ster)

I INTRODUCTION

The ever increasing volume of aviation operations requires nearly continual observations of sky cover, cloud base, visibility, etc., and to meet this need the development of an automated system for aviation-related weather measurements is required. Such a system has the potential advantage of making, recording, and communicating objective observations frequently and reliably, and would be valuable for general meteorological applications as well. It would replace the present system of visual observations of sky cover and interpretation of ceilometer readings, which depend heavily on the judgment and work load of human observers. While an automatic system would overcome these problems, the design of such a system is difficult because of the complexity of the relations between the atmospheric phenomena, the instrument responses, and the desired sky-state description.

The objective of the research described in this report was to provide a theoretical approach for designing an automatic system for describing the state of the sky--i.e., the amounts, kinds, directions of movement, and heights of all clouds. The approach taken was to develop a statistical cloud model that incorporates the most significant cloud characteristics, with particular emphasis on those characteristics that influence aircraft operations and ceilometer responses. This model describes the state of the sky in terms of cloud distributions as characterized by a number of cloud statistics, such as mean base height, mean length, etc.

An instrument model was also developed that allows the calculation of the responses of the three most commonly used ceilometers--fixed-beam, rotating-beam, and radar. The equations for this calculation are based on the basic physical principles governing the instruments.

This cloud/instrument model could, in principle, be used in the analysis of a proposed automatic system. However, it was primarily developed for computer simulation studies, in which a proposed automatic system could be tested and evaluated under a wide variety of simulated atmospheric conditions. To this end, the model was implemented as a digital computer program that generates layers of simulated clouds and calculates the resulting responses of a system of simulated instruments. This report describes the model and the simulation program, and gives the program documentation, including listings, flow charts, and user instructions.

II THE CLOUD MODEL

A. Types of Cloud Cover and Associated Hydrometeors--Qualitative Characteristics

Cloud cover in the atmosphere is composed of such a broad spectrum of distributions of condensed water vapor that it is not feasible to simulate all of the conditions that can arise. As a first approach to the simulation of cloud cover of primary concern to airport operations, the following basic conditions are postulated:

(1) A single dense, infinite layer with either a uniform base or an irregular base. Virga, drizzle, rain, or snow may be falling from the layer.

(2) Multiple thin sheets with either uniform or irregular bases, with or without precipitation.

(3) A single layer of ragged patches of clouds with either uniform or irregular bases, with or without precipitation.

(4) Multiple layers of ragged patches of clouds with either uniform or irregular bases, with or without precipitation.

These conditions, sketched in Figure 1, are admittedly simple, but by combining various portions of each it is possible to approximate many types of actual cloud distributions. To describe these conditions more precisely, we need to know the distributions for such parameters as height, thickness, size, density, and precipitation rate. Not all of the desired information is readily available, and it is difficult to give a succinct summary of complicated phenomena. Without attempting to be definitive, we shall record some general observations that have guided the development of the computer model.

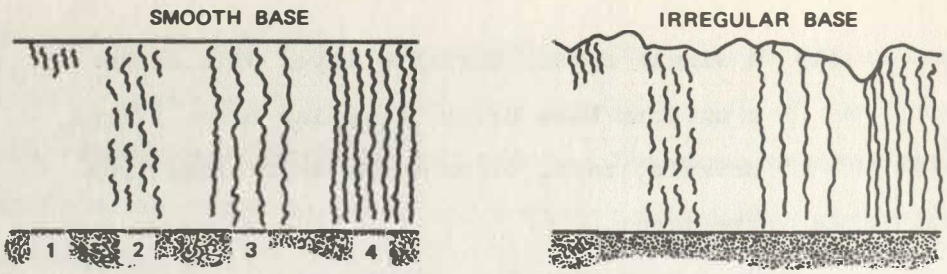

1. VIRGA
2. DRIZZLE
3. LIGHT RAIN or SNOW
4. HEAVY RAIN or SNOW

(a) DENSE SHEETS

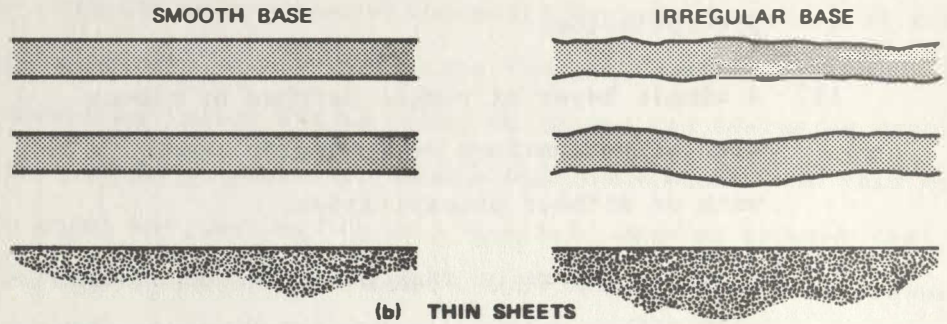

(b) THIN SHEETS

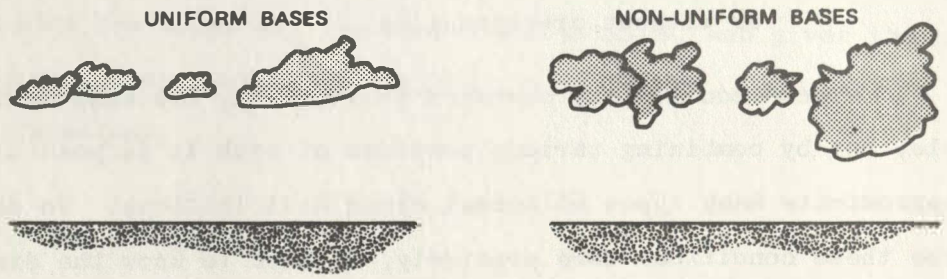

(c) SINGLE LAYER OF RAGGED PATCHES

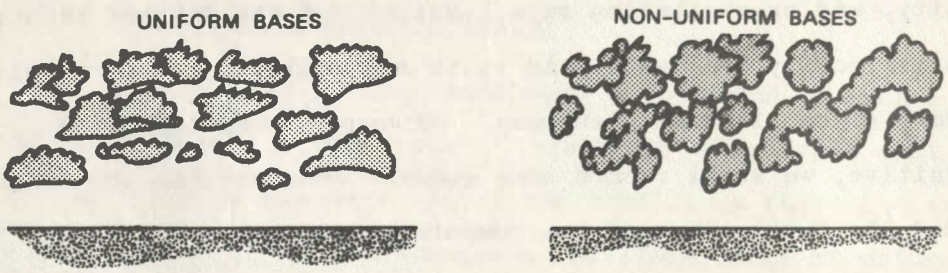

(d) MULTIPLE LAYER OF RAGGED PATCHES

TA-7935-13

FIGURE 1 BASIC CLOUD-COVER PATTERNS

B. Types of Cloud Cover and Associated Hydrometeors--Quantitative Characteristics

1. Single-Cloud Data

a. Size Distribution

Areas of the base of cloud elements probably range in size from a few thousand square feet to many square miles. For simulation, a maximum area of 500 square miles might be realistic. Several studies of clouds and radar echoes have shown that size distribution is approximately exponential, with smaller clouds greatly outnumbering larger ones. For example, in a study of Florida Cumulus, Plank (1969)* found that over the observed size range the number of clouds of various sizes could be specified approximately by the distribution function $n = K e^{-\alpha_d D}$, where n is the number density of clouds per unit surface area, D is the equivalent cloud diameter,† and K and α_d are parameters of the distribution. Plank compared his Florida data with data derived by Blackmer and Serebreny (1962) from U-2 photographs made on cross-country flights and found a comparable distribution. Dennis and Fernald (1963) studied the frequency distributions of shower radii (average of semimajor and semiminor areas for elliptical shower areas) as shown by radar and found a distribution of the form $N = N_0 e^{-\beta_d r_s}$, where N is the number density of showers,

---

*References are listed at the end of the report.

†The equivalent diameter is the diameter of the circle having the same area as the plan-projected area of the cloud.

r_s is the shower radius, and N_0 and β_d are parameters of the distribution. They also point out that the cloud data of Blackmer and Serebreny (1962) follow a similar distribution. They considered the similarity in distribution of showers and clouds significant, since the smallest showers they could measure were limited by the beamwidth of the radar and the spot size on the radar PPI. In their study they found that β_d varied with time of day as well as with location. For Blackmer's clouds, β_d ranges from 1.5 to 1.9. While all of these studies refer to cumuliform clouds and showers, it is not unreasonable to assume that a similar distribution may apply to certain conditions of stratiform-type cloud cover.

Cloud base may range from the surface (fog) to altitudes much greater than the upper limit of conditions of importance to airport operations. Thickness also may range from a few tens of feet (say 50) to much greater than 5000 feet. As an initial approximation, one can assume that the thickness equals the diameter for individual clouds of the cumuliform variety.

b. Density Variation and Optical Characteristics

Clouds can vary from tenuous wisps to very dense clouds in which visibility may be only a few feet. H. J. aufm Kampe (1950) reports measured visibilities in various types of clouds and shows values ranging from 10 to 300 meters. The mean values given by aufm Kampe are as follows:

Type of Cloud	Mean Visibility (meters)
Cumulus Congestus	20
Fair Weather Cumulus	40
Stratocumulus	100
Stratus	140
Altostratus	150

Obviously, if the cloud thickness is less than the visibility, higher clouds (if present) may be detectable by optical methods.

c. Velocity Distribution and Other Known Dynamic Characteristics

Cloud velocity can be considered comparable to the wind velocity in the layer in which the cloud is embedded. This may range from 0 to 60 knots. The most important exception is wave conditions. This exception may be important at a few airports where there are true wave clouds or similar conditions, such as coastal stratus that dissipates a short distance to the lee of elevated coastal terrain.

Cloud shapes continually change, with significant density changes occurring over periods from a few minutes to several hours. As a first approximation, however, we can consider the shapes to be fixed, with the primary variation being due merely to translation due to wind.

2. Multiple-Cloud Data--Spacing Distributions

Much of the available information on cloud spacing is based on studies of cumuliform clouds. With cloud cover that forms a ceiling we may be more concerned with holes in a cloud layer rather than spacing between elements. As a preliminary estimate, however, a range from 100 to 2500 feet may be useful. It should be noted that cloud size distribution, spacing distribution, and amount are interrelated, and that the specification of any two of these quantities highly constrains the third.

3. Cloud-Layer Data

a. Variations About Average Base Height

Borovikov et al. (1961) present an example of oscillations in the altitude of a cloud base. They claim there are two types of oscillations with an amplitude of 100 meters and over--one with a period of 1 to 6 hours, the other with a period of 10 to 15 minutes. They cite an example of even faster and sharper oscillations measured in fractions of a minute. These latter were on the order of 120 meters about the average base. Thus there are both long- and short-period fluctuations ranging from 0 to possibly 500 feet.

b. Cloud-Layer Thickness and Density Distributions

As with single clouds, layer thickness can vary from a few tens of feet to well over 5000 feet. The discussion of density variations for single clouds applies to cloud layers as well.

c. Spacing of Multiple Layers

Any postulated range of spacing between layers will probably be encountered in the atmosphere. Since we are concerned with clouds below 5000 feet, the spacings we will be concerned with will be rather small if we have two or more layers in the height interval. The exact value will depend on the assumed thickness of the layers.

4. Associated Precipitation

As indicated earlier, precipitation may be in the form of virga, drizzle, rain, or snow of various rates. In rare cases there may be hail of various sizes up to several inches in diameter. The precipitation will have various effects on optical and radar ceilometers depending on its form and intensity. Refraction phenomena during rainfall may cause optical ceilometers to give a spurious response at an elevation angle of 49°, and occasionally a secondary response at 36°. In snow, optical ceilometers may get a response down to zero elevation angle. Radar ceilometers are also affected by precipitation. Since precipitation particles are much larger than cloud droplets, and since radar ceilometers are designed to detect the weaker echoes from small cloud particles, precipitation produces a much stronger signal and much larger attenuation than the cloud layer. In its presence it may be impossible to locate either the base of the lower layer or the bases and tops of other layers. The computer program permits the simulation of these conditions.

C. Plan-View Parameters

Any attempt at modeling by definition results in an approximation to reality. Even with large computers and efficiently written programs, it is necessary to be very selective in choosing those aspects of cloud phenomena to simulate. The cloud model, as it finally developed, is based on the assumption that sky conditions can be described in terms of statistically homogeneous layers of clouds. The clouds in each layer are described in terms of a number of parameters that fix the probability distributions or the statistics, but not the actual clouds themselves. Since these parameters are not allowed to vary within a given layer, the layer is statistically homogeneous. The parameters fall naturally into three groups depending on whether they affect the plan view, the profile view, or the physical characteristics. In the following sections we describe these parameters in some detail.

In plan view, the clouds in any layer appear as scattered, possibly overlapping rectangles if the sky cover is five tenths or less. If the sky cover exceeds five tenths, the rectangular areas are interpreted as holes in an extensive layer of cloud cover. This change in interpretation is made to improve the efficiency of the computer simulation program. To make the following discussion more readable, we shall assume that the sky cover is five tenths or less, so that the rectangular areas are interpreted as clouds. If the sky cover exceeds five tenths, the following discussion should be interpreted as applying to holes rather than clouds.

Different cloud characteristics can be obtained by changing any or all of the following plan-view parameters:

(1)	Mean length	ℓ_m	(m)*
(2)	Aspect ratio	ρ	(-)
(3)	Cloud amount	c_a	(tenths)
(4)	Cloud speed	v	(m/s)
(5)	Cloud direction	ψ_c	(rad)
(6)	Layer beginning time	t_b	(s)
(7)	Layer ending time	t_e	(s).

The clouds generated by the model are rectangular, having length ℓ in the direction of motion and width $\rho\ell$ normal to the direction of motion, where ρ is the specified aspect ratio. The fact that the clouds are rectangular, rather than, say, elliptical or irregular, is not considered to be particularly significant. The size of the clouds and the percent cover is probably considerably more important than their exact shape. If ℓ_m is the specified mean cloud length, then the cloud lengths ℓ obey the exponential distribution

---

*Note that the units in this section of this report are usually given in MKS units to simplify the theoretical equations. In the computer program, other units are often used to obtain convenient magnitudes. The actual units used are given in the tables in Section IV.

$$p(\ell) = \begin{cases} \frac{1}{\ell_m} e^{-\ell/\ell_m} & \ell \geq 0 \\ 0 & \ell < 0 \end{cases} . \qquad (1)$$

The exponential distribution was chosen because it agreed with measured distributions of cloud sizes observed over large areas. The distribution tends to produce fewer large clouds than small clouds, with more than half of the clouds having $\ell < \ell_m$.* The total percentage area covered by the clouds is fixed by specifying the cloud amount c_a.

Some problems arise when we try to distribute the rectangular clouds over a prescribed area. Ideally, the clouds should be distributed in a uniform, nonoverlapping fashion such that a specified amount of the cloud cover is obtained. If the cloud centers are selected independently of the cloud sizes, there is a nonzero probability of overlap. If constraints are imposed to prevent overlap, computational complexities arise that seem out of proportion to the importance of preventing overlap. In either case, the clouds must be distributed over a finite portion of the prescribed area, and this introduces some statistical bias in their distribution.

The actual method used to distribute the clouds was chosen for its computational convenience, and will be described

---

*In some special circumstances it may be desirable to use another distribution. The program can be easily modified to accommodate such changes.

in Section IV. It produces a scattering of clouds that is essentially uniform, but that does lead to cloud overlap. This overlap is properly accounted for in computing the percentage cover, so that the desired cloud amount is achieved. However, the resulting distribution of the cloud "diameters" is not strictly exponential, since smaller clouds tend to be absorbed by larger ones. This effect is most noticeable when the cloud amount is near 50 percent, and is not very significant for either small or large percentage cover. Since neither the programming nor the use of the model relies on the cloud-length distribution being exactly exponential, this is believed to be a satisfactory solution.

The movement of the clouds is specified by the cloud speed v and cloud direction ψ_c. A conventional Cartesian coordinate system is used, with the origin locating any convenient point near the instruments, the x-axis pointing east, and the y-axis pointing north. All of the clouds in a layer are assumed to move together with a constant speed. The cloud direction is the direction from which the clouds are coming, expressed as an angle measured clockwise from north.

Finally, two plan-view parameters specify the extent of the cloud layer. The layer-beginning-time t_b specifies the time at which the leading edge of the layer is to pass over the origin, and the layer-ending-time t_e has the corresponding obvious meaning. The use of these parameters allows the simulation of abrupt changes in conditions such as those associated with an incoming front. By specifying the successive appearance of several layers having

different cloud sizes, cloud amounts, base heights, etc., a wide variety of quite complex sky conditions can be simulated. It should be noted, however, that given a specific set of cloud sizes and amounts, there is no provision for changes during the time interval t_b to t_e. That is, individual clouds are not growing or dissipating; only translation of the fixed cloud pattern takes place.

D. Profile-View Parameters

Viewed from the side, the clouds in any layer resemble rectangles having flat tops, vertical sides, and irregular bases. The following parameters control the characteristics of the profile view:

(1) Mean thickness $\bar{t}$ (m)

(2) Mean base height $\bar{h}$ (m)

(3) Base-height standard deviation σ_b (m)

(4) Base-height correlation distance d (m).

As shown in Figure 2, the height of the cloud top is the sum of the mean thickness $\bar{t}$ and the mean base height $\bar{h}$. The actual base height h(x) is an irregular function of x. Using the terminology of random processes, h(x) is a sample function of a stationary random process having mean $\bar{h}$ and standard deviation σ_b. That is,

$$\bar{h} = E[h(x)] \qquad (2)$$

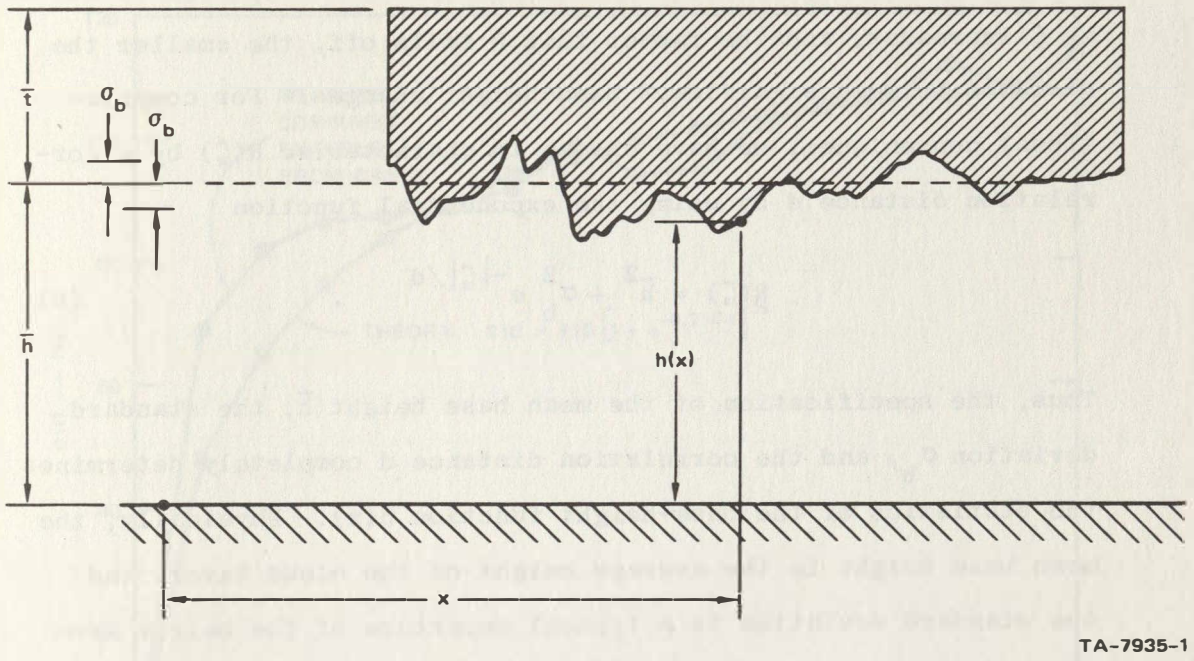

FIGURE 2 PROFILE VIEW OF A SIMULATED CLOUD

and

$$\sigma_b^2 = E\left[(h(x) - \bar{h})^2\right] \qquad (3)$$

where E[h] is the expected or mean value of the random variable h. In addition, the computer-generated random process is essentially gaussian, which means that all that is needed to complete its statistical description is the autocorrelation function $R(\zeta)$, where

$$R(\zeta) = E[h(x + \zeta)\, h(x)] \qquad (4)$$

$$= \bar{h}^2 + E[(h(x + \zeta) - \bar{h})\,(h(x) - \bar{h})] \quad . \qquad (5)$$

The autocorrelation function measures the rate at which the base height changes with x. Generally speaking, $R(\zeta)$ decreases as ζ increases, and the faster that R falls off, the smaller the distance between significant base-height changes. For computational convenience, we have chosen to characterise $R(\zeta)$ by a correlation distance d by using the exponential function

$$R(\zeta) = \bar{h}^2 + \sigma_b^2 \, e^{-|\zeta|/d} \quad . \tag{6}$$

Thus, the specification of the mean base height $\bar{h}$, the standard deviation σ_b, and the correlation distance d completely determines the statistics of the base-height function h(x). Physically, the mean base height is the average height of the cloud layer, and the standard deviation is a typical departure of the height from the average. The correlation distance tells how rapidly these departures occur. Roughly speaking, one does not expect the base height to change by an amount σ_b in a distance less than d, but one does expect such large changes in a distance greater than d.

While the exponential form for $R(\zeta)$ was chosen primarily for computational convenience, it apparently gives a reasonable first approximation to measured base-height statistics. In particular, Davis (1969) has reported measurements of the standard deviation of the difference between the lowest cloud base at one time and the lowest cloud base at periods of from 1 to 15 minutes later. The average (or combined) results for his measurements are shown in Figure 3. It is shown in Appendix A that for our model,

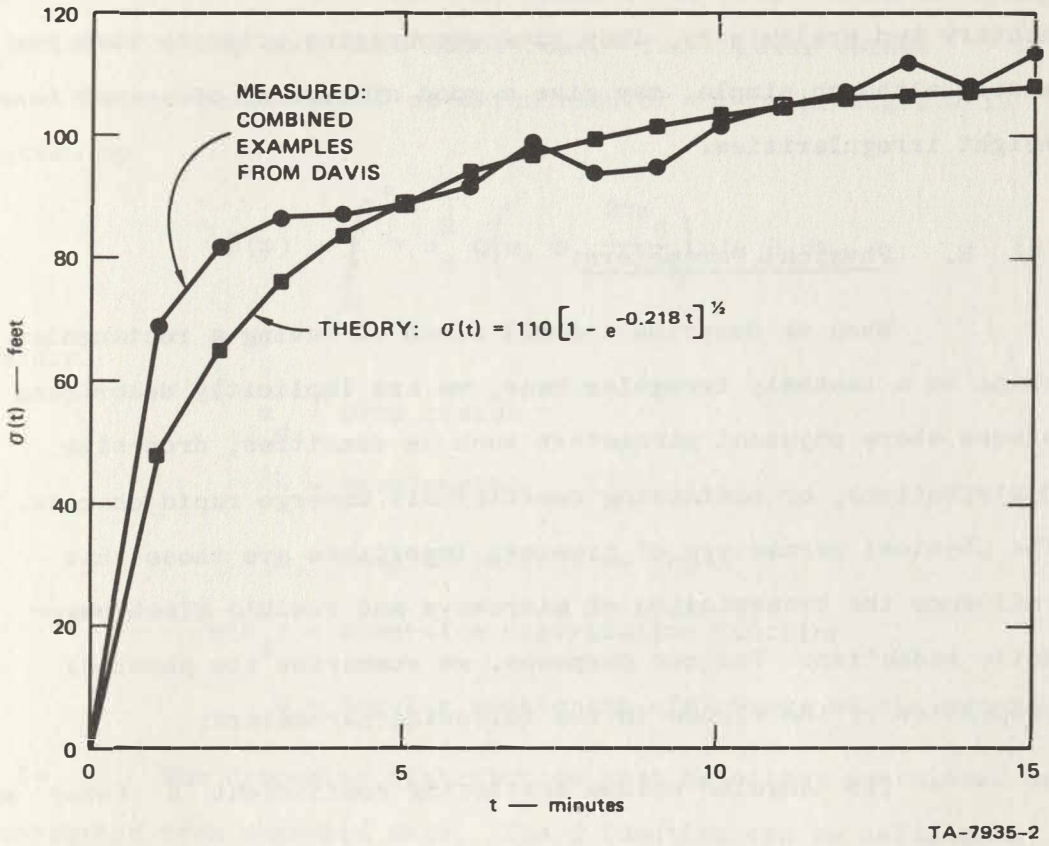

FIGURE 3 MEASURED AND THEORETICAL STANDARD DEVIATIONS

$$\sigma(t) = \sigma_b \left[1 - e^{-2vt/d}\right]^{1/2} \qquad (7)$$

where t is the elapsed time and v is the cloud velocity. The theoretical curve shown in Figure 3 for σ_b = 110 ft and d/v = 9.2 minutes gives a reasonably good approximation to the measured data. By fitting data of this type, one can obtain numerical

values for the standard deviation σ_b and the correlation distance d if the cloud velocity v is known. While these results are fragmentary and preliminary, they give encouraging evidence that the model, although simple, may give a good simulation of actual base-height irregularities.

E. Physical Parameters

When we describe a model cloud as having a rectangular shape or a randomly irregular base, we are implicitly describing places where physical parameters such as densities, drop-size distributions, or scattering coefficients undergo rapid changes. The physical parameters of greatest importance are those that influence the transmission of microwave and visible electromagnetic radiation. For our purposes, we summarize the physical properties of the clouds in the following parameters:

(1) Angular volume scattering coefficient β $(\text{ster}^{-1}\,\text{m}^{-1})$

(2) Volume scattering coefficient σ (m^{-1})

(3) Reflectivity per unit volume η (m^{-1})

(4) Atmospheric attenuation rate α_a (m^{-1}).

The scattering coefficients form the basis for computing the responses of fixed-beam and rotating-beam ceilometers. These coefficients can be measured experimentally (Barteneva and Polyakova, 1965) or they can be calculated from more basic considerations (Shifrin, 1951; van de Hulst, 1957). In particular, Mie theory can be used when scattering is due to the interaction

of a plane electromagnetic wave incident on a spherical body of uniform optical properties, and seems to be well suited to calculations for fog and cloud conditions. The angular volume scattering coefficient β as a function of the polar angle φ is given by

$$\beta(\varphi) = \int_0^\infty \pi a_d^2 Q\left(m, \varphi, \frac{2\pi a_d}{\lambda}\right) n(a_d)\, da_d \qquad (8)$$

where

a_d = Drop radius

λ = Wavelength

m = Complex refractive index

$n(a_d)$ = Drop-size distribution function

Q = Angular scattering efficiency of the sphere.

The drop-size distribution must be either postulated or estimated from measured data. The Q function can be calculated from electromagnetic theory (van de Hulst, 1957; Kattaway and Plass, 1967; Dave, 1968), and tables from which β can be calculated are available (Deirmendjian, 1969). Once β is known, the volume scattering coefficient σ can be computed directly from

$$\sigma = 2\pi \int_0^\pi \beta(\varphi) \sin\varphi \, d\varphi \qquad . \qquad (9)$$

The significance of σ can be seen from the fact that luminous flux travelling through an aerosol along a line from a to

b is attenuated by the factor $\exp - \int_a^b \sigma(x)\, dx$. Thus, the larger the value of σ, the less the light beam penetrates the aerosol.

The reflectivity per unit volume η and the atmosphere attenuation rate α_a are the principal physical parameters needed to calculate the responses of radar ceilometers. Both of these parameters are closely related to scattering coefficients, but at radar wavelengths approximations to Mie theory can be used. In particular, when the diameters d_i of the scattering particles are appreciably smaller than the wavelength λ, the Rayleigh approximation gives

$$\eta = \frac{\pi^5}{\lambda^4} \left| \frac{m^2 - 1}{m^2 + 2} \right|^2 Z \qquad (10)$$

where m is the complex refractive index and Z is the radar-reflectivity factor, given by

$$Z = \sum n_i d_i^6 \qquad (11)$$

where n_i is the number of particles per unit volume having diameter d_i (Wilk, 1958). It should be noted, however, that significant discrepancies have been observed between experimental and theoretical results based on this equation for Z, particularly for the case of water clouds. Naito and Atlas (1966) attribute the unexpectedly low measured scatter to partial coherence in the distribution of scattering particles, and their results suggest reducing the value of Z by the ratio of random particle concentration to total particle concentration. As an alternative, Z

can be estimated from measurable meteorological quantities. Collis and Stride give the following approximations:

$$Z = \begin{cases} 200\ R^{1.6} & \text{for rain} \\ 0.292\ W^{1.82} & \text{for liquid cloud droplets} \end{cases} \qquad (12)$$

where R is the precipitation rate in mm/hr, W is the liquid water content in gm/m^3, and Z is measured in mm^6/m^3 (Hansford, 1960). Another approximation is given by Wilk (1958), who also tabulates parameter values for various types of clouds.

The atmospheric attenuation rate α_a plays essentially the same role as the volume scattering coefficient σ. Microwave radiation travelling through an aerosol along a line from a to b is attenuated by the transmission factor

$$k = e^{-\int_a^b \alpha_a(x)\, dx} \quad . \qquad (13)$$

Wilk gives various expressions for α_a, depending upon whether the attenuation is due to water vapor and oxygen, precipitation, or clouds. These expressions are given for an attenuation A measured in dB/1000 ft. Thus, α_a, measured in m^{-1}, is related to A by

$$\alpha_a = 7.554 \times 10^{-4}\ A \quad . \qquad (14)$$

F. Examples

The significance of most of the cloud-model parameters is easily illustrated by a few examples. Figure 4 shows three examples of different random samples of computer-generated clouds having identical cloud parameters. Since the cloud amount is small, the square areas represent clouds, which are assumed to be moving from east to west. A vertically pointing instrument located at the place marked x in the center of the plan view cuts a slice through the cloud layer, and this intersection is shown in each plan view. The corresponding profile views show the true base heights, and represent the readings of an ideal, vertically pointing ceilometer.

When the cloud amount exceeds 0.5, it is more efficient to generate holes than clouds. Figure 5 illustrates this situation. Note that in the first and third examples the ceilometer, by chance, failed to spot a single hole, while the actual cloud amount is 90 percent. The model is naturally suited to determining such things as the length of time required to measure cloud amount to within some specified accuracy using one or more ceilometers.

The effects of changing some of the plan-view parameters are illustrated in Figure 6. Using Figure 6(a) as a reference, Figure 6(b) shows the effect of changing the aspect ratio, and Figure 6(c) shows the effect of changing the mean length. The time required to generate the clouds or holes depends on the value

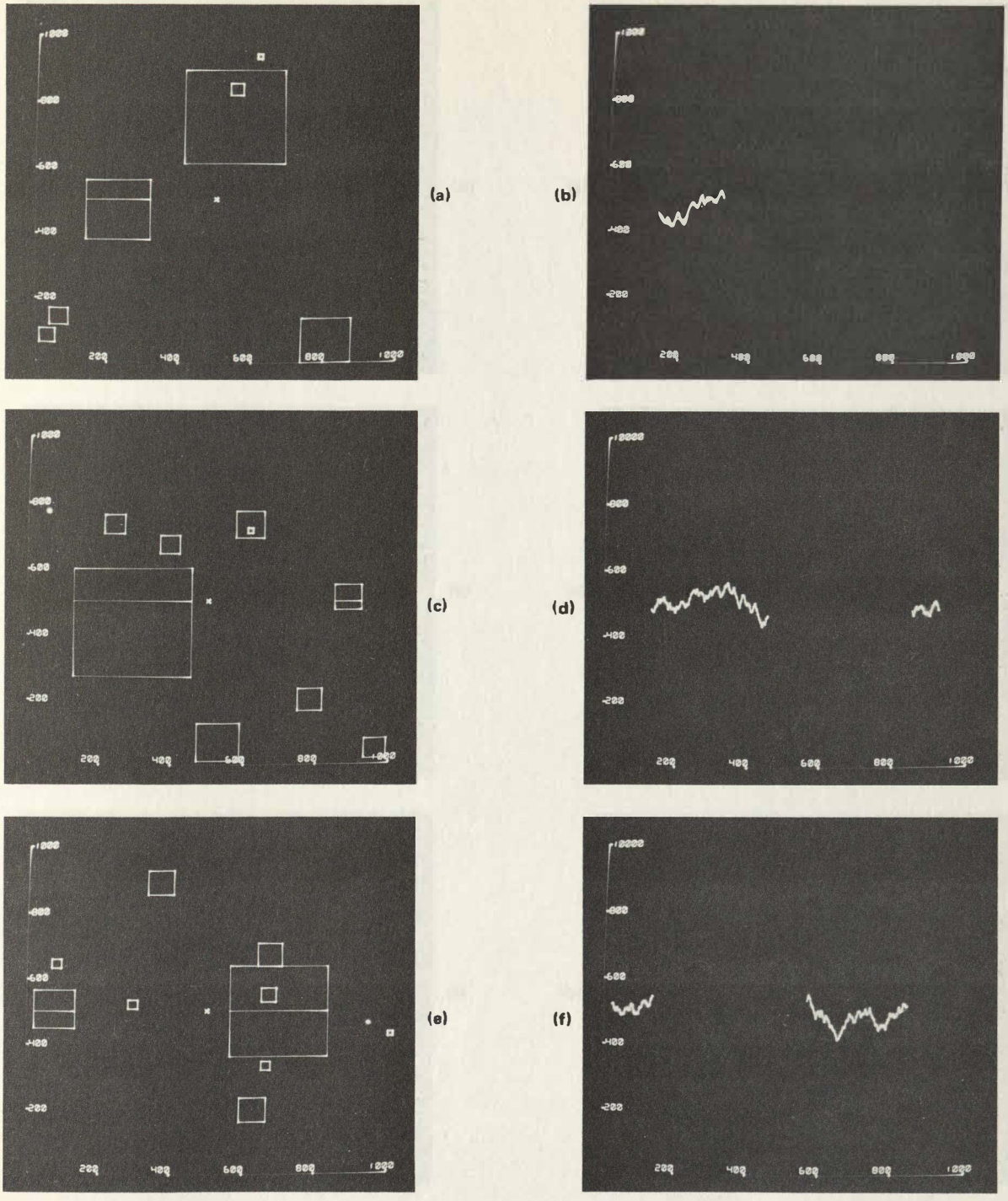

PLAN VIEW

Cloud amount = 0.1
Mean length = 100 m
Aspect ratio = 1

PROFILE VIEW

Mean base height = 500 m
Standard deviation = 20 m
Correlation distance = 100 m

TA-7935-3

FIGURE 4 THREE EXAMPLES OF COMPUTER-GENERATED CLOUDS

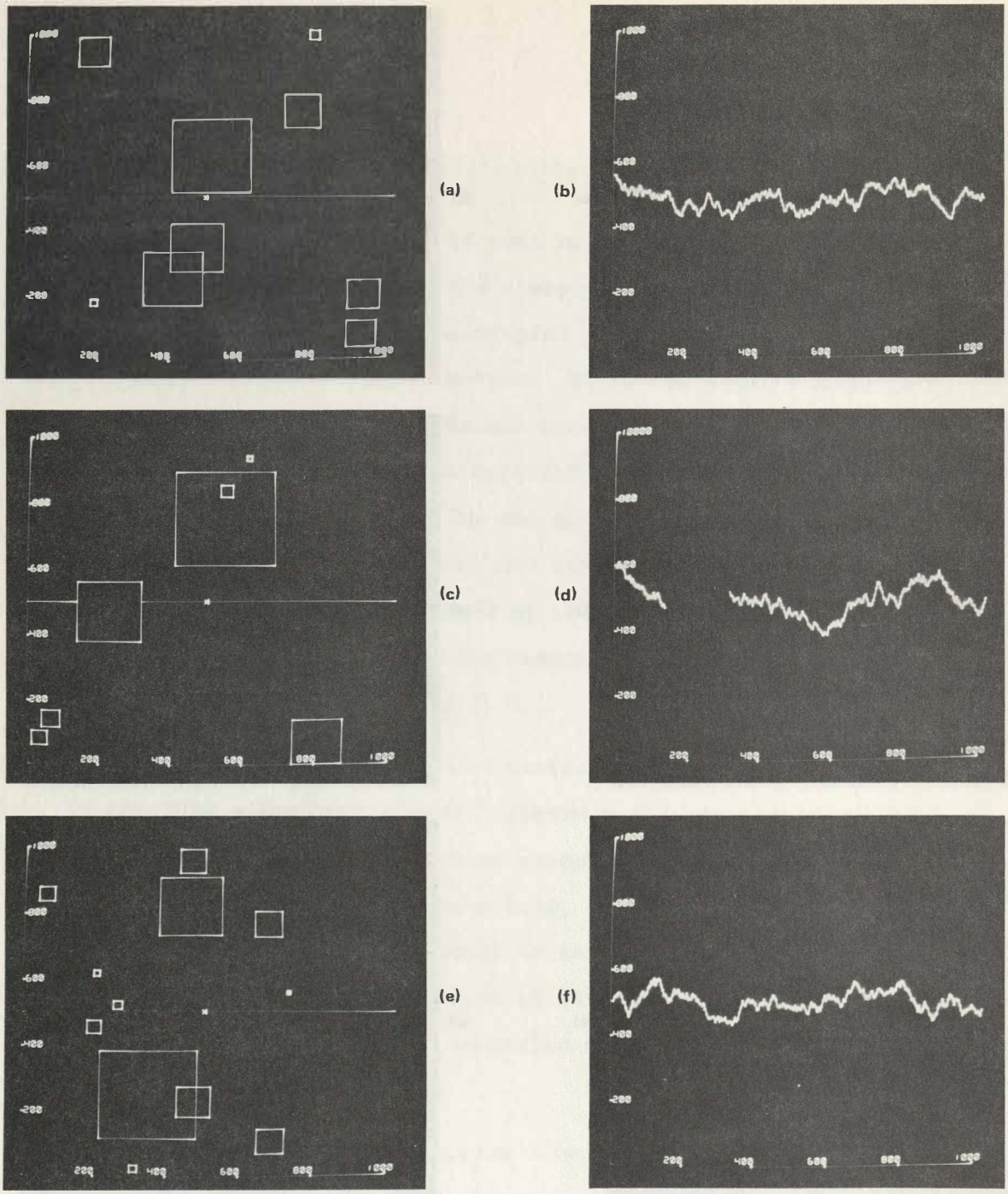

PLAN VIEW

Cloud amount = 0.9
Mean length = 100 m
Aspect ratio = 1

PROFILE VIEW

Mean base height = 500 m
Standard deviation = 20 m
Correlation distance = 100 m

TA-7935-4

FIGURE 5 THREE EXAMPLES OF COMPUTER-GENERATED HOLES

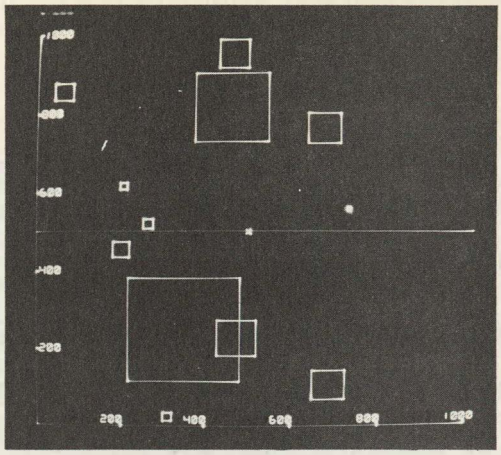

(a)

Mean length = 100 m
Aspect ratio = 1

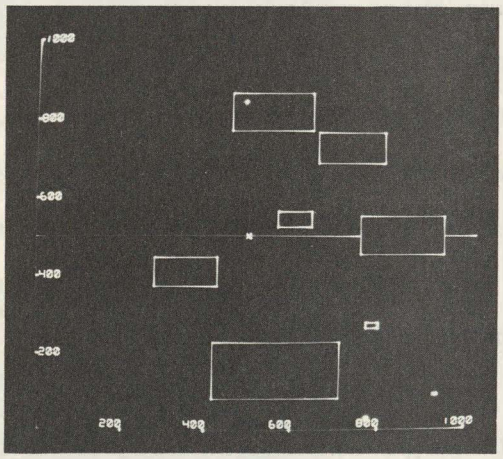

(b)

Mean length = 100 m
Aspect ratio = 0.5

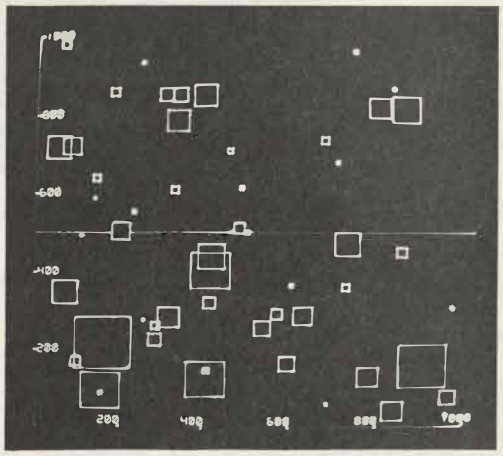

(c)

Mean length = 33 m
Aspect ratio = 1

TA-7935-5

FIGURE 6 PLAN-VIEW PARAMETER CHANGES, CLOUD AMOUNT = 0.9

of the mean length, and excessively small values should be avoided unless the cloud amount is either very small or very large.

Finally, Figure 7 illustrates the effects of changing profile-view parameters. Using Figure 7(a) as a reference, Figure 7(b) shows the effect of changing only the standard deviation. In Figures 7(c) and 7(d) the standard deviation is the same as in Figure 7(a), despite appearances to the contrary. In Figure 7(c) the correlation distance has been reduced, leading to a more erratic curve, while in Figure 7(d) the correlation distance has been increased, leading to a smoother curve. A common initial reaction to inspection of Figure 7(d) is that it has a smaller standard deviation. A closer inspection discloses that the higher spatial correlation results in the instantaneous value remaining significantly away from the mean value for longer lengths of time, and, even though extreme peaks occur much less frequently, the standard deviation is, in fact, unchanged.

III THE INSTRUMENT MODEL

A. Techniques for Cloud-Base-Height Measurement

Many different methods have been used to measure cloud-base heights. These methods have included the following:

(1) The altitude of obscuration of a known terrain feature

(2) The time required for a free-rising balloon to be lost to view

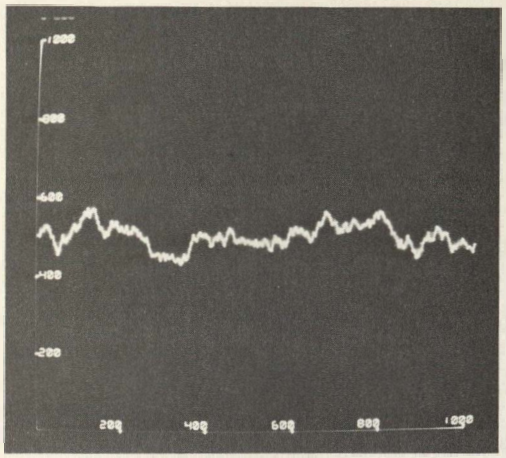

(a)

Standard deviation = 20 m
Correlation distance = 100 m

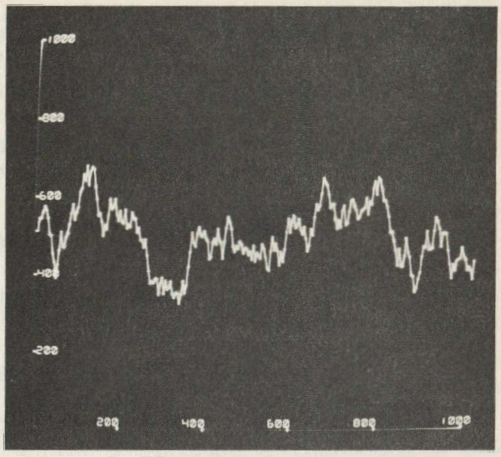

(b)

Standard deviation = 50 m
Correlation distance = 100 ft

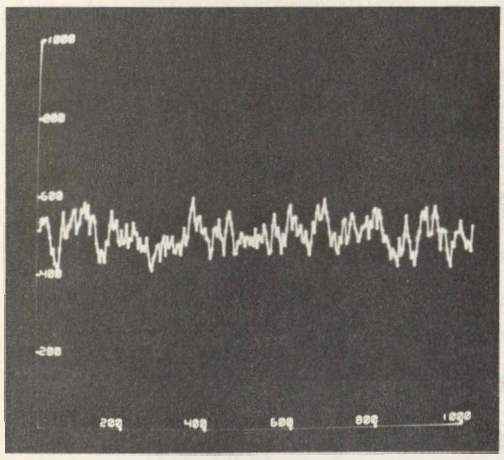

(c)

Standard deviation = 20 m
Correlation distance = 10 m

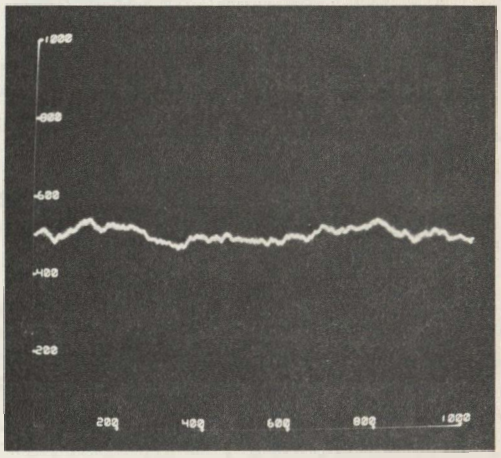

(d)

Standard deviation = 20 m
Correlation distance = 500 m

TA-7935-6

FIGURE 7 PROFILE-VIEW PARAMETER CHANGES, MEAN BASE HEIGHT = 500 m

(3) The altitude at which a tethered balloon is obscured as it is raised and lowered around cloud level

(4) The altitude at which a pilot can just see the ground

(5) The time required for a light pulse to make a round trip from the transmitter to the receiver (light radar and lidar*)

(6) The range at which a vertically pointing radar first detects a target (radar ceilometer)

(7) Triangulation using a vertically projected light and an observer with a clinometer

(8) Triangulation using a vertically projected light and a rotating photodetector (fixed-beam ceilometer)

(9) Triangulation using a vertically pointing photodector and a rotating light beam (rotating-beam ceilometer).

Of these, we have simulated the fixed-beam, rotating-beam and radar ceilometers because they have been fairly widely used and are obvious candidates for use in an automated observation

---

*Acronym for light detection and ranging. A lidar is a light radar that uses a laser light source.

system. Since the potentially interesting light radar and lidar ceilometers involve similar light-scattering principles, it should be possible to extend the present simulation techniques to include these instruments as well.

B. Fixed-Beam and Rotating-Beam Ceilometers

The basic geometry for a fixed-beam ceilometer is shown in Figure 8. Light projected vertically from the transmitter

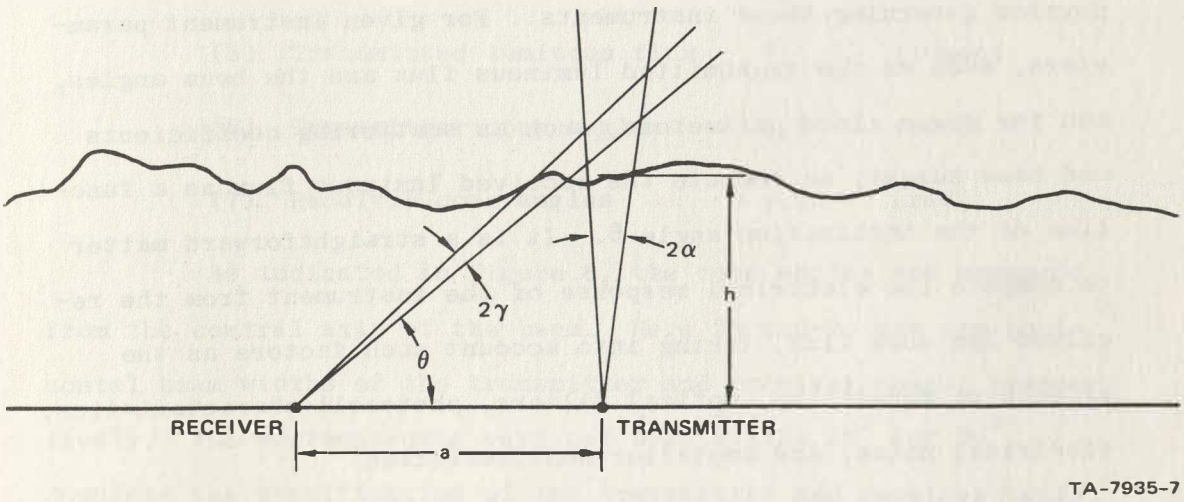

FIGURE 8 PROFILE VIEW OF A FIXED-BEAM CEILOMETER

penetrates the cloud and illuminates a region near the cloud base. A portion of the scattered light is picked up by the receiver's photodetector as the receiver scans along the projected beam. The light received usually reaches a maximum near $\theta = \tan^{-1} h/a$,

and h is usually estimated as $a\tan\theta$. The operation of the rotating-beam ceilometer is basically very similar. The main difference is that the receiver beam points vertically upward and the transmitter beam rotates, which has certain noise advantages due to reduced mechanical vibration of the sensitive detector and fewer opportunities for the pickup of stray interfering light sources. In addition, present instruments differ in the scanning rates, types of light sources, photocells, filters, electronic amplifiers, etc., used.

In our simulation, we have concentrated on the basic physics governing these instruments. For given instrument parameters, such as the transmitted luminous flux and the beam angles, and for given cloud parameters, such as scattering coefficients and base height, we compute the received luminous flux as a function of the inclination angle θ. It is a straightforward matter to compute the electrical response of the instrument from the received luminous flux, taking into account such factors as the effects of modulation, optical filters, photocell characteristics, electrical noise, and amplifier nonlinearities.*

The computation of the received luminous flux is based on single scattering theory, and accounts for light attenuation in the atmosphere, attenuation in the cloud, single scattering, penetration of thin lower layers, and refraction phenomena during precipitation. Although certain multiple-scattering effects

---

*The effects of some of these factors are discussed by Olbers (1955).

cannot be derived from this theory, the computational complexities of multiple scattering theory seem out of proportion to the possible benefits.

A fixed-beam ceilometer is described by specifying the following instrument parameters:

(1)	Instrument location	x,y	(m)
(2)	Sampling interval	t_s	(s)
(3)	Base-line distance	a	(m)
(4)	Receiver area	A_r	(m^2)
(5)	Transmitted luminous flux	F_T	(lumen)
(6)	Transmitter cone angles	α,α'	(rad)
(7)	Receiver cone angles	γ,γ'	(rad).

As indicated in Figure 8, the cone angles are measured from the central axis of the beam. Here 2α and 2γ are the horizontal beam widths of the transmitter and receiver cones, respectively. The corresponding vertical beam widths $2\alpha'$ and $2\gamma'$ complete the specification of the transmitter and receiver cones, which are rectangular in cross section. If the cone angles are small, the solid angle ω_T for the transmitter is approximately $4\alpha\alpha'$, and the solid angle ω_r for the receiver is approximately $4\gamma\gamma'$. For a rotating-beam ceilometer, the same parameters are needed; however, the receiver cone angles are now denoted by α and α', and the transmitter cone angles by γ and γ'.

The basic relation used to calculate the ceilometer response is

$$dF_r = \frac{F_T}{\omega_T}\beta(\varphi)\frac{A_r\cos\psi}{r^2 s^2}e^{-\int_0^r\sigma(r)dr-\int_0^s\sigma(s)ds}dv \qquad (15)$$

where

dF_r = Flux received from the scattering volume dv

$\beta(\varphi)$ = Angular volume scattering coefficient

$A_r\cos\psi$ = Normal component of receiver area

r = Distance from transmitter to scattering volume

s = Distance from receiver to scattering volume

σ = Volume scattering coefficient.

To determine the total flux received as a function of inclination angle θ, Eq. (15) must be integrated over the volume common to the transmitter and receiver beams for any given θ. This is very difficult to do exactly, both because of the awkward geometrical constraints and because of the variation of β and σ with altitude. A good approximate solution can be obtained, however, in which $F_r(\theta)$, shown in Figure 9, is characterized by four parameters: θ_{min}, θ_{max}, θ_{decay}, and F_{max}. It is shown in Appendix B that under reasonable assumptions the received flux begins to rise abruptly at $\theta = \theta_{min}$, reaching a peak of F_{max} at $\theta = \theta_{max}$, and decaying exponentially like $\exp -(\theta - \theta_{max})/\theta_{decay}$ thereafter. Explicit equations are given for computing these four

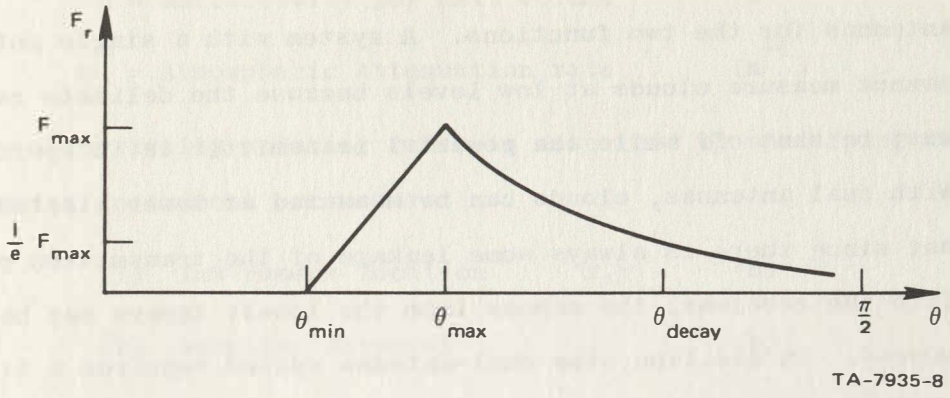

FIGURE 9 OPTICAL CEILOMETER RESPONSE CURVE

parameters, both for the response for the lowest cloud layer and the response for the second lowest cloud layer. Their computation at successive sampling times is the basic output of the optical-ceilometer simulation routine.

C. Radar Ceilometers

Vertically pointing radars operating at wavelengths of about 1 cm are capable of measuring the bases and tops of cloud layers, including layers above a lower overcast that obscures the layer from detection by a surface observer or an optical ceilometer. Such instruments are very sensitive to cloud-droplet temperature and rain, however. In addition, heights of clouds at very low altitudes cannot be measured; for the AN/TPQ-11 radar ceilometer, for example, this lower limit is about 500 feet.

A vertically pointing radar may have a single transmitting and receiving antenna, or separate but closely spaced antennas for the two functions. A system with a single antenna cannot measure clouds at low levels because the delicate receiver must be shut off while the powerful transmitter is in operation. With dual antennas, clouds can be measured at lower altitudes, but since there is always some leakage of the transmitted pulse into the receiver, the echoes from the lowest layers may be obscured. In addition, the dual-antenna system requires a tilt mechanism to converge the narrow beams at a selected altitude.

The computation of the average received power P_r backscattered by particles filling the beam at range r is based on the radar equation:

$$P_r = \frac{C}{r^2} \eta(r) e^{-2\int_o^r \alpha(r)dr} \tag{16}$$

where C is the radar constant given by

$$C = \frac{P_T G^2 \lambda^2 \theta_b \varphi_b c\tau}{128\pi^3} \tag{17}$$

and

P_T = Transmitted power (watts)

G = Antenna gain (-)

λ = Wavelength (m)

θ_b, φ_b = Horizontal and vertical beam widths (rad)

c = Speed of light (m/s)

τ = Pulse duration (s)

η = Reflectivity per unit volume (m^{-1})

α_a = Atmospheric attenuation rate (m^{-1}) .

Thus, a vertically-pointing radar is described by specifying the following instrument parameters:

(1) Instrument location x,y (m)

(2) Sampling interval t_s (s)

(3) Radar constant C (watts-m^3)

(4) Minimum range r_{min} (m) .

To determine the response of the instrument, Eq. (16) is evaluated using the values of η and α_a determined by the clouds intercepted by the radar beam. Complete equations for the response for the lowest two layers are derived in Appendix C. Except for attenuation, the result is a superposition of the responses for the separate layers. As illustrated in Figure 10, the response $F_r(r)$ for a single layer can be characterized by four parameters: P_1, r_1, $\hat{r}_1$, and α_1. Below r_1, the average height of the cloud base intercepted by the radar cone, the response is negligible. At or near r_1 it rises abruptly to P_1, and then falls off according to

$$P_r(r) = P_1\left(\frac{r_1}{r}\right)^2 e^{-2\alpha_1\left(r-r_1\right)} \qquad (18)$$

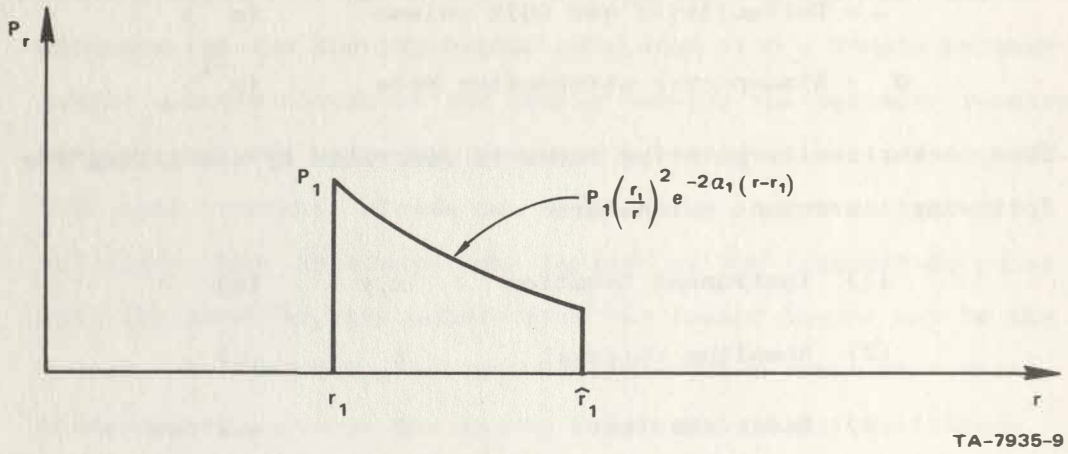

FIGURE 10 RADAR CEILOMETER RESPONSE CURVE

until $r = \hat{r}_1$, the height of the top of the cloud layer. Explicit equations for computing these four parameters, both for the lowest and the second lowest cloud layer, are given in Appendix C. Their computation at successive sampling times is the basic output of the radar-ceilometer simulation routine.

IV THE COMPUTER PROGRAM

A. Basic Program Organization

The simulation program uses the cloud/instrument model to compute the responses of a set of ceilometers to multiple layers of simulated clouds. The input to the program is a complete parametric description of the cloud layers and the instrument characteristics. The basic output is a record of the instrument responses at every sampling time. This output can be

listed on a line printer and/or written on magnetic tape for further analysis. In addition, graphical output can be obtained showing the actual clouds generated and the true ceiling heights.

The clouds generated in any given layer fall in a strip that is arbitrarily long in the direction of cloud motion, but of fixed extent normal to that direction. The instruments are placed in some configuration that lies within this strip. One of the basic subroutines in the program rotates coordinates so that this strip can always be thought of as moving from east to west. In the current version of the program, the strip represents an area 16-km wide, and after rotation the origin is centered in the north/south direction.

While the strip is arbitrarily long, the generation of clouds takes place in intervals, so that the strip effectively grows from west to east. As the clouds move from east to west, a new interval must be generated before the leading ceilometer encounters the end of the old interval. Since each layer can move at a different speed, these intervals are computed on the basis of time rather than distance. The x-axis for each layer is scaled by dividing by the layer speed, thereby converting it to a time axis. Each interval is a section of the strip of width 16 km and of length $v \cdot TD$, where v is the cloud speed and TD is the interval time duration, which is currently three hours. Thus, the stages for every layer end at the same time, and the process of growing the strip takes place at three-hour intervals.

This process of generating the strip in intervals has several implications. One is that a computer run continues for some specified number of three-hour intervals. Another is that the first three-hour interval will not produce a full three-hour record for a ceilometer unless the ceilometer is located at the extreme left edge. A third is that the maximum value for the x-coordinate of the ceilometer must be limited to $v \cdot TD/2$ to keep it within the interval. For this reason, we require the cloud speed to be at least 2.5 m/s, corresponding to a maximum x-coordinate of 13.5 km after rotation.*

A flowchart for the basic steps in the program is shown in Figure 11. The first step is to establish a number of basic constants, such as TD and the strip size (see Table I for details). The next step is to read cards specifying (1) the options selected, (2) basic parameters, such as the number of layers and the number of instruments, (3) the cloud-layer parameters, and (4) the instrument parameters. Next, four subroutines are called to compute various quantities that depend on the cloud and instrument parameters, but that do not vary as the simulated clouds are generated and translated.

At this point, computation for the first three-hour interval begins. This computation is done in two phases--a cloud-generation phase and an instrument response phase. In the

---

*Parameter limitations such as these limitations on speed and range are noted in the parameter tables.

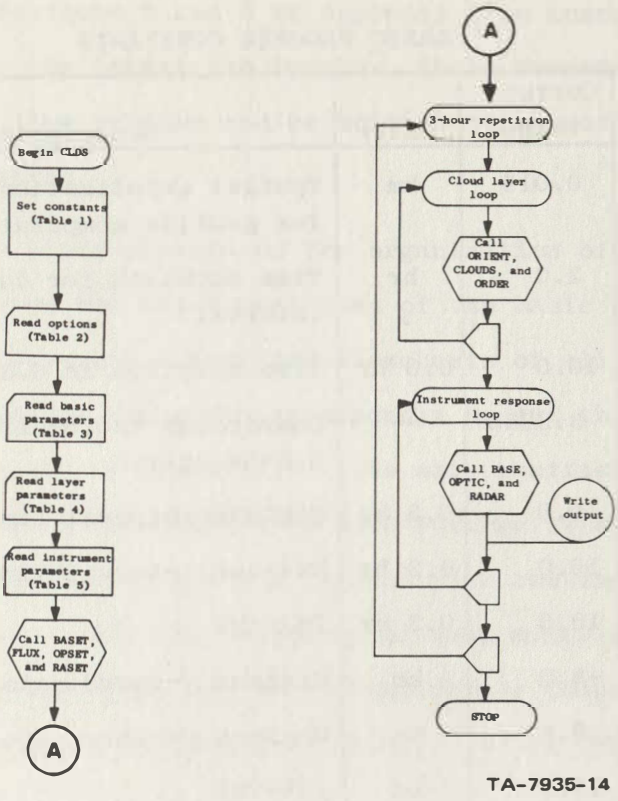

FIGURE 11 BASIC FLOWCHART FOR SIMULATION PROGRAM

cloud-generation phase, the layers are generated in succession. For each layer, subroutine ORIENT rotates the instrument configuration to the standard position and scales the x-axis by the cloud speed. Subroutine CLOUDS generates the rectangular clouds (or holes) until the specified cloud amount is attained. The intersections of these clouds with the line traced by the ceilometers as the layer moves are saved, and subroutine ORDER arranges these segments sequentially, merging overlapping traces.

Table I

BASIC PROGRAM CONSTANTS

Symbol	Current Value	Units	Description
DELX	0.015	km	Spatial quantization interval for profile computations
TD	3.0	hr	Time duration for computation interval
T10	10.0	0.3 hr	Time duration in 0.3-hr units
DDT	3.3333	--	Conversion factor from hr to 0.3-hr units
TMI	0.0	0.3 hr	Minimum interval time
TMA	10.0	0.3 hr	Maximum interval time
TMR	10.0	0.3 hr	TMA-TMI
TMS	-8.0	km	Minimum y-coordinate for strip
TMN	8.0	km	Maximum y-coordinate for strip
TMR	16.0	km	YMN-YMS

After the plan view for the highest layer has been computed, calculation of the instrument responses begins, with each instrument being considered in turn. For each instrument, subroutine BASE uses Eq. (A-1) of Appendix A to compute the true base-height profile for every layer. The average height in the vertical cone is also computed, and the results for the two lowest layers having clouds directly above the instrument are saved. These average heights are used by subroutine OPTIC and subroutine RADAR to compute the instrument response. OPTIC uses the equations in Section 8 of Appendix B to compute F_{max}, θ_{min},

θ_{max}, and θ_{decay} for the lowest two layers. RADAR uses the equations in Sections 5 and 6 of Appendix C to compute P_1, r_1, $\hat{r}_1$, and α_1 for the lowest two layers. These responses can be listed on the line printer and/or written on magnetic tape for further processing.

This broad picture of the organization of the simulation program indicates the major functions of the basic subroutines in the simulation program. Detailed flowcharts of all of the Fortran IV routines are given in Appendix D, and the source code listings are given in Appendix E. The only routines that are not part of the standard CDC 6400/6600 Fortran IV system and that are not documented are the various plot routines for the CalComp plotter. With the exception of some minor modifications, these routines are described in the California Computer Products manual, "Programming CalComp Pen Plotters" (June 1968).

B. Input Data

1. Data Cards

Data for the program are punched on a series of cards specifying (1) the options selected, (2) basic parameters, (3) cloud-layer parameters, and (4) instrument parameters. The cards for these functions are referred to as the A, B, C, and D cards, respectively. For a given run, there is only one A card and one B card, but there are seven C cards per layer and two D cards per instrument.

The user of the simulation program controls its operation by the choices he makes for the data on these cards. The A card controls the type of output obtained: printout, magnetic-tape output, and/or graphical output. The B card controls such things as the number of cloud layers and the number of instruments. For each layer, the C cards specify the statistical parameters for the layer. Similarly, for each instrument, the D cards specify the physical parameters of the instruments.

In Sections II and III we described the significance of these parameters, and in some cases described how one might obtain numerical values for them. The problem of choosing values for all of the parameters naturally depends on the conditions one wishes to simulate. Because of the wide variety of conditions that can be simulated, we cannot give any further specific advice on how the parameter values should be selected. However, the following sections give a complete and exact description of the parameters at the user's disposal. Example values are also given, but they are for illustrative purposes only, and should not be regarded as being representative of any real situation.

2. Output Options--A Card

The output options are controlled by the three parameters NLINE, NTAPE, and NCALC. Table II summarizes their effects and gives the required format. Every run of the program produces a line-printer listing of the parameters for that run.

Table II

OUTPUT OPTIONS--A CARD

Column	Format	Symbol	Units	Value Limits	Typical Value	Description
1-10	I10	NLINE	--	0,1	1	0: no line printer output 1: line printer output
11-20	I10	NTAPE	--	0,1	0	0: no magnetic tape output 1: magnetic tape output
21-30	I10	NCALC	--	0,1,2	2	0: no graphical output 1: plot profile view 2: plot profile and plan view

If NLINE = NTAPE = NCALC = 0, no additional output is obtained. The principal output of the run--the ceilometer responses--is listed on the line printer if NLINE = 1, and both the parameters and the output are written on magnetic tape (input/output unit 41) if NTAPE = 1.

If desired, graphical output showing the actual simulated cloud conditions can be obtained. When this option is exercised, data are written on magnetic tape (input/output unit 46) in a format suitable for off-line operation of a CalComp plotter. If NCALC = 1, profile views of the actual ceiling heights at the ceilometer locations are plotted. In addition, if NCALC = 2, plan views of the clouds in each layer are plotted.

3. Basic Parameters--B Card

The basic program parameters under user control are the six quantities, NL, NI, RN, TT, ASC, and AAT listed in Table III. NL specifies the number of cloud layers and NI specifies the number of instruments. As Table III indicates, the current program is limited to five cloud layers and ten instruments during any one run. Repeated runs can be used to obtain the responses for any number of instruments.

Since a pseudo-random number generator is used to generate clouds and cloud-base irregularities, repetition of a run without changing any parameters will result in an exact duplication of previous results. RN allows the starting number

Table III

BASIC PARAMETERS--B CARD

Column	Format	Symbol	Units	Value Limits	Typical Value	Description
1-10	I10	NL	--	1-5	2	Number of cloud layers
11-20	I10	NI	--	1-10	3	Number of instruments
21-30	F10.5	RN	--	Odd no.	3.0	Controls initialization of random number generators
31-40	F10.5	TT	--	>0.0	3.0	Total time for run
41-50	F10.5	ASC	km^{-1}	≥ 0.0	0.1	Atmospheric volume scattering coefficient, σ_o
51-60	F10.5	AAT	km^{-1}	≥ 0.0	0.04	Atmospheric attenuation rate, α_o

for the pseudo-random number generator to be changed, thereby allowing the variations due only to random factors to be studied. RN can be set to any convenient odd number. A change in RN results in a change in every effect involving randomness. Ways of obtaining selective changes are described in the next two subsections.

TT specifies the total time period for the simulation. Because operations take place in three-hour intervals, if TT is not an exact multiple of three, the program will generate successive three-hour intervals until TT is exceeded.

The last two parameters, ASC and AAT, are atmospheric parameters. ASC is the volume scattering coefficient σ_0 and AAT is the atmospheric attenuation rate α_0. Note that σ_0 is measured at optical wavelengths and α_0 at radar wavelengths. The wavelengths selected must correspond to the operating wavelengths of the instruments. The simulation of different optical (or different radar) ceilometers operating at significantly different wavelengths can only be done by making repeated runs.

4. Cloud-Layer Parameters--C Cards

Of the seven C cards, the first two specify a variety of cloud-layer parameters, while the last five merely specify a table of values for the normalized angular volume scattering coefficient β/σ. Information about these cards is summarized in Table IV.

Table IV

CLOUD LAYER PARAMETERS--C CARDS

Card	Column	Format	Symbol	Units	Value Limits	Typical Value	Description
C1	1-10	I10	LCOD	--	1-15	2	Layer code for random numbers
	11-20	I10	LTYP	--	-1,0,1	1	1: generates clouds -1: generates holes 0: generates clouds if cloud amount ≤0.5; holes otherwise
	21-30	F10.5	CBT	hrs	--	-3.0	Time at which beginning of layer passes over origin, t_b
	31-40	F10.5	CET	hrs	>CBT	12.0	Time at which end of layer passes over origin, t_e
	41-50	F10.5	CSP	m/s	2.5-25.	5.0	Cloud speed, v
	51-60	F10.5	CDR	degrees	--	90.0	Cloud direction, clockwise from north, ψ
	61-70	F10.5	CAM	tenths	0.0-1.0	0.6	Cloud amount, c If LTYP $\neq$ 0, CAM ≤0.8 If LTYP = -1, CAM is interpreted as hole amount
	71-80	F10.5	CML	km	>0.0	2.0	Mean cloud (or hole) length, ℓ_m
C2	1-10	F10.5	CAR	--	>0.0	0.5	Cloud (or hole) aspect ratio, ρ
	11-20	F10.5	CTH	km	>0.0	0.03	Mean cloud thickness, $\bar{\tau}$
	21-30	F10.5	CBH	km	0.0-1.5*	0.1	Mean cloud base height, $\bar{h}$
	31-40	F10.5	CBSD	km	0.0-0.5	0.02	Base-height standard deviation, σ
	41-50	F10.5	CBCD	km	≥0.0	0.5	Base-height correlation distance, d
	51-60	F10.5	CSC	km^{-1}	≥0.0	30.0	Cloud-volume scattering coefficient, σ
	61-70	F10.5	CAT	km^{-1}	≥0.0	0.1	Cloud attenuation rate, α
	71-80	F10.5	CRF	$10^{-6}km^{-1}$	≥0.0	1.0	Cloud reflectivity per unit volume, η
C3-C7	--	F10.5	RATBS	--	≥0.0	0.01	37 values for the normalized angular volume scattering coefficient $\beta(\varphi)/\sigma$ given in 5° increments from φ = 0° to φ = 180°

*This limitation is due to graphical output; by modifying the statement after Statement 68 in TYPE1, replacing 1.5 by the desired maximum height, this restriction can be removed.

The first parameter, LCOD, is a code number for the random number generator for the layer. If neither RN, LCOD, nor any other plan-view parameter is changed, repeated runs will have identical plan-view cloud patterns. If LCOD is the only parameter changed, a different random sample having the same statistics will result. Fifteen different random samples can be obtained merely by changing LCOD; additional samples can be obtained by changing RN. As a side effect, whenever two layers are given identical valves for LCOD and identical plan-view parameters, identical cloud patterns will result.

The second parameter, LTYP, can be used to control the mode of cloud generation: 1 for clouds and -1 for holes. If LTYP = 0, the program selects between clouds and holes depending on the cloud amount. This is the preferred mode of operation, since it places no limits on the cloud amount.

CBT and CET specify the beginning and ending times for the layer, indicating the times at which an edge of the layer passes over the origin. CSP gives the cloud speed, and CDR gives the cloud direction. If CDR = 90°, the clouds are moving in from the east.

CAM gives the cloud amount in tenths. If LTYP = 0, CAM can have any value from 0.0 to 1.0. Note, however, that if LTYP = ±1, CAM must not exceed 0.8. Furthermore, if LTYP = -1, CAM is interpreted as the hole amount, rather than the cloud amount. These possible sources of confusion are eliminated by taking LTYP = 0.

The remaining parameters need little comment, since they are merely the remainder of the plan-view, profile-view, and physical parameters described in Section II. It should be noted again, however, that certain parameters, such as σ and β, are wavelength-dependent, and the values selected must correspond to the wavelengths of the instruments used. Thus, if two optical or two radar ceilometers operating at significantly different wavelengths are used, the responses will have to be computed in separate runs.

5. Instrument Parameters--D Cards

The two D cards specify the instrument parameters as summarized in Table V. The first parameter, ICOD, is a code number for the random number generator for the instrument. If neither RN, ICOD, nor any other profile-view parameter is changed, repeated runs will have identical profile-view cloud patterns. If ICOD is the only parameter changed, a different random sample having the same statistics will result. Fifteen different random samples can be obtained merely by changing ICOD; additional samples can be obtained by changing RN. As a side effect, whenever two instruments are given identical values for ICOD, identical profile-view base irregularities will result.

The meanings of the other parameters are easy to understand from Table V. Note, however, that the contents of the second D card distinguish the optical ceilometers from the radar ceilometers. Since the radar ceilometer uses fewer parameters, it turns out that one of the parameters, RAR, is

Table V

INSTRUMENT PARAMETERS--D CARDS

Card	Column	Format	Symbol	Units	Value Limits	Typical Value	Description
D1	1-10	I10	ICOD	--	1-15	1	Instrument code for random numbers
	11-20	I10	ITYP	--	1,2,3	2	Instrument type 1: fixed beam 2: rotating beam 3: radar
	21-30	F10.5	XIS	km	XIS^2 $-YIS^2$	2.0	Instrument x-coordinate
	31-40	F10.5	YIS	km	≤64	-3.0	Instrument y-coordinate
	41-50	F10.5	TIS	min	≥0.1	3.0	Instrument sampling interval, t_s
D2o	1-10	F10.5	TFX	lumens	>0.0	500.0	Transmitted flux, F_T
(optical)	11-20	F10.5	TRD	km	>0.0	0.1	Base line, a
	21-30	F10.5	RAR	m	>0.0	0.5	Effective diameter of receiver area, $\sqrt{4A_r/\pi}$
	31-40	F10.5	RA1	degrees	0.0-10.0	4.0	Receiver cone half-angle, α or γ
	41-50	F10.5	RA2	degrees	0.0-10.0	4.0	Receiver cone half-angle, α' or γ'
	51-60	F10.5	TA1	degrees	0.0-10.0	0.4	Transmitter cone half-angle, γ or α
	61-70	F10.5	TA2	degrees	0.0-10.0	0.4	Transmitter cone half-angle, γ' or α'
D2r	1-10	F10.5	TFX	watts-km^3	>0.0	0.001	Radar constant, C
(radar)	11-20	F10.5	TRD	km	≥0.0	0.05	Minimum range, r_{min}
	21-30	F10.5	RAR	--	--	0.0	Dummy
	31-40	F10.5	RA1	degrees	0.0-10.0	0.25	Radar beam width, θ

meaningless for that instrument. A value, typically 0.0, must be included on the card, however, or else the beam width θ will be lost.

C. Output Data

The three output options serve three quite different purposes. Output on the line printer is useful for short runs and preliminary studies. Output on magnetic tape is intended for further processing and fairly large-scale studies. Graphical output is useful for diagnostic purposes, and may be helpful when the user encounters puzzling phenomena.

Regardless of the type of output requested, every run results in a line printer listing of the parameters used. The sample printout shown in Appendix F illustrates this output. In addition, when magnetic tape output is requested, the data on the A, B, C, and D cards are written at the front of the magnetic tape in the card format. For details, see statements 80 to 300 in subroutine TYPE1 listed in Appendix E.

The records of ceilometer responses form the principal output of the program. As illustrated in Appendix F, these responses are produced in blocks corresponding to the three-hour computation intervals. Each block contains records of the responses of Ceilometer 1, Ceilometer 2, etc., in sequence. Each ceilometer record consists of $3/t_s$ responses, where t_s is the sampling interval in hours. For an optical ceilometer, a response consists of eleven numbers--the sampling time, the five

quantities $\text{atan}\theta_{max}$, F_{max}, θ_{max}, θ_{min}, and θ_{decay} for the lowest layer, and the same five quantities for the next higher layer. For a radar ceilometer, a response consists of nine numbers, the sampling time, the four quantities P_1, r_1, $\hat{r}_1$, and α_1 for the lowest layer, and the same four quantities for the next higher layer. On tape, the optical responses appear in an 11F12.4 format and the radar responses in an 9E12.4 format.

The sample printout in Appendix F illustrates some other interesting aspects of the program. In this run, the responses of hypothetical fixed-beam, rotating-beam, and radar ceilometers are simulated. The cloud conditions consist of a thin lower layer producing 0.4 cover and moving slowly from east to west, and a thick higher layer producing 0.8 cover and moving more rapidly from south to north. Figure 12 shows the fixed-beam ceilometer response as reconstructed from a portion of the record listed in Appendix F. Note that sometimes there is a response for both layers, but that this need not always be the case. When there is a missing response, all numerical output is assigned the value 99.99.

This example also serves to illustrate the kind of graphical output produced by the program. Figure 13 shows the plan view of Layer 1 for the first three-hour interval. The overlapping rectangular clouds shown cover forty percent of the area, as specified. Note that the y-axis runs from -8 km to 8 km, while the t-axis runs from -1.5 hrs to 1.5 hrs. This

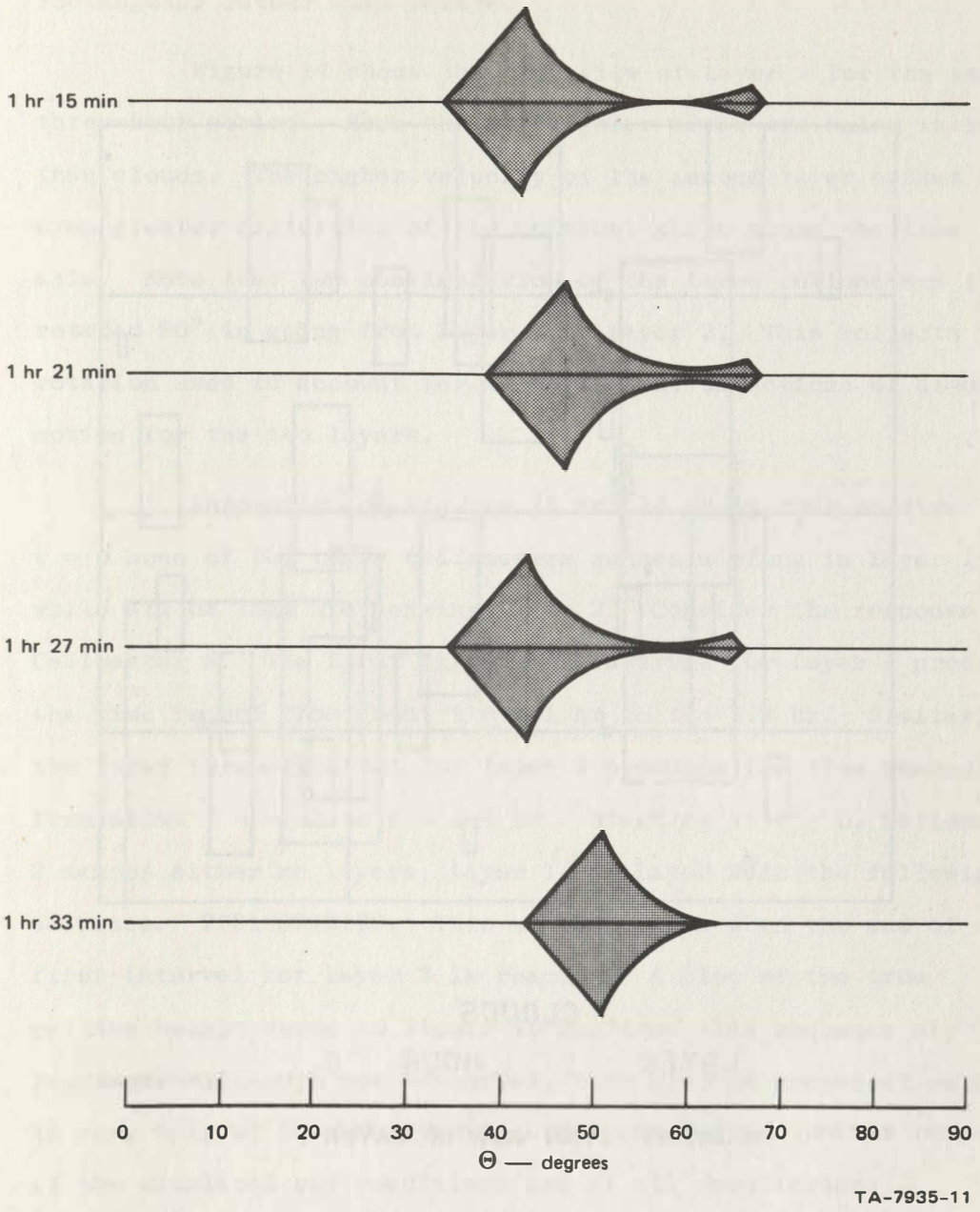

FIGURE 12 SIMULATED FIXED-BEAM CEILOMETER RESPONSE

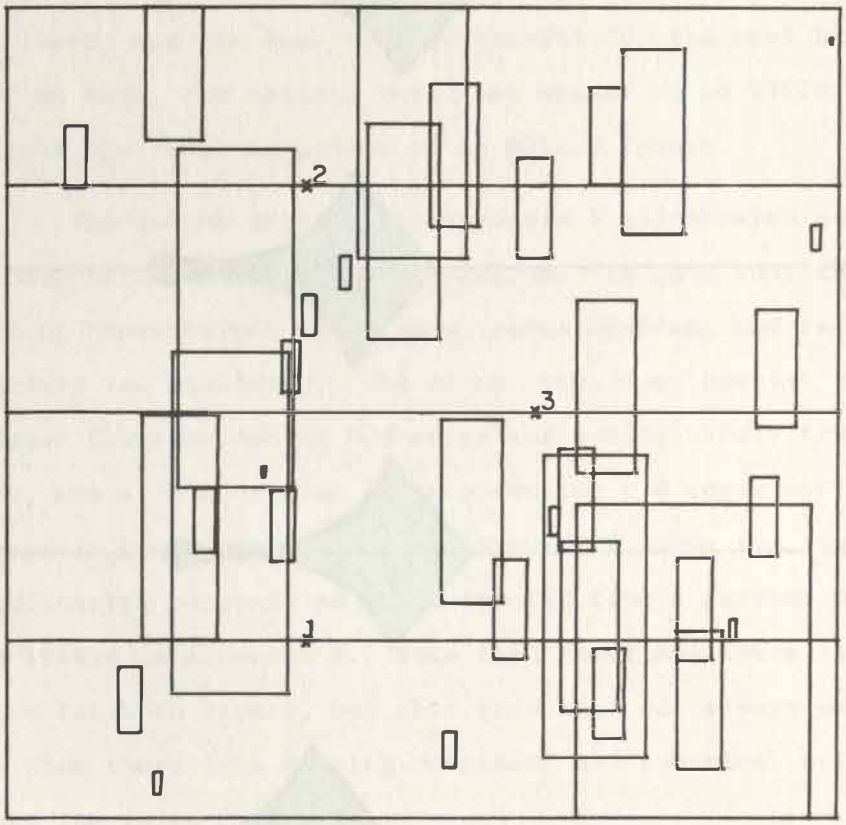

CLOUDS

LAYER 1 HOUR 0

TA-7935-45

FIGURE 13 PLAN VIEW OF LAYER 1

difference in scale is the reason that the clouds appear to be rectangular rather than square.

Figure 14 shows the plan view of Layer 2 for the same three-hour period. Here the rectangular areas are holes rather than clouds. The higher velocity of the second layer causes an even greater distortion of the apparent shape along the time axis. Note that the configuration of the three ceilometers is rotated 90° in going from Layer 1 to Layer 2. This reflects the rotation used to account for the different directions of cloud motion for the two layers.

Inspection of Figures 13 and 14 shows that at time t = 0 none of the three ceilometers senses a cloud in Layer 1, while all of them are sensing Layer 2. Consider the response of Ceilometer 2. The first three-hour interval for Layer 1 produces the time record from about t = 1.1 hr to t = 1.9 hr. Similarly, the first three-interval for Layer 2 produces the time record from about t = -1.3 to t = 1.7 hr. Starting at t = 0, Ceilometer 2 senses either no layers, Layer 1, or Layer 2 in the following sequence: 202120212120. This sequence ends when the end of the first interval for Layer 3 is reached. A plot of the true ceiling height shown in Figure 15 confirms this sequence of readings. Although not essential, this kind of graphical output is very helpful in understanding the computed ceilometer responses if the simulated sky conditions are at all complicated.

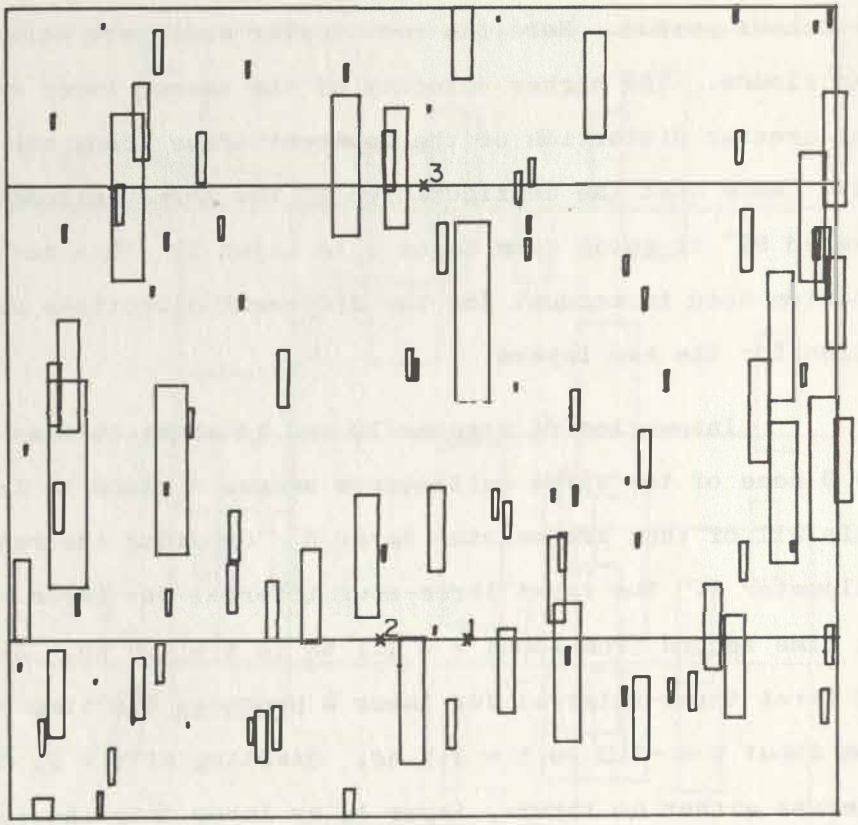

FIGURE 14 PLAN VIEW OF LAYER 2

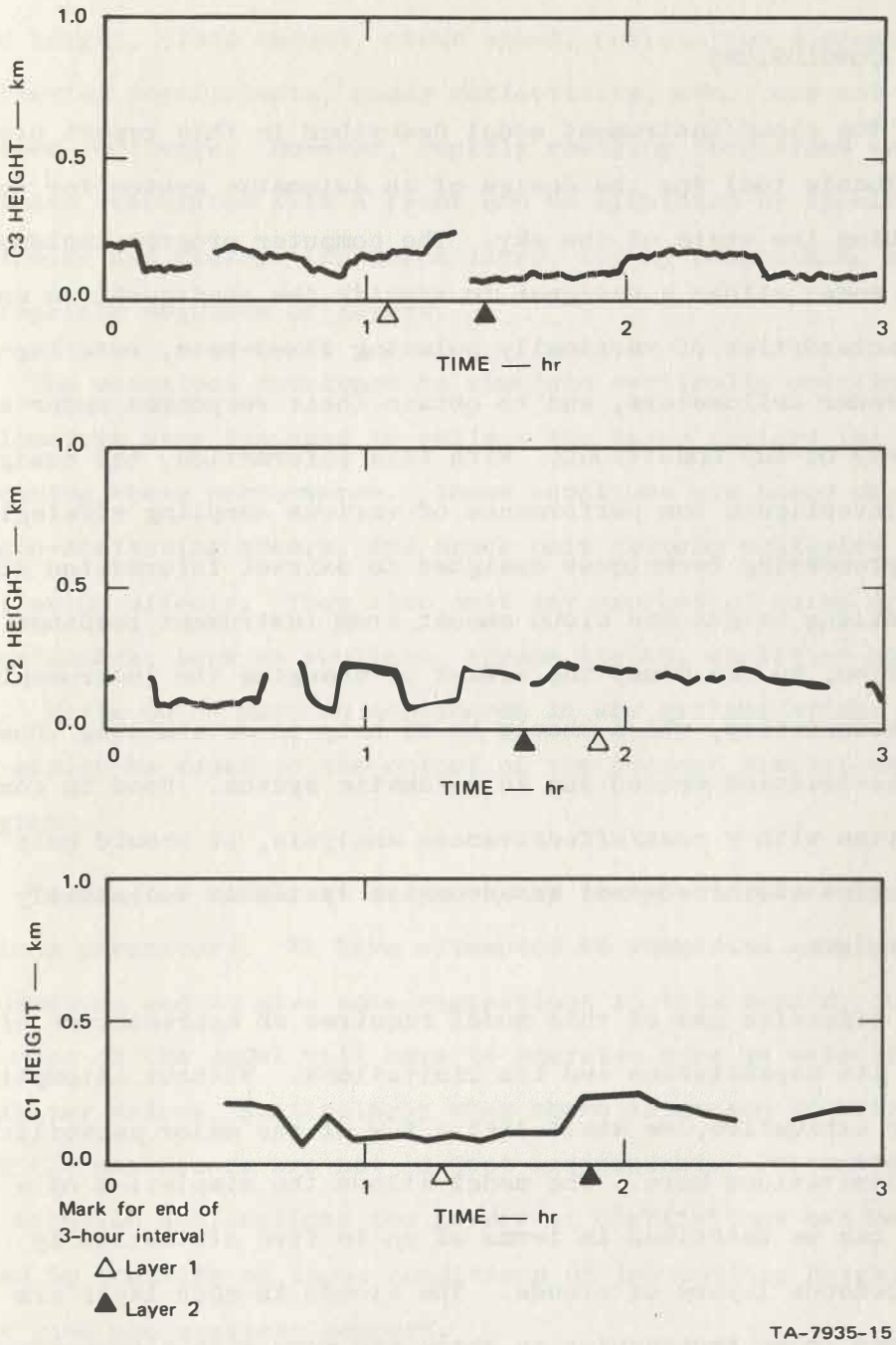

FIGURE 15 PROFILE VIEW: IDEAL CEILOMETER RESPONSES

V CONCLUSIONS

The cloud/instrument model described in this report provides a valuable tool for the design of an automatic system for describing the state of the sky. The computer program implementing this model allows a designer to specify the configuration and characteristics of vertically pointing fixed-beam, rotating-beam, and radar ceilometers, and to obtain their responses under a wide variety of sky conditions. With this information, the designer can investigate the performance of various sampling strategies and processing techniques designed to extract information such as ceiling height and cloud amount from instrument readings. In addition, he can study the effect of changing the instrument characteristics, which should be of help in determining those characteristics needed for an automatic system. Used in conjunction with a cost/effectiveness analysis, it should help determine whether or not an automatic system is technically feasible.

Effective use of this model requires an appreciation of both its capabilities and its limitations. Without attempting to be exhaustive, we shall list a few of the major capabilities and limitations here. The model allows the simulation of a sky that can be described in terms of up to five statistically homogeneous layers of clouds. The clouds in each layer are assumed to be rectangular in shape and move with a common velocity. Random irregularities in size, position, and base height

are allowed, but the parameters for a layer (mean size, mean base height, cloud amount, cloud speed, correlation distance, scattering coefficients, radar reflectivity, etc.) are not allowed to change. However, rapidly changing conditions such as those associated with a front can be simulated by specifying beginning and ending time for a layer, and by programming an appropriate sequence of layers.

The equations developed to simulate vertically pointing ceilometers were designed to reflect the major factors influencing their performance. These equations are based on single-scattering theory, and hence omit certain multiple-scattering effects. They also omit any sources of noise or interference, such as sunlight, strobe lights, amplifier noise, etc. While noise must be considered in any systems study, it can easily be added to the output of the present simulation program.

To use the model, it is necessary to select values for the various parameters. We have attempted to summarize some useful information and to give some suggestions in this regard. However, the user of the model will have to exercise care in selecting parameter values, particularly when there is reason to believe that the parameters are not in fact independent. Fortunately, for aviation applications the number of combinations can be reduced by focusing on those conditions of low ceiling height that give the greatest concern.

Appendix A

STATISTICS OF CLOUD-BASE PROFILES

1. Introduction

All of the ceilometers simulated in our model sample a limited portion of the sky. A given instrument essentially samples a given cloud layer along a vertical plane through the instrument location and in the direction of motion of the clouds. The intersection of this plane with the layer produces the cloud-base profile, a record of the ceiling-height readings of a perfect ceilometer. This cloud-base profile is irregular, with fluctuations about some average or mean value. In this appendix we shall give the equations used to simulate these irregularities, and shall derive their statistical properties.

2. The Base-Height Difference Equation

Let $h(x)$ give the height of the cloud base above a given instrument as a function of distance along the direction of cloud motion. In the computer model, this function is computed for a discrete sequence of points, $x = 0, \Delta x, 2\Delta x, \ldots$. Let $h_k = h(k\Delta x)$. Then the sequence of heights $h_0, h_1, h_2 \ldots$ is generated from the initial height h_0 using the first-order difference equation

$$h_{k+1} = \theta h_k + (1 - \theta)\bar{h} + \sigma_b\sqrt{1 - \theta^2}\, u_k \qquad \text{(A-1)}$$

where

$$\theta = e^{-\Delta x/d} \tag{A-2}$$

Δx = Spatial sampling interval

d = Correlation distance

$\bar{h}$ = Mean base height

σ_b = Standard deviation for base height

u_k = k^{th} random disturbance.

The term θh_k links previous base heights and is responsible for continuity, or, more precisely, for correlation along the cloud-base profile. If the correlation distance d is very large, θ approaches unity and the base height changes very slowly. If the correlation distance is very small, θ approaches zero and the base height fluctuates rapidly with each random disturbance u_k. The random disturbances are assumed to be statistically independent, identically distributed, zero-mean, unit-variance random variables. Thus, if E[u] denotes the expected value of u,

$$E[u_k] = 0 \tag{A-3}$$

$$E[u_k^2] = 1 \tag{A-4}$$

$$E[u_i u_j] = \delta_{ij} \tag{A-5}$$

where δ_{ij} is the so-called Kronecker delta. While some theoretical properties are simplified by giving the u_k a normal distribution, for computational simplicity we assume that the u_k are uniformly distributed from $-\sqrt{3}$ to $\sqrt{3}$.

3. Solution of the Difference Equation

In the following analysis it is somewhat simplier to work with the deviations $z_k = h_k - \bar{h}$ than with the base heights themselves. It follows at once from Eq. (A-1) that

$$z_{k+1} = \theta z_k + \sigma_b \sqrt{1 - \theta^2}\, u_k \quad . \tag{A-6}$$

It is a straightforward matter to solve this difference equation and obtain

$$z_n = \theta^n z_0 + \sigma_b \sqrt{1 - \theta^2} \sum_{k=0}^{n-1} \theta^k u_{n-1-k} \quad . \tag{A-7}$$

Since $0 < \theta < 1$, this solution shows that the effect of the initial value z_0 eventually becomes negligible, and that z_n approaches an exponentially weighted sum of statistically independent random variables. It might be thought that the central-limit theorem immediately implies that the distribution of z_n is asymptotically normal. Strictly speaking, however, this is not true as long as $\theta < 1$. Since $u_k \leq \sqrt{3}$,

$$z_n \le \theta^n z_0 + \sigma_b\sqrt{1 - \theta^2}\,\sqrt{3}\sum_{k=0}^{n-1}\theta^k$$

$$\le \theta^n z_0 + \sigma_b\sqrt{1 - \theta^2}\,\sqrt{3}\,\frac{1 - \theta^n}{1 - \theta}$$

$$\le \theta^n z_0 + \sqrt{3}\,\sigma_b\sqrt{\frac{1 + \theta}{1 - \theta}} \quad .$$

Thus, for small θ, z_n may never significantly exceed $\sqrt{3}\,\sigma_b$, so that its distribution is certainly not normal. It is true, however, that as θ approaches unity the distribution of z_n becomes asymptotically normal. From Eq. (A-2) we see that to use a normal approximation the basic requirement is that the spatial sampling interval Δx be small relative to the correlation distance d.

4. Base-Height Means and Variances

Let $\bar{z}_n$ and σ_k^2 be the mean and the variance of z_k, respectively. Then, from Eqs. (A-3) and (A-7),

$$\bar{z}_n = \theta^n z_0 \qquad \text{(A-8)}$$

and

$$\sigma_n^2 = E\left[\left(z_n - \theta^n z_0\right)^2\right]$$

$$\sigma_n^2 = E\left[\theta^{2n}\left(z_0 - \bar{z}_0\right)^2\right] + E\left[2\theta^n z_0 \sigma_b \sqrt{1 - \theta^2} \sum_{k=0}^{n-1} \theta^k u_{n-1-k}\right] + E\left[\sigma_b^2\left(1 - \theta^2\right) \sum_{i=0}^{n-1} \sum_{j=0}^{n-1} \theta^{i+j} u_{n-1-i} u_{n-1-j}\right] .$$

Assuming that the disturbances u_k are independent of the initial deviation z_0 and using Eq. (A-5) we obtain

$$\sigma_n^2 = \theta^{2n}\sigma_0^2 + \sigma_b^2\left(1 - \theta^2\right)\sum_{i=0}^{n-1} \theta^{2i}$$

$$= \sigma_b^2 + \theta^{2n}\left(\sigma_0^2 - \sigma_b^2\right) . \qquad \text{(A-9)}$$

There are two different simple assumptions that can be made about the distribution of the initial deviation z_0. One is that it has mean zero and variance σ_b^2, in which case z_n also has mean zero and variance σ_b^2 for all n. The other assumption is that z_0 is known exactly, so that $\sigma_0 = 0$. In this case, z_n asymptotically approaches the mean-zero variance-σ_b^2 condition. Although slightly more cumbersome mathematically, this is the situation that prevails in the computer simulation, where we arbitrarily take $z_0 = 0$.

Since $h_n = \bar{h} + z_n$, the base-height mean and variance is given by

$$E\left[h_n\right] = \bar{h}_n = \bar{h} + \bar{z}_n = \bar{h} + \theta^n\left(\bar{h}_0 - \bar{h}\right) \qquad \text{(A-10)}$$

and

$$E\left[\left(h_n - \bar{h}_n\right)^2\right] = E\left[\left(z_n - \bar{z}_n\right)^2\right]$$

$$= \sigma_n^2 = \sigma_b^2 + \theta^{2n}\left(\sigma_0^2 - \sigma_b^2\right) \quad . \qquad \text{(A-11)}$$

Thus, the base-height mean approaches $\bar{h}$ and the base-height variance approaches σ_b^2 asymptotically. If the initial height h_0 has mean $\bar{h}$ and variance σ_b^2, then so do all succeeding base heights. In the computer model we take $h_0 = \bar{h}$ and $\sigma_0 = 0$, so that $\bar{h}$ is the true mean base height, but the variance only approaches σ_b^2 asymptotically:

$$E\left[\left(h_n - \bar{h}\right)^2\right] = \sigma_b^2\left(1 - \theta^{2n}\right) \quad . \qquad \text{(A-12)}$$

This equation forms a basis for comparing the model to the experimental results reported by Davis (1969). Davis measured the standard deviation of the difference between the lowest cloud base at one time and the lowest cloud base at periods of from 1 to 15 minutes later. This corresponds exactly to the situation where $\sigma_0 = 0$ and $\sigma_n^2 = \sigma_b^2(1 - \theta^{2n})$. Thus, if we assume that the clouds are moving with velocity v and measure the variance at time t_n, where

$$t_n = \frac{x_n}{v} = \frac{n\Delta x}{v} \qquad \text{(A-13)}$$

we have from Eq. (A-2) that

$$\theta^{2n} = e^{-2n\Delta x/d}$$

$$= e^{-2vt_n/d} \qquad \text{(A-14)}$$

and hence that

$$\sigma_n^2 = \sigma_b^2\left[1 - e^{-2vt_n/d}\right] \quad . \qquad \text{(A-15)}$$

With proper choices for σ_b and v/d, this result appears to be in good general agreement with the data reported by Davis. It also suggests the use of data such as those of Davis for selecting values for such parameters as σ_b and d.

5. Base-Height Autocorrelation Function

Let us now calculate the autocorrelation function R_{mn} for the base height under the assumption that $h_0 = \bar{h}$ and $\sigma_0 = 0$. By definition,

$$R_{mn} = E\left[h_m h_n\right]$$

$$= E\left[\left(\tilde{h} + z_m\right)\left(\tilde{h} + z_n\right)\right]$$

$$= h^{-2} + E\left[z_m z_n\right] \qquad \text{(A-16)}$$

since $\bar{z}_m = \bar{z}_n = 0$ if $h_0 = \bar{h}$. Now, from Eq. (A-7),

$$z_n = \sigma_b\sqrt{1 - \theta^2} \sum_{k=0}^{n-1} \theta^k u_{n-1-k}$$

so that

$$z_m z_n = \sigma_b^2\left(1 - \theta^2\right)\sum_{i=0}^{m-1}\sum_{j=0}^{n-1} \theta^{i+j} u_{m-1-i} u_{n-1-j} \quad . \tag{A-17}$$

Thus, from Eq. (A-5)

$$E\left[z_m z_n\right] = \begin{cases} \sigma_b^2\left(1 - \theta^2\right)\sum_{j=0}^{n-1} \theta^{2j+m-n} & m \geq n \\ \sigma_b^2\left(1 - \theta^2\right)\sum_{i=0}^{m-1} \theta^{2i+n-m} & m < n \end{cases}$$

$$= \sigma_b^2 \theta^{|m-n|}\left(1 - \theta^{2\min(m,n)}\right) \tag{A-18}$$

where min(m,n) is the smaller of m and n. Thus the autocorrelation function is given by

$$R_{mn} = \bar{h}^2 + \sigma_b^2\, \theta^{|m-n|}\left(1 - \theta^{2\min(m,n)}\right) \tag{A-19}$$

which asymptotically approaches the exponential form $\bar{h}^2 + \sigma_b^2\theta^{|m-n|}$. To relate this to the autocorrelation function for the continuous base height,

$$R(\zeta) = E[h(x + \zeta)h(x)] \qquad \text{(A-20)}$$

we take $x + \zeta = m\Delta x$ and $x = n\Delta x$ so that

$$m - n = \frac{\zeta}{\Delta x} \quad . \qquad \text{(A-21)}$$

Then, from Eqs. (A-2) and (A-19), the asymptotic form for $R(\zeta)$ is

$$R(\zeta) = \bar{h}^2 + \sigma_b^2 e^{-|\zeta|/d} \qquad \text{(A-22)}$$

6. Summary

The ceiling base height is generated recursively using the first-order difference equation

$$h_{k+1} = \theta h_k + (1 - \theta)\bar{h} + \sigma_b \sqrt{1 - \theta^2}\, u_k \qquad \text{(A-1)}$$

where

$$\theta = e^{-\Delta x/d} \qquad \text{(A-2)}$$

Δx = Spatial sampling interval

d = Correlation distance

$\bar{h}$ = Mean base height

σ_b = Standard deviation for base height

u_k = Zero-mean, unit variance random disturbance.

If the spatial sampling interval is small relative to the correlation distance so that θ is near unity, the resulting ceiling heights are approximately jointly normally distributed with mean $\bar{h}$ and autocorrelation function

$$R_{mn} = E\left[h_m h_n\right] \cong \bar{h}^2 + \sigma^2 \theta^{|m-n|}$$

or

$$R(\zeta) = E\left[h(x + \zeta)h(x)\right] \cong \bar{h}^2 + \sigma_b^2 e^{-|\zeta|/d} \quad . \qquad \text{(A-22)}$$

This is an asymptotic result, obtained under the assumption that $\theta^m \ll 1$ and $\theta^n \ll 1$. For small m and n, the standard initial condition $h_0 = \bar{h}$ constrains the succeeding base heights, reducing the variance of h_n^2 from σ_b^2 to

$$E\left[h_n - \bar{h}^2\right] = \sigma_b^2\left(1 - \theta^{2n}\right) \qquad \text{(A-12)}$$

$$= \sigma_b^2\left[1 - e^{-2vt_n/d}\right] \qquad \text{(A-15)}$$

where v is the cloud velocity and t_n is the n^{th} observation time. This result can be used to estimate the parameters σ_b and d from data such as those reported by Davis (1969).

Appendix B

SIMULATION OF OPTICAL CEILOMETERS

1. Introduction

Our statistical cloud model produces a sky containing several layers of clouds passing over a configuration of ceilometers. Any given ceilometer senses the sky conditions in its immediate vicinity, producing a trace related to the ceiling height. The exact response of the ceilometer depends on a variety of factors involving both the characteristics of the instrument and the physical characteristics of the clouds. In this appendix we shall derive the equations to be used in simulating the major characteristics of fixed-beam and rotating-beam ceilometers.

2. Qualitative Characteristics

The basic geometry for a fixed-beam ceilometer is shown in Figure B-1. The transmitter projects light into the cloud, illuminating a region near the cloud base. A portion of the scattered light is picked up by the receiver, which scans along the transmitter beam. The light received normally reaches a maximum near $\theta = \tan^{-1} h/a$, and thus h can be estimated as $a\tan\theta$.

One disadvantage of rotating the receiver is that the mechanical vibration is picked up by the sensitive photodetector. Another disadvantage is that other light sources can be intercepted,

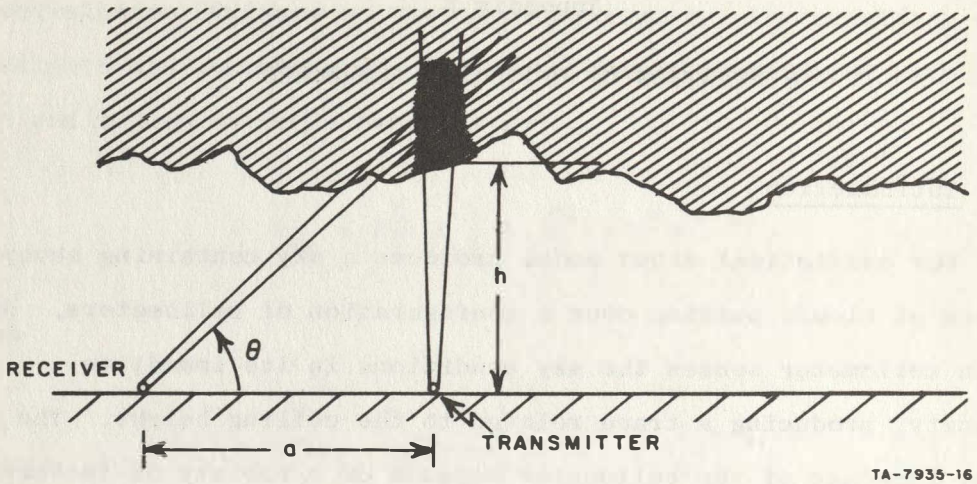

FIGURE B-1 SIDE VIEW OF A FIXED-BEAM CEILOMETER

resulting in false responses. The rotating-beam ceilometer eliminates these problems by interchanging the receiver and the transmitter, rotating the transmitting beam rather than the receiver. It also happens that current rotating-beam ceilometers scan more rapidly than fixed-beam ceilometers. However, the basic principles are essentially the same, and the same analysis holds for both instruments.

The details of the physics of the scattering of light by the water drops in the cloud are extremely complicated. However, a first-order theory based on the assumption that any light scattered is scattered only once gives a computationally feasible approximate solution. Basically, this theory predicts that the luminous flux

entering the cloud will be exponentially attenuated. A certain fraction of the flux within the common volume of the transmitter and receiver beams is scattered back toward the receiver, being further attenuated as it returns through the cloud. In the next sections we set up the general equations based on this single-scattering theory.

3. Basic Relations

Let a point source of light radiate a luminous flux of F lumens through a solid angle ω. If an amount of flux dF passes through an area dA normal to the flow of flux subtending a solid angle $d\omega = dA/r^2$, then the illuminance E and luminous intensity I are given by

$$E = \frac{dF}{dA} \tag{B-1}$$

$$I = \frac{dF}{d\omega} \tag{B-2}$$

so that

$$E = \frac{I}{r^2} \quad . \tag{B-3}$$

When an aerosol is illuminated with incident illuminance E, each volume element dv scatters light and looks like a point source of light. The luminous intensity varies with the polar angle φ, but is independent of θ (see Figure B-2). Specifically,

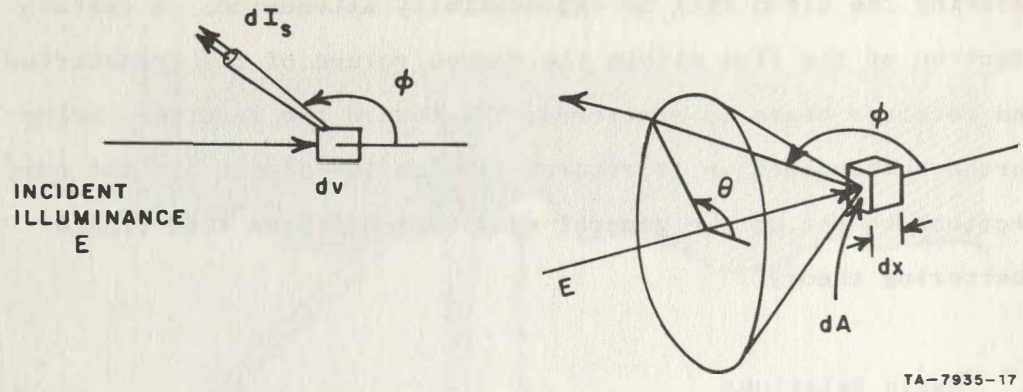

FIGURE B-2 BACKSCATTER FROM A VOLUME ELEMENT

$$dI_s = \beta(\varphi)Edv \tag{B-4}$$

where $\beta(\varphi)$ is the angular volume scattering coefficient and is measured in (steradian-meter)$^{-1}$. The actual value of $\beta(\varphi)$ depends on the wavelength of the light involved, the drop-size distribution, and the index of refraction for water. At this point we shall merely assume that $\beta(\varphi)$ is known.

The total flux scattered dF_s is found by integrating dI_s over a unit sphere. Thus,

$$dF_s = \int_0^{\pi}\int_0^{2\pi} dI_s \sin\varphi d\varphi d\theta$$

$$= \int_0^{\pi}\left[\beta(\varphi)\frac{F}{A}Adx\ 2\pi \sin\varphi d\varphi\right] \tag{B-5}$$

where F is the luminous flux entering the volume element dv = Adx. If we define the volume scattering coefficient σ by

$$\sigma = 2\pi \int_0^{\pi} \beta(\varphi)\sin\varphi d\varphi \qquad \text{(B-6)}$$

we have

$$dF_s = \sigma F dx \quad . \qquad \text{(B-7)}$$

Since this represents flux lost, if we neglect absorption we can write

$$F(x + dx) = F(x) - dF_s \qquad \text{(B-8)}$$

or

$$\frac{dF}{dx} = -\sigma F \qquad \text{(B-9)}$$

so that

$$F(x_1) = F(x_0)e^{-\int_{x_0}^{x_1} \sigma(x)dx} \quad . \qquad \text{(B-10)}$$

Equations (B-4), (B-6), and (B-10) are the key equations. Equation (B-4) shows how incident illuminance is scattered in various directions. Equation (B-10) shows that the flux in a beam

of light decays exponentially due to scattering losses. Equation (B-6) relates the scattering to this decay. If we assume that all of the illuminance E is due to the light beam, and none comes from light scattered elsewhere, we are ignoring multiple scattering effects. We shall make this assumption in the next section when we develop the general equations for fixed-beam and rotating-beam ceilometers.

4. General Ceilometer Equations

Let P be a point within the common volume of the receiver and transmitter cones as shown in Figure B-3, and let I_T be the luminous intensity radiated in the direction of P. If a volume element dv subtends a solid angle $d\omega_T$, the flux received at P is given by

$$dF = I_T d\omega_T e^{-\int_0^r \sigma(r')dr'} \qquad \text{(B-11)}$$

where r' locates a point on the ray from T to P. If we write $d\omega_T = dA/r^2$, the illuminance at P is given by

$$E(r) = \frac{I_T}{r^2} e^{-\int_0^r \sigma(r')dr'} . \qquad \text{(B-12)}$$

By Eq. (B-4), the volume element at P looks like a point source having luminous intensity

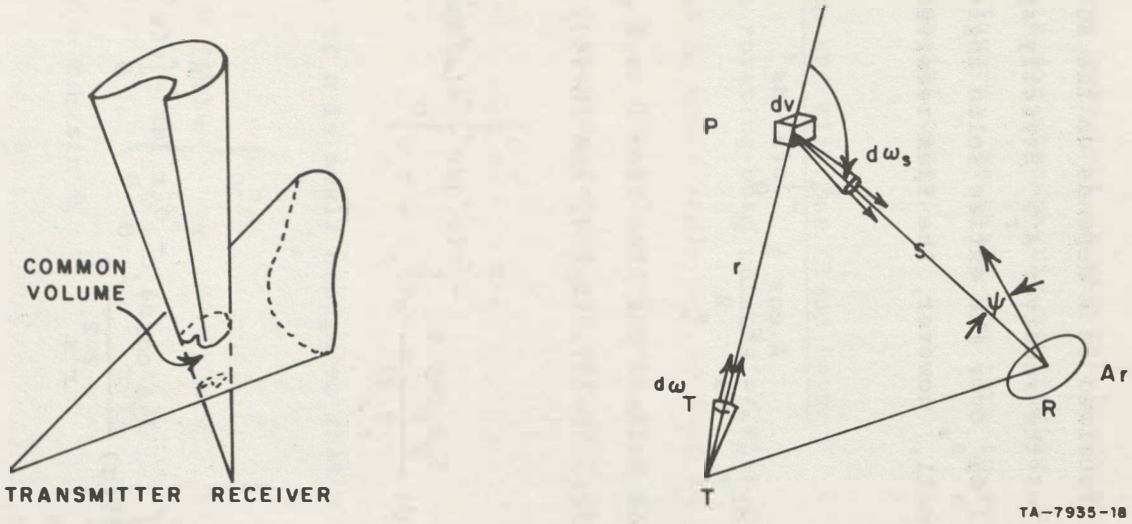

FIGURE B-3 GEOMETRY FOR A GENERAL CEILOMETER

$$dI_s = \beta(\varphi)E(r)dv \quad . \tag{B-13}$$

The amount of flux received at R depends on the solid angle subtended by the area of the receiver A_r. Strictly speaking, we should integrate $dI_s d\omega_s$ over the entire solid angle subtended by A_r. If A_r/s^2 is small,* however, the flux received is given by

$$dF_r = dI_s \frac{A_r \cos \psi}{s^2} e^{-\int_0^s \sigma(s')ds'} \tag{B-14}$$

where ψ is the angle between the line from P to R and the normal to A_r. Combining Eqs. (B-12), (B-13), and (B-14), we have

$$dF_r = \beta(\varphi) \frac{I_T A_r \cos \psi}{r^2 s^2} e^{-\int_0^r \sigma(r')dr' - \int_0^s \sigma(s')ds'} dv$$

and

$$F_r = \iiint_{\text{Common Volume}} \beta(\varphi) \frac{I_T A_r \cos \psi}{r^2 s^2} e^{-\int_0^r \sigma(r')dr' - \int_0^s \sigma(s')ds'} dv \tag{B-15}$$

---

*If we allow very low clouds and very low points P, this approximation breaks down. These equations then yield erroneously large values for the received flux. In using these equations, $A_r \cos \psi/s^2$ should never be allowed to exceed 2π.

This is the general equation for the received flux for both rotating-beam and fixed-beam ceilometers. Since the scattering coefficients have been left as general functions of position, this equation accounts for atmospheric scattering, precipitation, and multiple cloud layers. We shall now turn to evaluating this integral for some special cases.

5. Narrow-Beam RBC With One Cloud Layer

Consider a rotating-beam ceilometer with a very narrow transmitting beam having solid angle ω_T, so that if a flux F_T is transmitted, $I_T \cong F_T/\omega_T$. The volume element $dv = \omega_T r^2 dr$ (see Figure B-4). Because σ changes from σ_0 in air to σ_1 in the cloud,

$$\int_0^r \sigma(r')dr' = \begin{cases} \sigma_o r & r < r_0 \\ \sigma_o r + \sigma_1(r - r_0) & , \quad r > r_0 \end{cases} .$$

Similarly, if α is small enough so that $s \cong h$,

$$\int_0^s \sigma(s')ds' = f(h) = \begin{cases} \sigma_o h & , \quad h < h_0 \\ \sigma_0 h + \sigma_1(h - h_0) & , \quad h > h_0 \end{cases} .$$

Furthermore, if $r \cong h/\sin\theta$,

$$e^{-\int_0^r \sigma(r')dr' - \int_0^s \sigma(s')ds'} = e^{-f(h)\left(\frac{1}{\sin\theta} + 1\right)} .$$

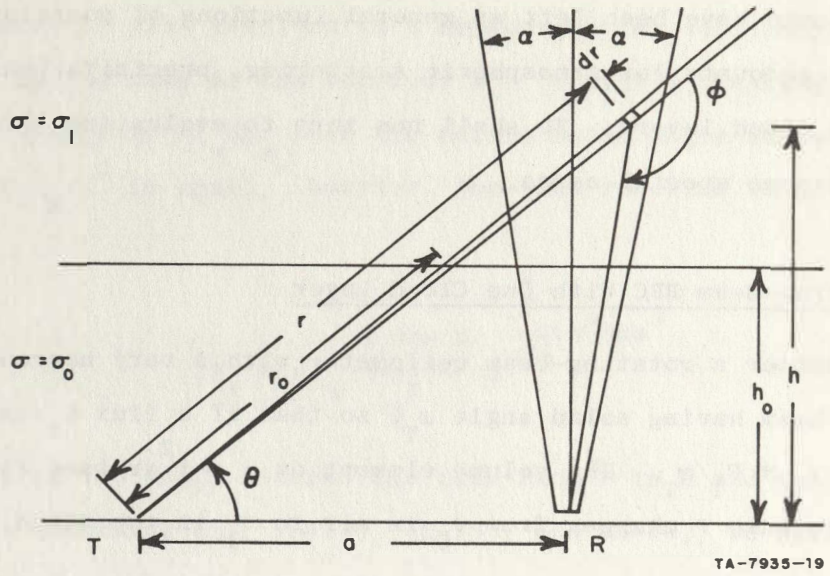

FIGURE B-4 GEOMETRY FOR A NARROW-BEAM ROTATING-BEAM CEILOMETER

Finally, taking $\psi = 0$ and $\varphi \cong \pi/2 + \theta$, we have from Eq. (B-15)

$$F_r = \int_{\substack{\text{Common}\\ \text{Volume}}} \beta\left(\frac{\pi}{2} + \theta\right) \frac{F_T/\omega_T}{r^2 h^2} A_r e^{-f(h)\left(\frac{1}{\sin\theta}+1\right)\omega_T r^2} dr$$

$$= F_T A_r \int_{h_1}^{h_2} \beta\left(\frac{\pi}{2} + \theta\right) \frac{1}{h^2} e^{-f(h)\left(\frac{1}{\sin\theta}+1\right)} \frac{dh}{\sin\theta}$$

where h_1 and h_2 are the heights at which the transmitted beam enters and leaves the receiver cone, respectively. Note that both β and σ vary with H.

An exact evaluation of this integral is difficult. We must consider three cases:

$$\text{Case 1: } h_2 < h_0$$

$$\text{Case 2: } h_1 < h_0 < h_2$$

$$\text{Case 3: } h_0 < h_1 \quad .$$

In Case 1 all received flux is due to air scattering. The equation for F_r breaks down for small θ because of the solid-angle approximation $A_r \cos \psi / s^2$, and must be interpreted with care. If it is presumed that β is negligibly small for $h < h_0$, F_r can be neglected for Case 1.

If σ_1 is significantly greater than σ_0, Case 2 represents a transitional phase in which the received flux builds up to a peak at $h_1 = h_0$. For Case 3, a small-angle approximation for α gives

$$h_2 = a \tan \theta (1 + \alpha \tan \theta)$$

$$h_1 = a \tan \theta (1 - \alpha \tan \theta)$$

and if we assume that the $1/h^2$ factor in the integral is roughly $1/a^2 \tan^2 \theta$, we obtain the approximate solution

$$F_r \cong \frac{2\beta\left(\frac{\pi}{2} + \theta\right) F_T A_r e^{-\sigma_0 h_0 \left(\frac{1}{\sin \theta}+1\right)}}{\sigma_1 a^2 \tan^2 \theta \left(1 + \sin \theta\right)} e^{-\sigma_1 (a \tan \theta - h_0)\left(\frac{1}{\sin \theta}+1\right)}$$

$$\times \sinh\left[\sigma_1 a \alpha \tan^2 \theta \left(\frac{1}{\sin \theta} + 1\right)\right] \quad .$$

Basically, this quantity is near its peak when $h_1 = h_0$--i.e., when

$$\theta = \theta_0 + \Delta\theta$$

where $\tan \theta_0 = h_0/a$ and $\Delta\theta \cong \alpha \sin^2 \theta_0$. It decays roughly exponentially for larger values of θ at a rate set by a σ_1.

In summary, the response for a narrow-beam rotating-beam ceilometer is shown in Figure B-5, where

$$\theta_0 = \tan^{-1} \frac{h_0}{a}$$

$$\theta_{min} = \theta_0 - \alpha \sin^2 \theta_0$$

$$\theta_{max} = \theta_0 + \alpha \sin^2 \theta_0$$

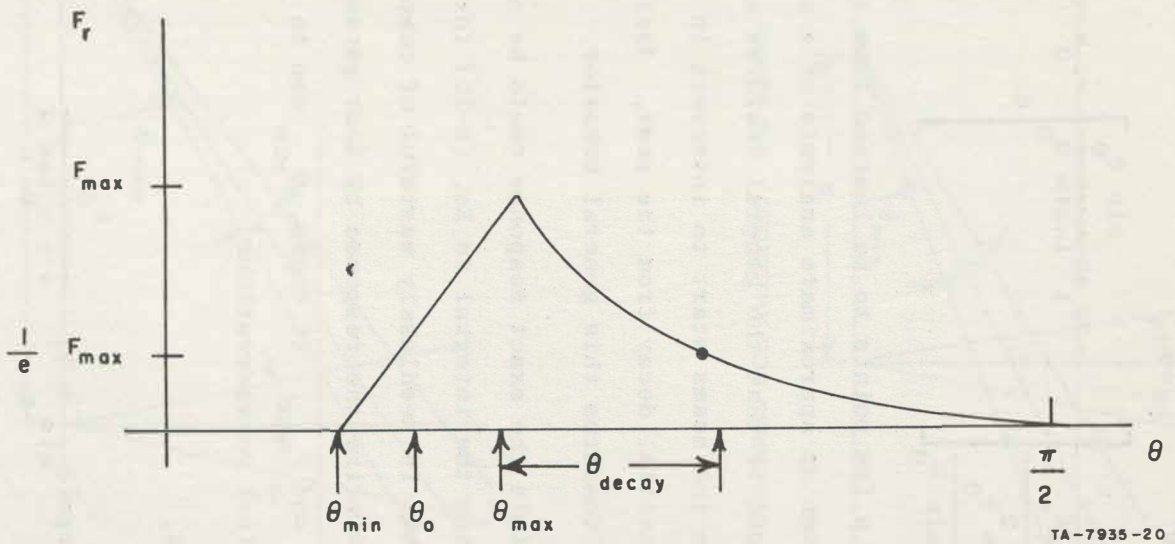

FIGURE B-5 CEILOMETER RESPONSE CURVE

$$\theta_{decay} = \frac{1}{a\sigma_1} \sin\theta_0(1 - \sin\theta_0)$$

$$F_{max} = \frac{\beta\left(\theta + \frac{\pi}{2}\right)F_T A_r}{\sigma_1 a^2 \frac{\sin^2\theta_0}{1 - \sin\theta_0}}\left[1 - e^{-2\sigma_1 a\alpha\frac{\sin\theta_0}{1-\sin\theta_0}}\right] e^{-\sigma_0 a \tan\theta_0 \frac{1+\sin\theta_0}{\sin\theta_0}}$$

There are only a few points to be learned from this analysis. The first is that even an approximate analysis of a simple case is difficult. The second is that the general features are clear--a rapid buildup when the beams start to intersect in the cloud, followed by an exponential decay from the peak. Analysis of other special cases confirms this general behavior.

While in principle the exact response could be obtained by numerically evaluating the integral in Eq. (B-15) for every value of θ, in practice this is needlessly wasteful of computing time. We propose to characterize the response by four parameters: θ_{min}, θ_{max}, θ_{decay}, and F_{max}. Of these, θ_{min} can be computed from simple geometrical considerations.

From Figure B-6,

$$\tan(\theta_{min} + \gamma) = \frac{h_0}{a + h_0 \tan\alpha}$$

or, using small-angle approximations,

$$\theta_{min} = \theta_0 - (\alpha \sin^2\theta_0 + \gamma) \quad , \qquad \text{(B-16)}$$

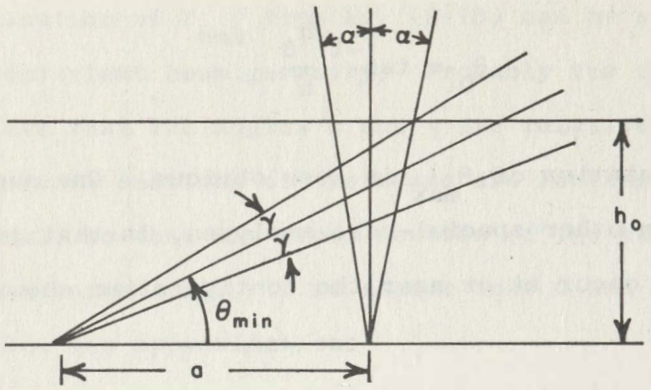

FIGURE B-6 GEOMETRY FOR COMPUTING θ_{min}

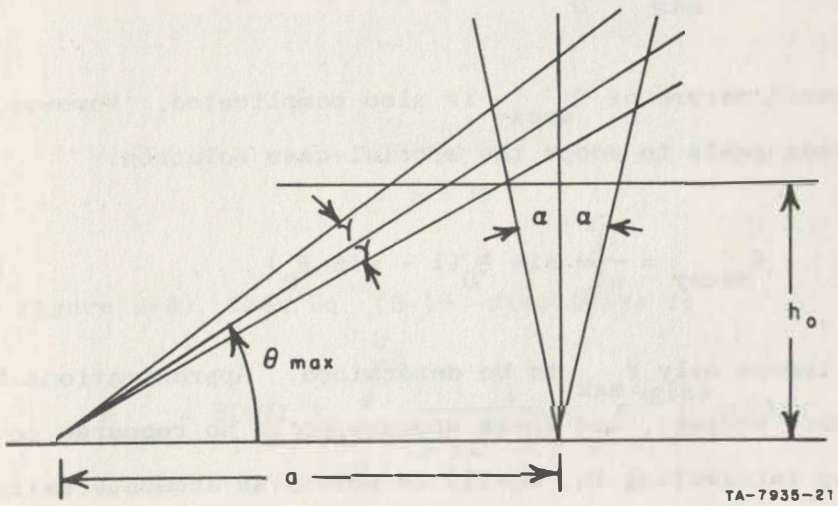

FIGURE B-7 GEOMETRY FOR COMPUTING θ_{max}

where

$$\theta_0 = \tan^{-1} \frac{h_0}{a} \quad . \tag{B-17}$$

The calculation of θ_{max} is less obvious. One suggestion, resulting from other special-case analyses, is that the maximum response will occur at or near the configuration shown in Figure B-7. Thus,

$$\tan(\theta_{max} - \gamma) = \frac{h_0}{a - h_0 \tan \alpha}$$

so that

$$\theta_{max} = \theta_0 + (\alpha \sin^2 \theta + \gamma) \quad . \tag{B-18}$$

The exact nature of θ_{decay} is also complicated. However, it seems reasonable to adopt the special-case solution:

$$\theta_{decay} = \frac{1}{a\sigma_1} \sin \theta_0 (1 - \sin \theta_0) \quad . \tag{B-19}$$

This leaves only F_{max} to be determined. Approximations here are much more suspect, and there appears to be no recourse to numerically integrating Eq. (B-15) to obtain an accurate estimate. In the next section we shall simplify this triple integral to a single integral, however.

6. Calculation of the Maximum Response

The evaluation of F_{max} from Eq. (B-15) can be simplified by assuming a convenient beam geometry. Probably the simplest assumptions are that the angles α and γ are relatively small, and that the cross sections of the beams are rectangular rather than elliptical, so that any cross section of the common volume is a polygon of area A(h). If we assume that α and γ are small enough to allow the approximations

$$s = h \tag{B-20}$$

$$r = \left(h^2 + a^2\right)^{1/2} \tag{B-21}$$

$$\varphi = \frac{\pi}{2} + \theta \tag{B-22}$$

and

$$\psi = 0 \tag{B-23}$$

(see Figure B-8), then Eq. (B-15) simplifies to

$$F_{max} = \beta(\varphi) I_T A_r \int_{h_0}^{h_3} \frac{1}{h^2(h^2 + a^2)} e^{-g(h)} A(h)dh \tag{B-24}$$

where

$$g(h) = \left[\sigma_0 h_0 + \sigma_1 (h - h_0)\right]\left[1 + \frac{\left(h^2 + a^2\right)^{1/2}}{h}\right] . \tag{B-25}$$

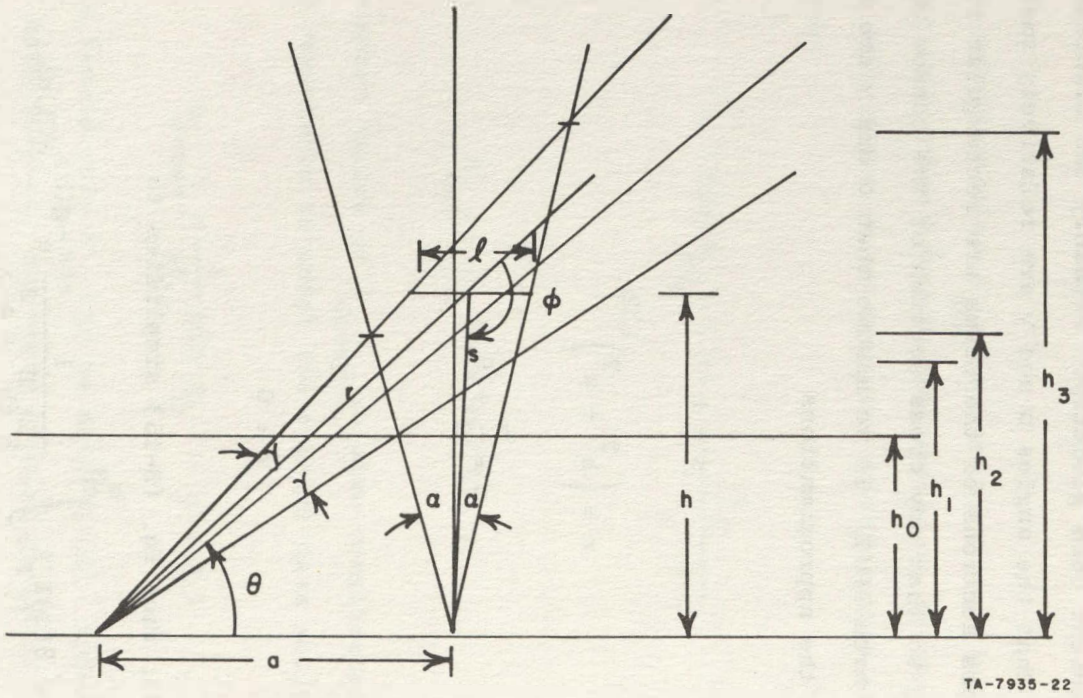

FIGURE B-8 GEOMETRY FOR COMPUTING F_{max}

We now turn to the calculation of A(h), the area of a cross section of the common volume. This calculation is simple but tedious due to the number of special cases that must be considered. The cross section of the common volume is the intersection of the cross sections of the receiver cone and the transmitter cone, and these can overlap each other in various ways.

The cross section of the receiver cone is a rectangle with the dimensions shown in Figure B-9. Assuming that α and α' are small, the area is approximately $4h^2\alpha\alpha'$, corresponding to a solid angle of approximately $4\alpha\alpha'$.

The cross section of the transmitter cone is a trapezoid, shown in Figure B-10, with

$$\ell_T(h) = \frac{h}{\tan(\theta - \gamma)} - \frac{h}{\tan(\theta + \gamma)} \qquad \text{(B-26)}$$

$$\cong 2h\gamma/\sin^2\theta \qquad \text{(B-27)}$$

for small γ. Thus the area is approximately $4h^2\gamma\gamma'/\sin^3\theta$, which agrees with the fact that the solid angle is approximately $4\gamma\gamma'$.

In the following analysis we shall treat the cross section of the transmitter cone as if it were a rectangle of length ℓ_t and width w_T, where

$$w_T(h) = \frac{2h\gamma'}{\sin\theta} \quad . \qquad \text{(B-28)}$$

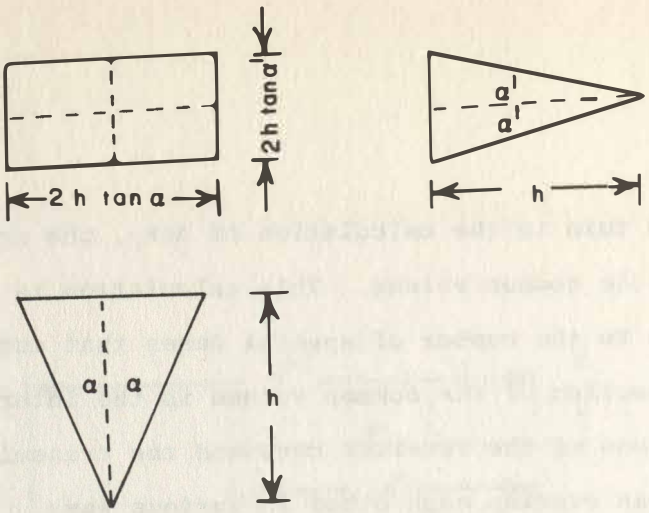

FIGURE B-9 PLAN AND ELEVATION VIEWS OF RECEIVER CONE

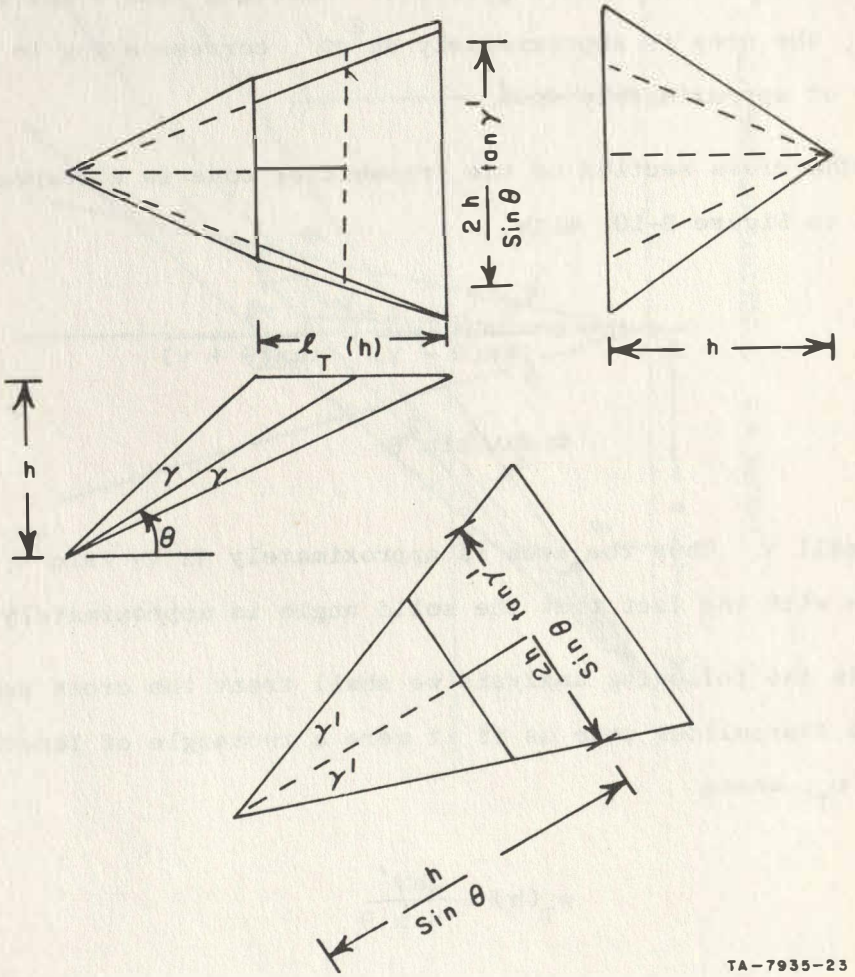

FIGURE B-10 VIEWS OF THE TRANSMITTER CONE

The cross section of the common volume is then a rectangle of length ℓ and width w. Clearly,

$$w(h) = \min\left(2h\alpha', \frac{2h\gamma'}{\sin\theta}\right) . \tag{B-29}$$

That is,

$$w(h) = \begin{cases} 2h\alpha' & , \text{ if } \sin\theta < \frac{\gamma'}{\alpha'} \\ \frac{2h\gamma'}{\sin\theta} & , \text{ if } \sin\theta > \frac{\gamma'}{\alpha'} \end{cases} . \tag{B-30}$$

Clearly, if $\gamma' > \alpha'$, then w(h) is always given by $2h\alpha'$. However, this corresponds to the unusual case in which the transmitting beam is broader than the receiving beam, and ordinarily there will be a crossover angle.

As can be seen from Figure B-8, there are three distinct zones for computing the length $\ell(h)$, depending on whether h is between h_0 and h_1, h_1 and h_2, or h_2 and h_3. To complicate things further, if α is sufficiently small relative to γ, h_2 can be less than h_1. It can be shown that $h_2 > h_1$ if

$$3\tan\alpha + \frac{1}{\tan(\theta + \gamma)} < \frac{a}{h_0} \tag{B-31}$$

or, for small γ, if

$$\gamma\left[1 + \left(\frac{a}{h_0}\right)^2\right] > \alpha . \tag{B-32}$$

Thus, if $\gamma > \alpha$, then h_2 is always greater than h_1. However, this is the unusual case, and generally there will be a crossover value of h_0. Exact equations for h_1, h_2, and h_3 can be derived from the geometry and the relation defining our assumed condition for maximum response:

$$\tan(\theta - \gamma) = \frac{h_0}{a - h_0 \tan \alpha} \tag{B-33}$$

which gives

$$\tan \theta = \frac{h_0 + (a - h_0 \tan \alpha)\tan \gamma}{a - h_0(\tan \alpha + \tan \gamma)} \quad . \tag{B-34}$$

The results for h_1, h_2, and h_3 are as follows:

$$h_1 = \frac{ah_0}{a - 2h_0 \tan \alpha} \tag{B-35}$$

$$h_2 = \frac{a \tan(\theta + \gamma)}{1 + \tan \alpha \tan (\theta + \gamma)} \tag{B-36}$$

$$h_3 = \frac{a \tan(\theta + \gamma)}{1 - \tan \alpha \tan(\theta + \gamma)} \tag{B-37}$$

where

$$\tan(\theta + \gamma) = \frac{\tan(\theta - \gamma) + \tan 2\gamma}{1 - \tan(\theta - \gamma)\tan 2\gamma} \quad . \tag{B-38}$$

These expressions are awkward to deal with and can be simplified by the usual small-angle approximations to yield

$$h_1 = h_0 + \frac{2h_0^2}{a}\alpha \qquad \text{(B-39)}$$

$$h_2 = h_0 + \frac{2(h_0^2 + a^2)}{a}\gamma \qquad \text{(B-40)}$$

$$h_3 = h_0 + \frac{2}{a}\left[h_0^2\alpha + (h_0^2 + a^2)\gamma\right] \quad . \qquad \text{(B-41)}$$

It should be remarked at this point that these small-angle approximations can break down for large θ. In particular, h_3 is infinite when $\theta + \gamma + \alpha = \pi/2$, a fact that is recognized in Eq. (B-37) but not in Eq. (B-41). However, since scattering from the top of the common volume contributes little to F_{max}, this is probably not significant. In fact, the approximations given above are probably preferable for numerical treatment.

The values for $\ell(h)$ can now be computed from the geometry of Figure B-8.

Case 1: $h_2 > h_1$

$$\ell(h) = \begin{cases} \dfrac{h - h_0}{h_0}\, a & h_0 < h < h_1 \\ 2h\alpha & h_1 < h < h_2 \\ a - h\left[\dfrac{a}{h_0} - 2\alpha - \left(1 + \left(\dfrac{a}{h_0}\right)^2\right)2\gamma\right] & h_2 < h < h_3 \end{cases}$$

Case 2: $h_1 > h_2$

$$\ell(h) = \begin{cases} \dfrac{h - h_0}{h_0}\, a & , \quad h_0 < h < h_2 \\ 2h\left[1 + \left(\dfrac{a}{h_0}\right)^2\right]\gamma & , \quad h_2 < h < h_1 \\ a - h\left[\dfrac{a}{h_0} - 2\alpha - \left(1 + \left(\dfrac{a}{h_0}\right)^2\right)2\gamma\right] & , \quad h_1 < h < h_3 \end{cases} .$$

This essentially completes the analysis for the maximum response for the rotating-beam ceilometer. F_{max} is found by integrating as indicated in Eq. (B-24), where I_T is essentially $F_T/4\gamma\gamma'$, g(h) is given by Eq. (B-25), A(h) is given by the product of the w(h) of Eq. (B-30) and $\ell(h)$ of Eqs. (B-42) and (B-43), and h_1, h_2, and h_3 are given by Eqs. (B-39), (B-40), and (B-41).

So far we have done our calculations assuming a rotating-beam ceilometer configuration. However, the general equation for the flux received, Eq. (B-15), is the same for fixed-beam and rotating-beam ceilometers. Furthermore, the geometry is the same, provided only that we now associate γ with the receiver and α with the transmitter. In fact, the only thing that changes is that the transmitted luminous intensity I_T is now computed as $F_T/4\alpha\alpha'$ rather than $F_T/4\gamma\gamma'$. This is significant, since it indicates that for maximum response it is $\alpha\alpha'$ rather than $\gamma\gamma'$ that we want to be as small as possible.

Another significant point is that the cloud layer may be so thin that the final intersection point at h_3 is outside of the

cloud. What this really means is that our expression for g(h) given by Eq. (B-25) is incorrect, since σ drops back to σ_0 above the cloud. An approximate, but probably adequate solution is to stop the integration in Eq. (B-24) at the top of the cloud.

Finally, there is the matter of light penetrating a lower layer and being scattered from a higher layer. Again, the solution is given by integrating Eq. (B-24), provided that the correct expression is used for g(h). If σ^* is the volume scattering coefficient in the lower layer of thickness t^*, a reasonable approximation for the correct g(h) is

$$g^*(h) = g(h) + (\sigma^* - \sigma_0)t^*\left(\frac{1}{\sin\theta} + 1\right) \quad . \qquad \text{(B-44)}$$

Thus F_{max} can be obtained by integrating Eq. (B-24) as it stands and multiplying the final result by the factor

$$e^{-(\sigma^*-\sigma_0)t^*\left(\frac{1}{\sin\theta}+1\right)} \quad . \qquad \text{(B-45)}$$

7. Precipitation and Refraction Effects

Throughout this treatment we have tacitly assumed that β does not change very rapidly with φ in the vicinity of the maximum response. Furthermore, we have assumed that σ_1 is sufficiently larger than σ_0 to cause the maximum response to occur near the base of the cloud. When the ceilometer response is due to precipitation, neither of these conditions holds.

While the general equations hold for precipitation as well as for clouds, the point of maximum response is primarily determined by β. Typically, $\beta(\varphi)$ shows a pronounced peak near $\varphi = 139^\circ$ ($\theta = 49^\circ$). The exact angle for peak response varies with wavelength, which is the well-known cause of rainbows. As usual, an exact integration of Eq. (B-15) is very difficult. However, a reasonable approximate solution can be obtained by taking $\beta(\varphi)$ outside the integral and by writing

$$F_r = \frac{\beta(\varphi)}{\beta(\varphi_{max})} F_{max} , \qquad (B-46)$$

where φ_{max} is the angle for which β is maximum, and F_{max} is the value of F_r at $\theta = \theta_{max} = \varphi_{max} - \pi/2$. A little thought shows that F_{max} can be computed exactly as described in the previous section, provided that h_0 is determined from

$$h_0 = a \tan \theta_{max} - \alpha a \tan^2 \theta_{max} - \gamma a \sec^2 \theta_{max} \qquad (B-47)$$

and that a precipitation value for σ is substituted for both σ_0 and σ_1.

8. Summary

The basic results of this analysis are summarized below. The geometrical parameters are illustrated in Figures B-11, B-12, and B-13.

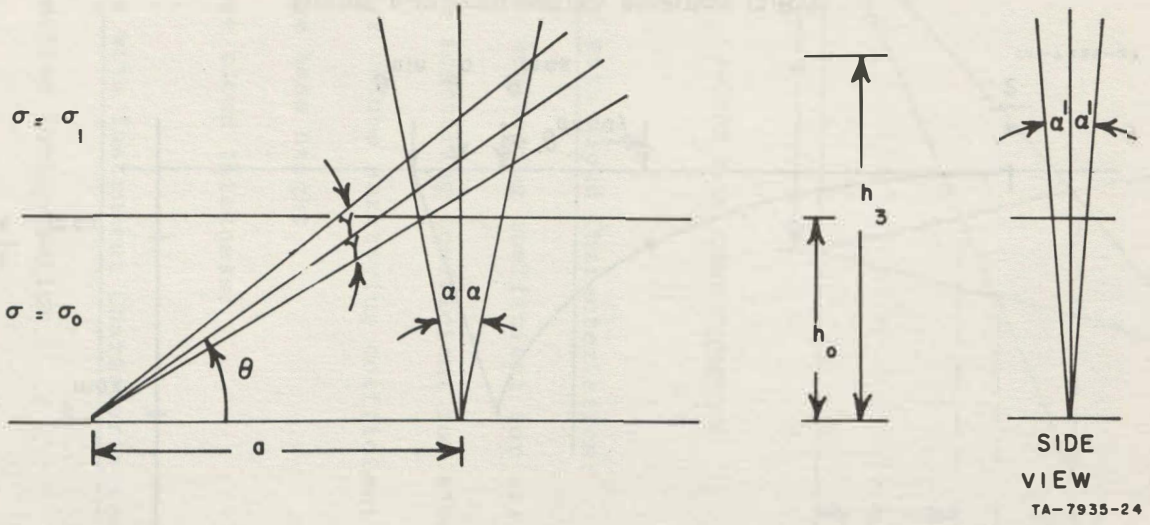

FIGURE B-11 CEILOMETER GEOMETRY

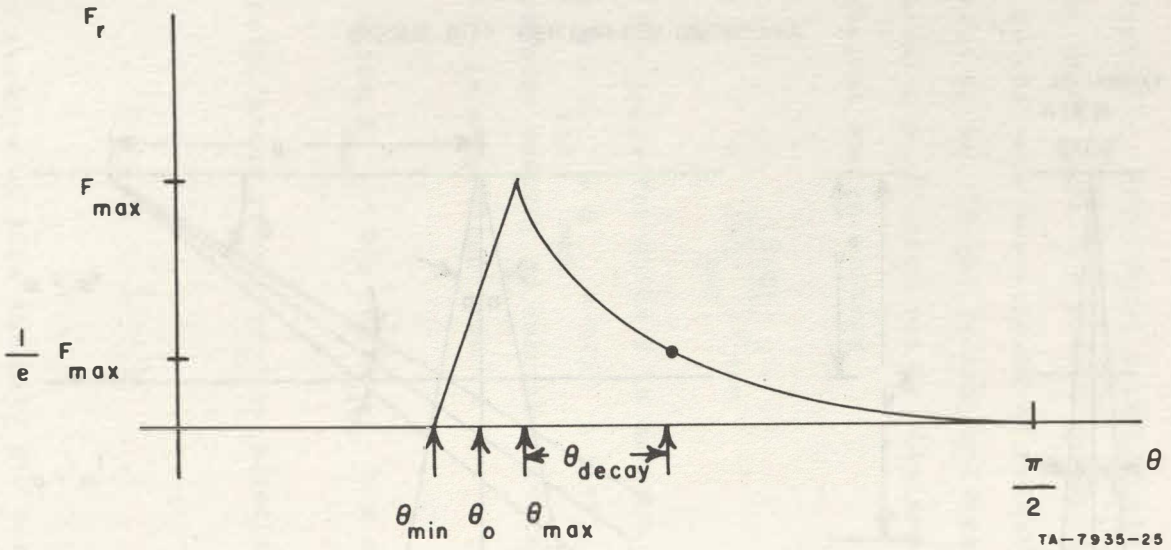

FIGURE B-12 CEILOMETER RESPONSE CURVE

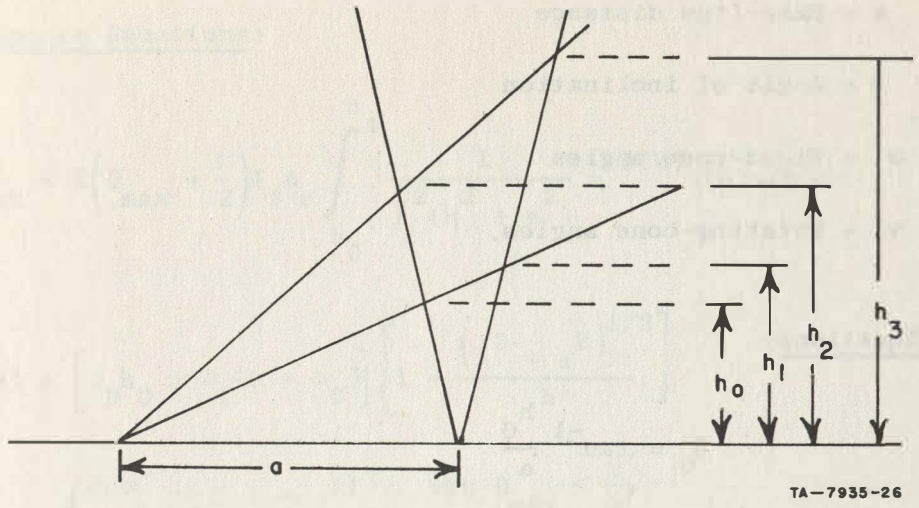

FIGURE B-13 CONE GEOMETRY

Symbols Associated with Cloud Characteristics:

σ_0 = Volume scattering coefficient for air

σ_1 = Volume scattering coefficient for cloud

β = Angular volume scattering coefficient for cloud

h_0 = Average base height

t = Average cloud thickness.

Symbols Associated with Instrument Characteristics

F_T = Transmitted luminous flux

I_T = Transmitted flux intensity

F_R = Received luminous flux

A_r = Area of receiver

a = Base-line distance

θ = Angle of inclination

α, α' = Fixed-cone angles

γ, γ' = Rotating-cone angles.

Angle Equations:

$$\theta_0 = \tan^{-1} \frac{h_0}{a}$$

$$\sin \theta_0 = \frac{h_0}{\left(h_0^2 + a^2\right)^{1/2}}$$

$$\theta_{min} = \theta_0 - \left(\alpha \sin^2 \theta_0 + \gamma\right)$$

$$\theta_{max} = \theta_0 + \left(\alpha \sin^2 \theta_0 + \gamma\right)$$

$$\theta_{decay} = \frac{1}{a\sigma_1} \sin \theta_0 (1 - \sin \theta_0) \quad .$$

Height Equations:

$$h_1 = h_0 + \frac{2h_0^2}{a} \alpha$$

$$h_2 = h_0 + \frac{2\left(h_0^2 + a^2\right)}{a} \gamma$$

$$h_3 = h_0 + \frac{2}{a}\left[h_0^2 \alpha + \left(h_0^2 + a^2\right)\gamma\right] \quad .$$

$$h_4 = \min(h_3, h_0 + t) \quad .$$

Response Equations:

$$F_{max} = \beta\left(\theta_{max} + \frac{\pi}{2}\right) I_T A_r \int_{h_0}^{h_4} \frac{1}{h^2(h^2 + a^2)} e^{-g(h)} \ell(h) w(h) dh$$

$$g(h) = \left[\sigma_0 h_0 + \sigma_1 (h - h_0)\right]\left[1 + \frac{\left(h^2 + a^2\right)^{1/2}}{h}\right]$$

$$w(h) = \begin{cases} 2h\alpha' & , \text{ if } \sin\theta_{max} < \frac{\gamma'}{\alpha'} \\ \frac{2h\gamma'}{\sin\theta_{max}} & , \text{ if } \sin\theta_{max} > \frac{\gamma'}{\alpha'} \end{cases}$$

$$\ell(h) = \begin{cases} \ell_1(h) & , \text{ if } h_2 > h_1 \\ \ell_2(h) & , \text{ if } h_1 > h_2 \end{cases}$$

$$\ell_1(h) = \begin{cases} \frac{h - h_0}{h_0} a & , \quad h_0 < h < h_1 \\ 2h\alpha & , \quad h_1 < h < h_2 \\ a - h\left[\frac{a}{h_0} - 2\alpha - \frac{2\gamma}{\sin^2\theta_0}\right] & , \quad h_2 < h < h_3 \end{cases}$$

$$\ell_2(h) = \begin{cases} \dfrac{h - h_0}{h_0}\, a & , \quad h_0 < h < h_2 \\ \dfrac{2h\gamma}{\sin^2 \theta_0} & , \quad h_2 < h < h_1 \\ a - h\left[\dfrac{a}{h_0} - 2\alpha - \dfrac{2\gamma}{\sin^2 \theta_0}\right] & , \quad h_1 < h < h_3 \end{cases} .$$

If a layer of thickness t^* and volume scattering coefficient σ^* intervenes, multiply the expression for F_{max} by

$$e^{-(\sigma^* - \sigma_0)t^*\left(\frac{1}{\sin \theta_{max}} + 1\right)} .$$

Relations for Fixed-Beam Ceilometer:

α, α' = Transmitter cone angles

γ, γ' = Receiver cone angles

$$I_T = \frac{F_T}{4\alpha\alpha'} .$$

Relations for Rotating-Beam Ceilometer:

α, α' = Receiver cone angles

γ, γ' = Transmitter cone angles

$$I_T = \frac{F_T}{4\gamma\gamma'} .$$

Appendix C

SIMULATION OF VERTICALLY POINTING RADAR CEILOMETERS

1. Introduction

Like optical ceilometers, radar ceilometers sense the presence of clouds by detecting the electromagnetic energy scattered back from a transmitted beam. Although the basic physics is essentially the same, the differences due to wavelength, geometry, and pulsed instead of continuous-wave operation require separate simulation equations. In this appendix we shall derive the equations used in simulating the major characteristics of vertically pointing radar ceilometers.

2. Qualitative Characteristics

A single-antenna, vertically pointing radar transmits a powerful short-duration pulse of electromagnetic energy directly upward. Soon after the pulse leaves, the antenna is switched to a sensitive receiver tuned to the frequency of the transmitter. If the pulse travels in a straight line at the speed of light c, a target at range r will return an echo to the receiver after the time 2r/c required for a round trip. The target range is thus determined, provided that the power received exceeds the minimum detectable signal.

The received power is affected by a number of factors, including the transmitted power, the area of the receiver antenna, the duration of the pulse, the wave length, the target range, the scattering properties of the target, and the attenuation of the wave as it passes through the medium. For atmospheric targets, the received power is subject to numerous disturbances due to the random or quasi-random distribution of scattering particles, and various sources of noise. Thus, in the following analysis it is to be understood that we are speaking of average power, and that only the most significant effects are taken into account.

3. Basic Relations

Derivations of the basic radar equation for scattering by clouds and precipitation can be found in various references (Austin, 1947; Battan, 1959; Hansford, 1960). We sketch a derivation here primarily to define notation and to expose some of the approximations involved. Let the transmitter emit a pulse having peak power P_T, time duration τ, and wavelength λ. The antenna directs this pulse along a cone of solid angle $\omega_T \cong \theta_b \varphi_b$ where θ_b and φ_b are the 3-dB horizontal and vertical beam widths in radians. As the pulse moves away, the power per unit area decreases with range r like $P_T/\omega_T r^2$. Were the pulse to strike a target of cross-sectional area A_t that scattered the incident power isotropically, the scattered power P_r received by the antenna would be given by

$$P_r = \frac{P_T A_t}{\omega_T r^2} \cdot \frac{A_r}{4\pi r^2} \qquad \text{(C-1)}$$

where A_r, the effective area of the receiving antenna, is assumed to be small relative to r^2. This equality can be expressed in a more illuminating form by introducing the antenna gain G, where

$$G = \frac{4\pi}{\omega_T} \cong \frac{4\pi}{\theta_b \varphi_b} \quad . \qquad \text{(C-2)}$$

It can be shown (Ridenour, 1947) that the gain of a uniformly fed aperture is given by

$$G = \frac{4\pi A_r}{\lambda^2} \quad . \qquad \text{(C-3)}$$

Since antenna dimensions are often selected to yield a desired value for G (beamwidth) at the operating wavelength, it is convenient to use these relations to eliminate ω_T and A_r from Eq. (C-1) and obtain

$$P_r = \frac{P_T G^2 \lambda^2}{(4\pi)^3 r^4} A_t \quad . \qquad \text{(C-4)}$$

For meteorological purposes, this basic radar equation must be modified to account for (1) nonisotropic scattering by particles in the pulse volume, and (2) attenuation of the signal by scattering and absorption. The conventional way to handle nonisotropic scattering is to introduce a backscattering cross

section per unit volume σ_i for a particle of diameter d_i. By definition, the target area A_i for particles of diameter d_i occupying a volume V is

$$A_i = \sigma_i V \quad . \tag{C-5}$$

When there is a distribution of particle sizes, with n_i particles per unit volume having diameter d_i, the target area A_t is given by

$$A_t = \sum_{\text{vol.}} n_i \sigma_i V \quad . \tag{C-6}$$

Consider now the reflected power reaching the antenna at time t, where t is measured from the time that the end of the pulse left the transmitter. Clearly, that part of the power reflected from the end of the pulse is due to particles at range ct/2, and that part reflected from the start of the pulse is due to particles at range $c(t + \tau)/2$, where τ is the pulse duration. Thus, the total power received is due to particles in what is approximately a rectangular parallelepiped whose length is $c\tau/2$ and whose cross-sectional area is $\theta_b \varphi_b r^2$. Thus,*

$$V = \theta_b \varphi_b r^2 c\tau/2 \tag{C-7}$$

---

*We are assuming that the pulse volume is sufficiently small that properties such as the drop-size distribution can be considered to be constant. This may not be true at the edges of clouds or at great ranges where a cloud only partially fills the beam. The effects of pulse length, beam width, and side lobes are discussed by Battan (1959).

and, from Eqs. (C-4) and (C-6),

$$P_r = \frac{P_T G^2 \lambda^2 \theta_b \varphi_b c\tau \eta}{128 \pi^3 r^2} \qquad \text{(C-9)}$$

where the reflectivity per unit volume* η is given by

$$\eta = \sum n_i \sigma_i \quad . \qquad \text{(C-10)}$$

Finally, we must account for attenuation of the signal due to atmospheric losses. In a uniform medium, scattering and absorption subtract a fixed percentage of the power propagating through the medium. If α_a is the fraction of power removed per unit distance, the power transmitted over a range r is reduced by the factor $e^{-\alpha_a r}$. If the attenuation rate α_a varies with range, the exponent $\alpha_a r$ must be replaced by the integral of α_a over the path. Finally, taking into account the round-trip transmission of the signal, we obtain the desired equation

$$P_r = \frac{P_T G^2 \lambda^2 \theta_b \varphi_b c\tau \eta k}{128 \pi^3 r^2} \qquad \text{(C-11)}$$

where the transmission factor k is given by

$$k = e^{-2\int_0^r \alpha_a(r')dr'} \quad . \qquad \text{(C-12)}$$

---

*Note that dimensionally η is an area per unit volume, and is frequently measured in cm^{-1}.

4. Response to a Single Cloud Layer

If we combine those factors in Eq. (C-11) that do not depend on range, we obtain

$$P_r = \frac{C}{r^2}\,\eta(r)\, e^{-2\int_0^r \alpha_a(r')\,dr'} \qquad \text{(C-13)}$$

where

$$C = \frac{P_t\, G^2\, \lambda^2\, \theta_b \varphi_b\, c\tau}{128\,\pi^3} \quad . \qquad \text{(C-14)}$$

Thus, the variation of P_r with range depends on three factors, the r^{-2} decrease, the particle reflectivity per unit volume η, and the attenuation rate α_a. Consider the case of a single cloud layer whose base* is at height r_1, and whose top is at height $\hat{r}_1$. If we assume that η is η_1 in the cloud and negligible outside, and that α_a is α_1 in the cloud and α_0 outside, we obtain

$$P_r = \begin{cases} 0 & 0 < r < r_1 \\ P_1\left(\dfrac{r_1}{r}\right)^2 e^{-2\alpha_1(r-r_1)} & r_1 < r < \hat{r}_1 \\ 0 & \hat{r} < r \end{cases} \qquad \text{(C-15)}$$

where

$$P_1 = \frac{C\eta_1}{r_1^2}\, e^{-2\alpha_0 r_1} \quad . \qquad \text{(C-16)}$$

---

*If the cloud base is irregular, we take h_1 to be the average base height within the transmitter cone.

Thus, the response to a single cloud layer is characterized by four numbers, P_1, r_1, $\hat{r}_1$, and α_1. The computation of the response for a single layer is equivalent to the computation of these four parameters. Since r_1 is the only quantity that changes in our model, this means that the only computation of consequence is that of P_1. While Eq. (C-16) is acceptable for that computation, an even simpler procedure is to use the average value of r_1, $\bar{r}_1$, to compute $\bar{P}_1$ once, and thereafter compute only changes in P_1 by

$$\Delta P_1 = \left.\frac{dP_1}{dr_1}\right|_{\bar{r}_1} \Delta r_1 \qquad \text{(C-17)}$$

or

$$\Delta P_1 = -2 \bar{P}_o \left(\alpha_0 + \frac{1}{\bar{r}_1}\right) \Delta r_1 \quad . \qquad \text{(C-18)}$$

5. Response to Two Cloud Layers

Because less energy is scattered at radar wavelengths than at optical wavelengths, a weather radar frequently penetrates two or more layers of clouds. In our simulation, we have restricted our attention to the response from the lowest two layers, although it would not be difficult to extend the technique to treat an arbitrary number of layers. Consider the case of two cloud layers, the first extending from r_1 to $\hat{r}_1$, and the second from r_2 to $\hat{r}_2$. Let η be η_1 in the first layer,

η_2 in the second layer, and negligible elsewhere. Similarly, let α_a be α_1 in the first layer, α_2 in the second layer, and α_0 elsewhere. Then, from Eq. (C-13),

$$P_r = \begin{cases} 0 & 0 < r < r_1 \\ P_1 \left(\frac{r_1}{r}\right)^2 e^{-2\alpha_1 (r-r_1)} & r_1 < r < \hat{r}_1 \\ P_2 \left(\frac{r_2}{r}\right)^2 e^{-2\alpha_1 (r-r_2)} & r_2 < r < \hat{r}_2 \\ 0 & \hat{r}_2 < r \end{cases} \tag{C-19}$$

where

$$P_1 = \frac{C\eta_1}{r_2^2} e^{-2\alpha_0 r_1} \tag{C-20}$$

and

$$P_2 = \frac{C\eta_2}{r_2^2} e^{-2\left[(\alpha_1-\alpha_0)(\hat{r}_1-r_1) + \alpha_0 r_2\right]} . \tag{C-21}$$

These results are illustrated in Figure C-1. Note that the abrupt changes in reflected power at the cloud boundaries result from our simplifying assumption that the pulse length is short. If desired, a more accurate curve can be obtained by averaging these results using a window of length $c\,\tau/2$.

6. Recovery-Time Effects

Because a certain time must be allowed to elapse between the time the pulse is transmitted and the receiver can be used,

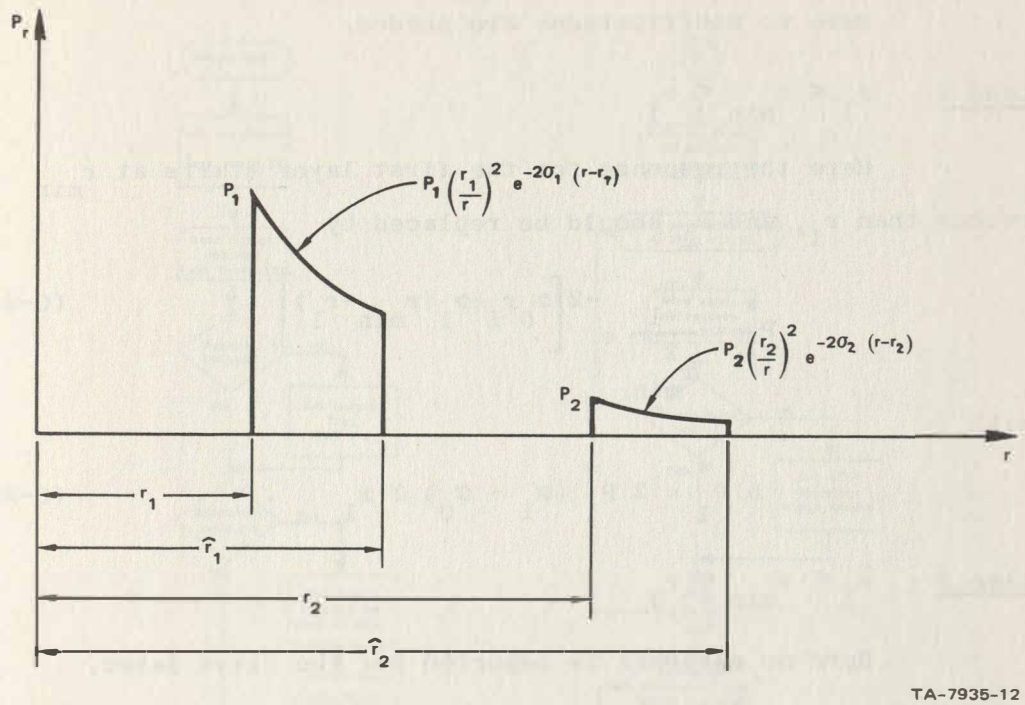

FIGURE C-1 RADAR RESPONSE TO TWO CLOUD LAYERS

targets closer than a corresponding minimum range r_{min} cannot be detected. Of course, if the clouds are beyond r_{min}, this problem does not arise. However, since the simulation program treats rain as a zero-altitude layer, this minimum range is obviously important here. For the general two-layer situation, five cases arise that call for various degrees of modification of Eqs. (C-19) through (C-23).

Case 1: $r_{min} < r_1$.

Here no modifications are needed.

Case 2: $r_1 < r_{min} < \hat{r}_1$.

Here the response for the first layer starts at r_{min} rather than r_1, and P_1 should be replaced by

$$P_1^* = \frac{C\eta_1}{r_{min}^2} e^{-2\left[\alpha_0 r_1 + \alpha_1 (r_{min} - r_1)\right]} \qquad \text{(C-24)}$$

with

$$\Delta P_1^* = 2 P_1^* (\alpha_1 - \alpha_0) \Delta r_1 \quad . \qquad \text{(C-25)}$$

Case 3: $\hat{r}_1 < r_{min} < r_2$.

Here no response is reported for the first layer.

Case 4: $r_2 < r_{min} < \hat{r}_2$.

Here no response is reported for the first layer, and the response fot the second layer starts at r_{min}, with P_2 replaced by

$$P_2^* = \frac{C\eta_2}{r_{min}^2} e^{-2\left[(\alpha_1 - \alpha_0)(\hat{r}_1 - r_1) + \alpha_0 r_2 + d_2 (r_{min} - r_2)\right]} \qquad \text{(C-26)}$$

with

$$\Delta P_2^* = 2 P_2^* \left[(\alpha_1 - \alpha_0) \Delta r_1 + (\alpha_2 - \alpha_0) \Delta r_2\right] \quad . \qquad \text{(C-27)}$$

Case 5: $\hat{r} < r_{min}$.

Here no response at all is reported.

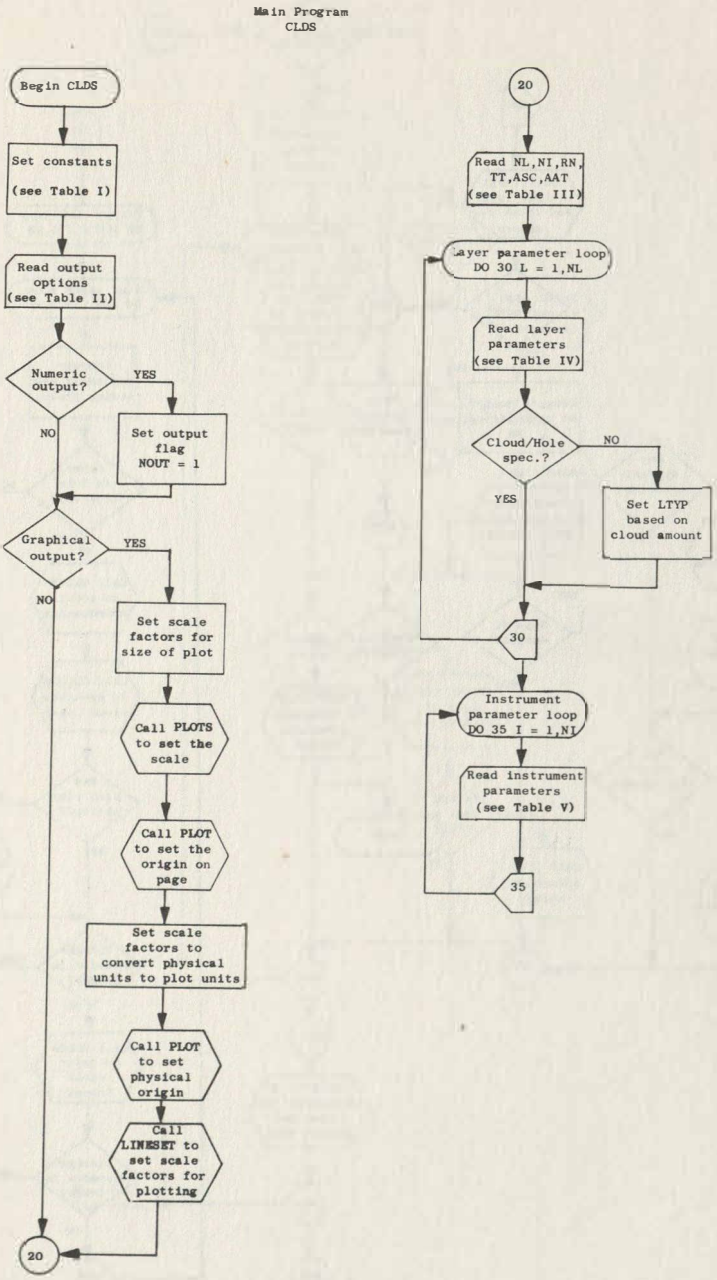

TA-7935-14

APPENDIX D PROGRAM FLOW CHARTS

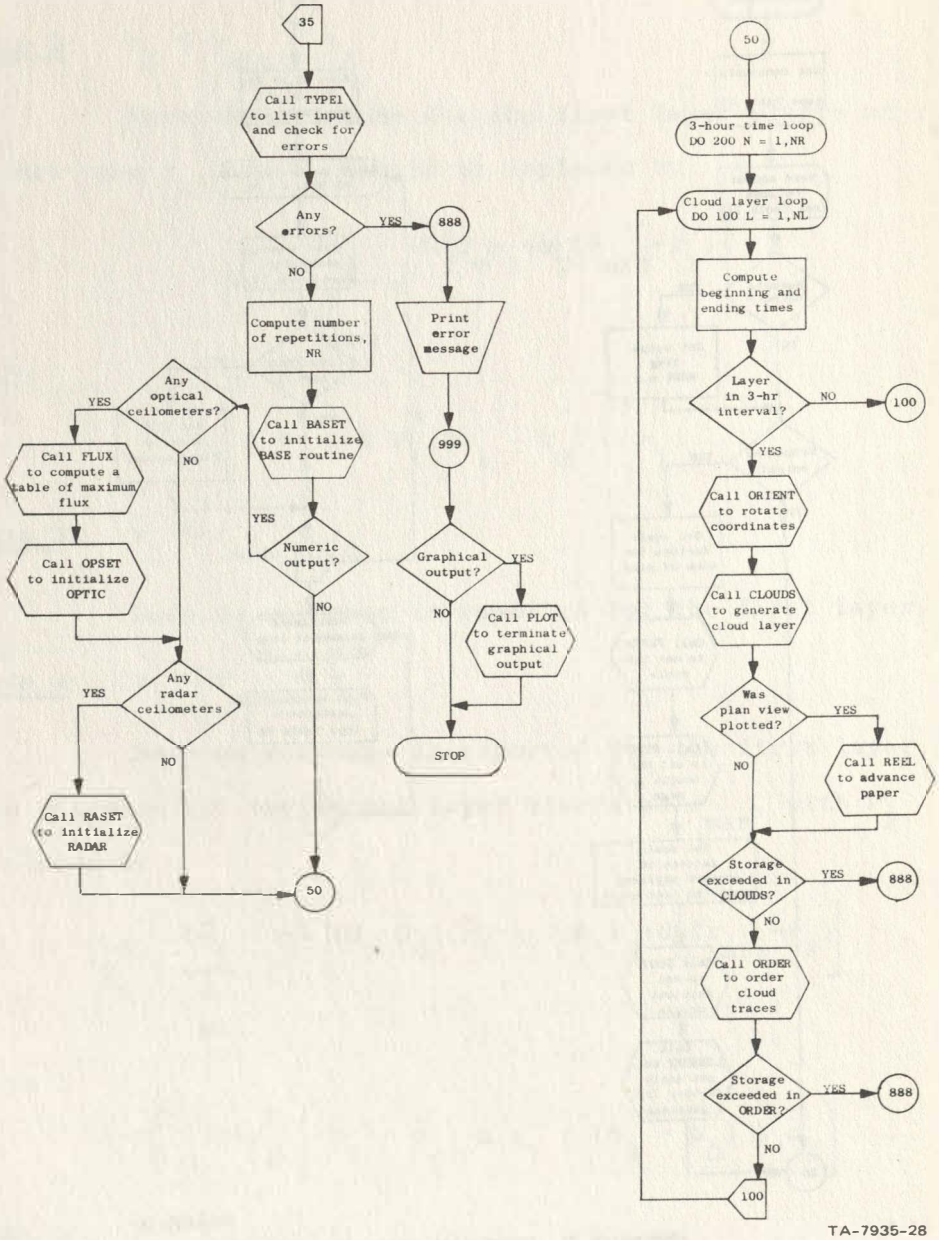

TA-7935-28

APPENDIX D PROGRAM FLOW CHARTS continued

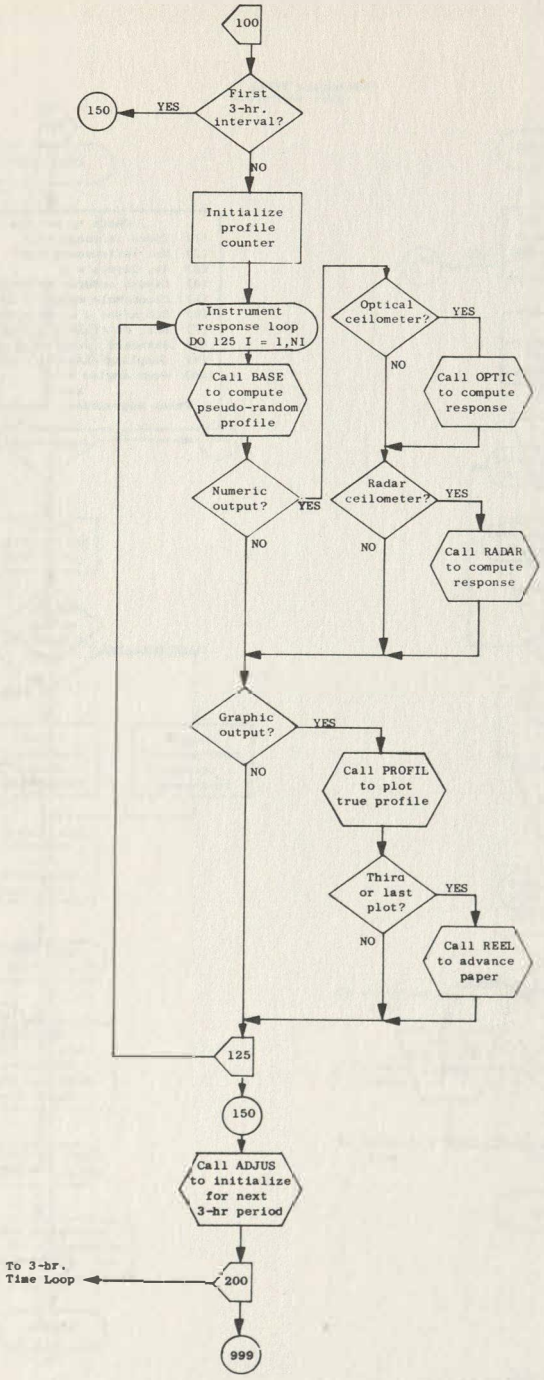

TA-7935-29

APPENDIX D PROGRAM FLOW CHARTS continued

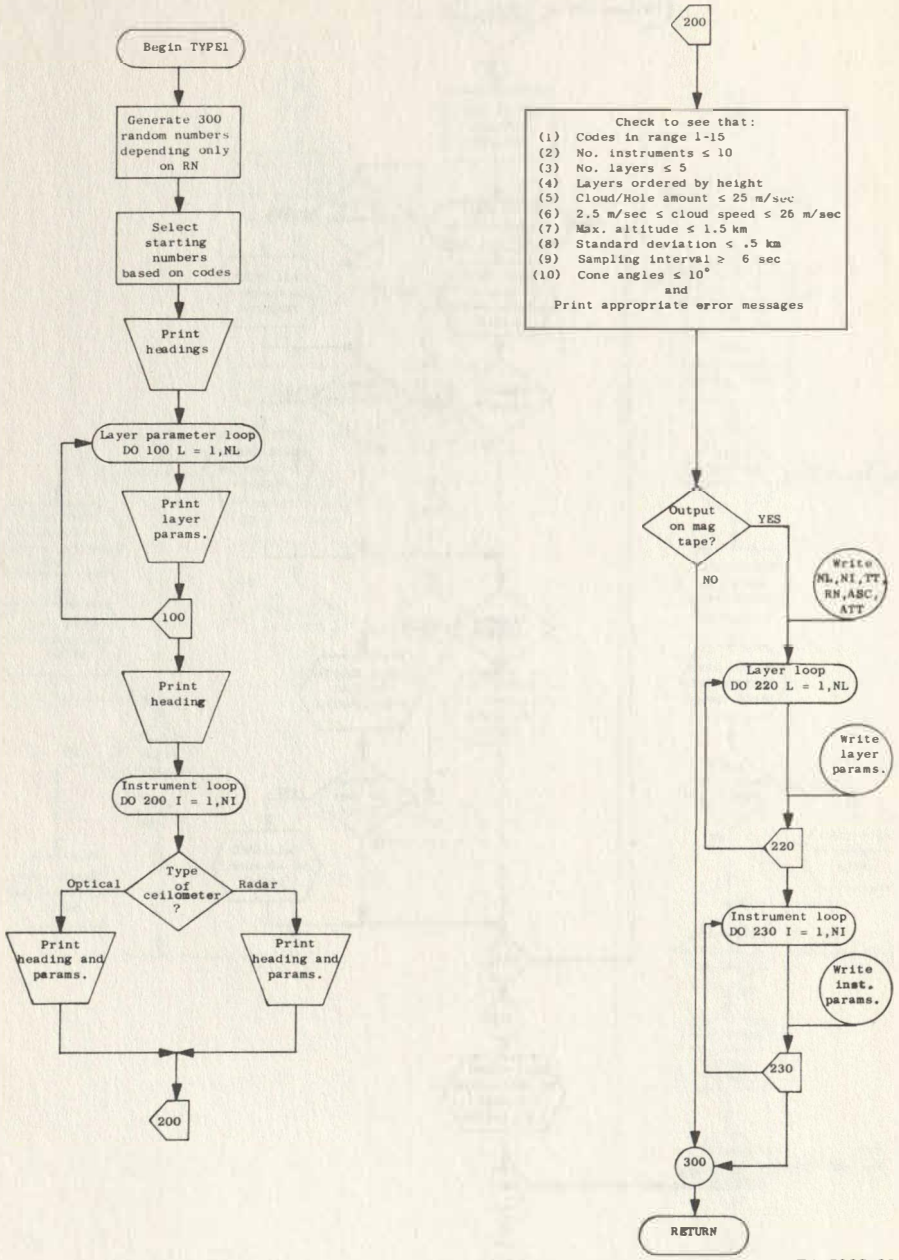

TA-7935-32

APPENDIX D PROGRAM FLOW CHARTS continued

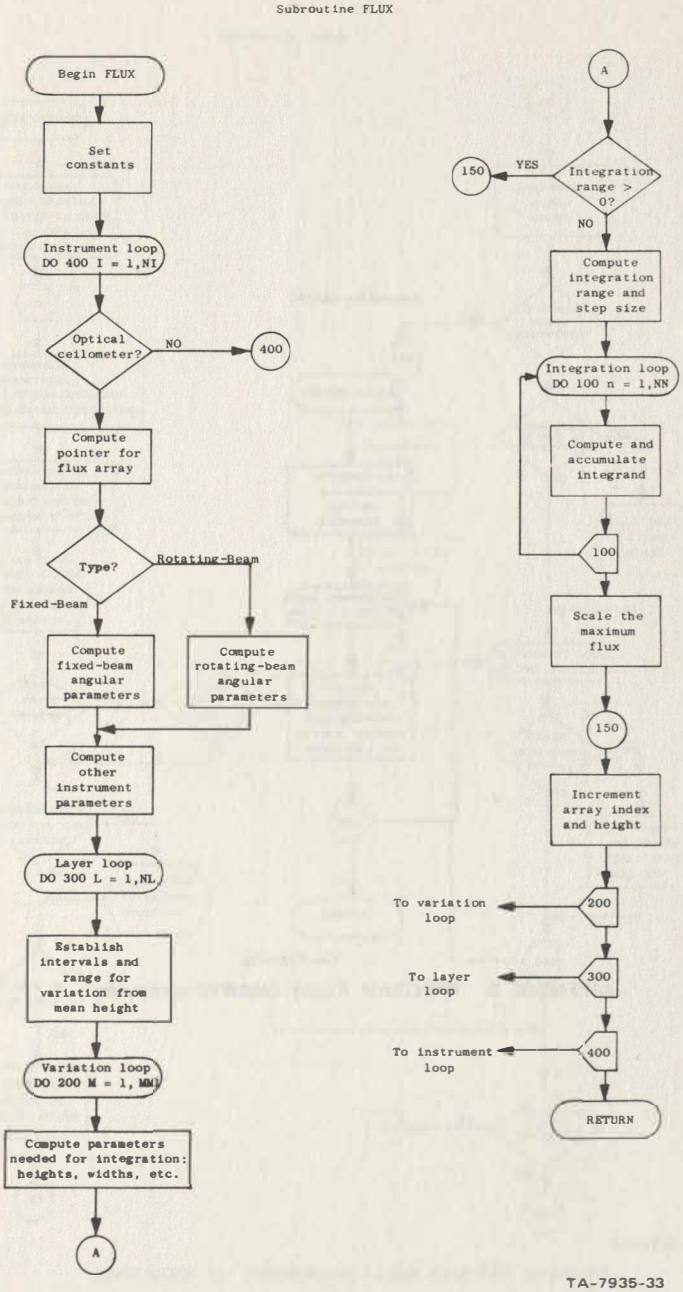

TA-7935-33

APPENDIX D PROGRAM FLOW CHARTS continued

Subroutine ORIENT

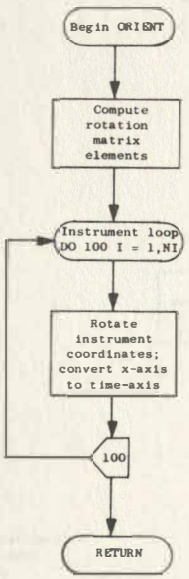

TA-7935-30

APPENDIX D PROGRAM FLOW CHARTS continued

Subroutine CLOUDS

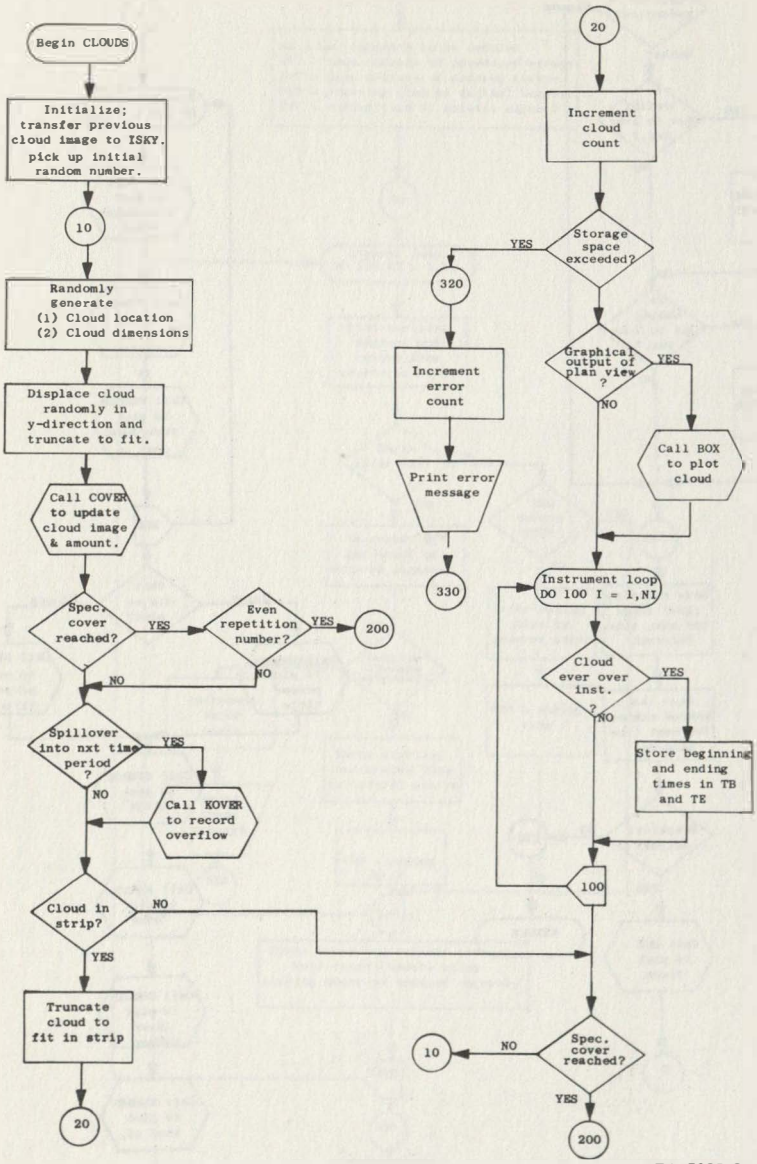

TA-7935-31

APPENDIX D PROGRAM FLOW CHARTS continued

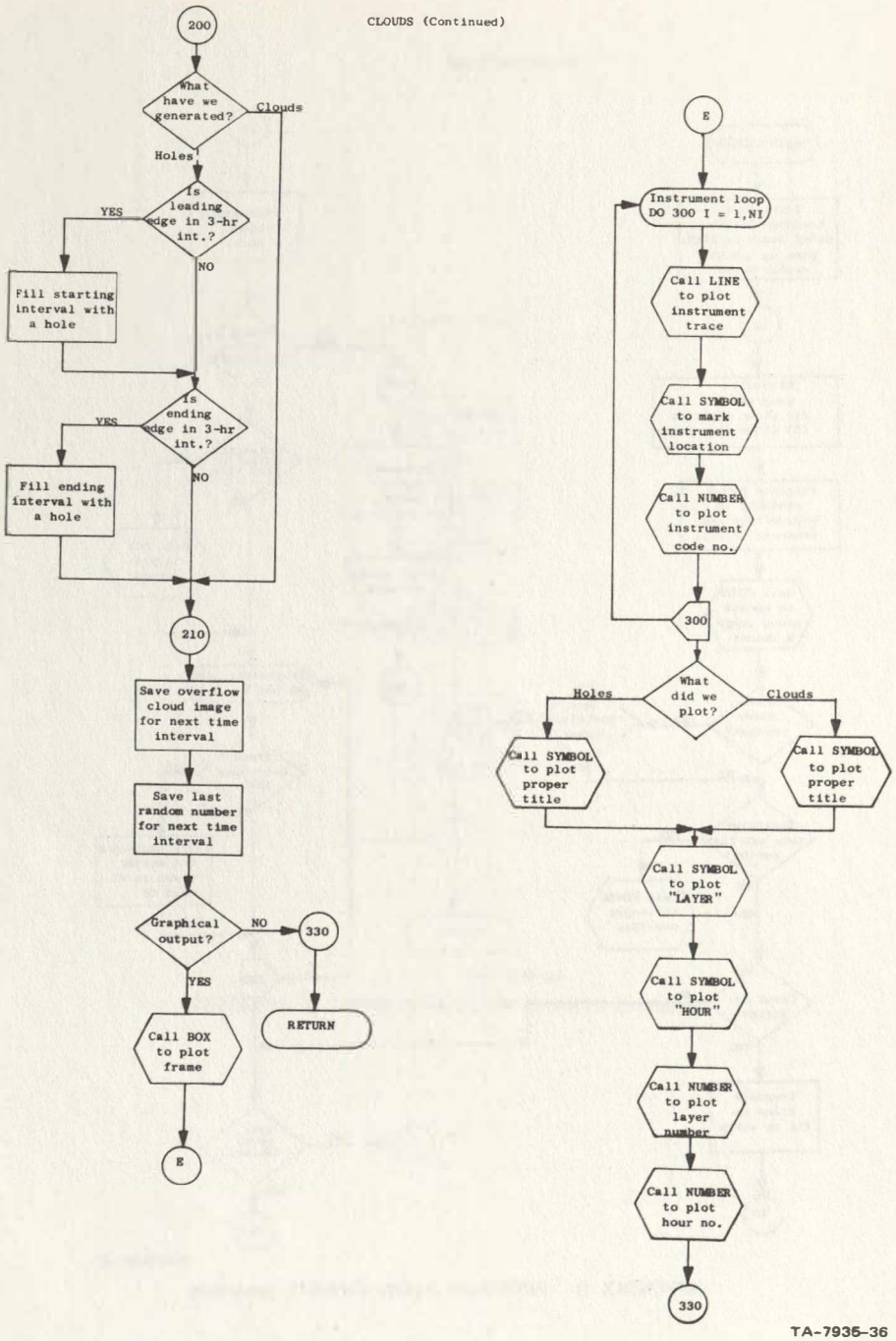

TA-7935-36

APPENDIX D PROGRAM FLOW CHARTS continued

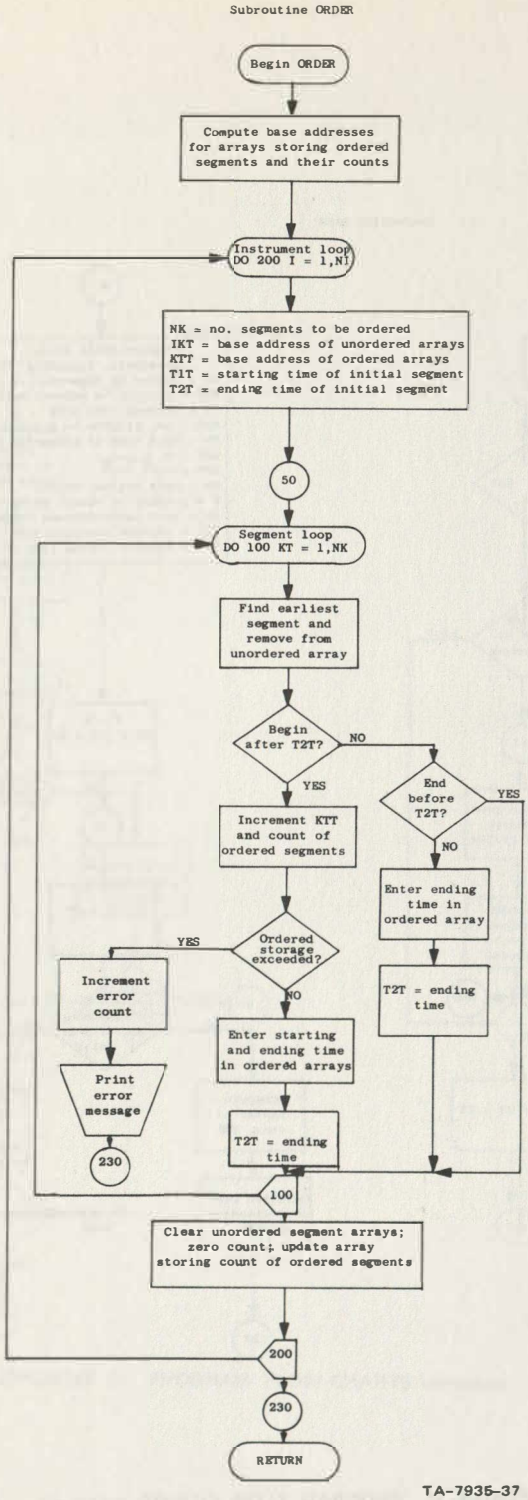

TA-7935-37

APPENDIX D PROGRAM FLOW CHARTS continued

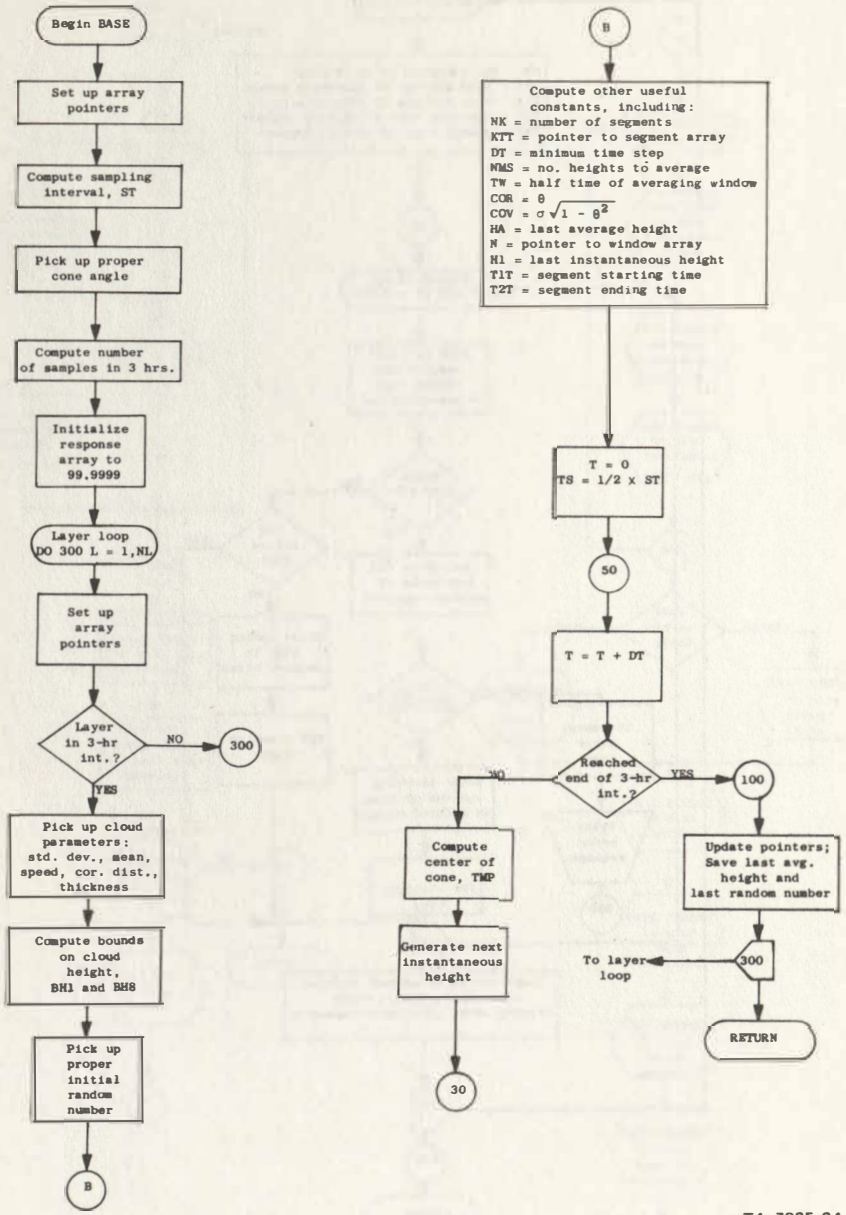

TA-7935-34

APPENDIX D PROGRAM FLOW CHARTS continued

BASE (Continued)

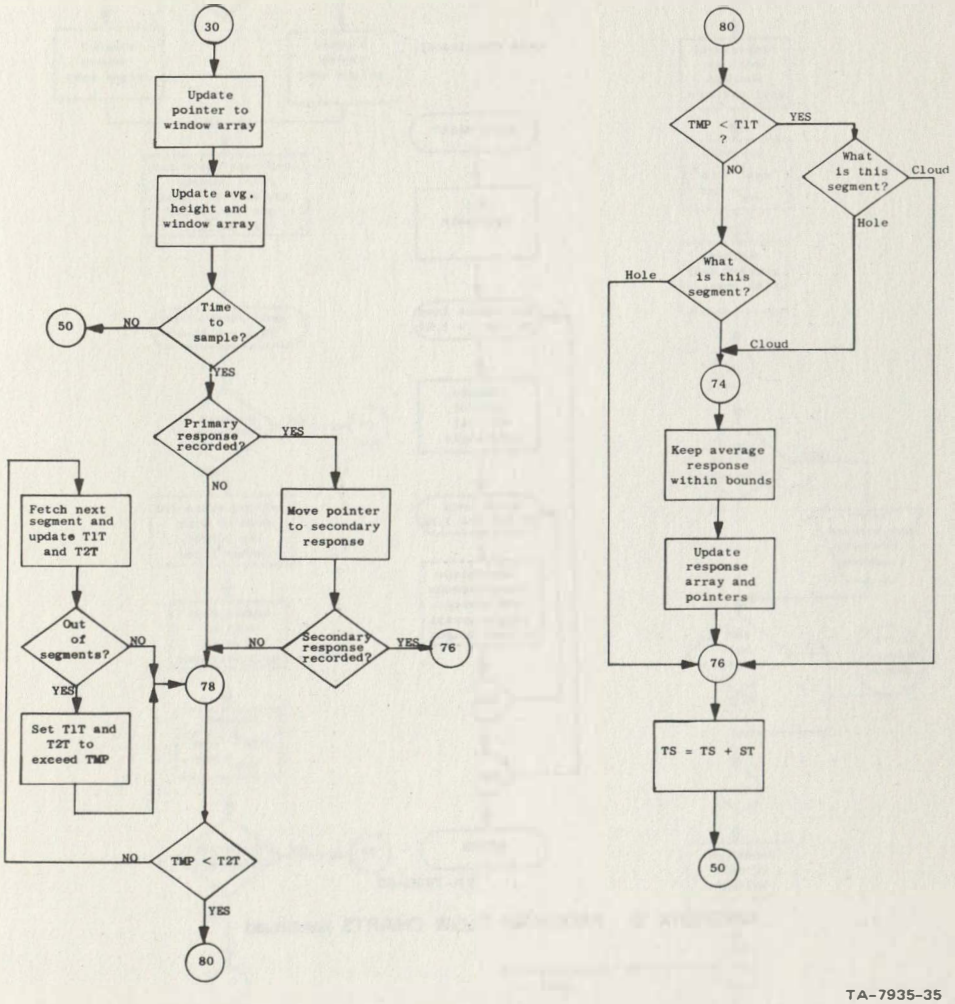

TA-7935-35

APPENDIX D PROGRAM FLOW CHARTS continued

BASE (Continued)

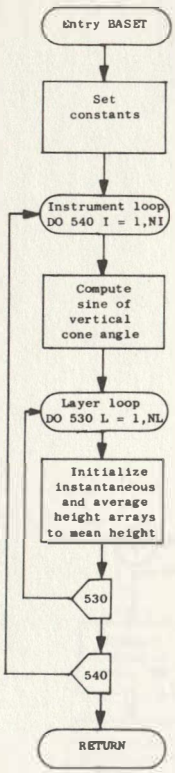

TA-7935-40

APPENDIX D PROGRAM FLOW CHARTS continued

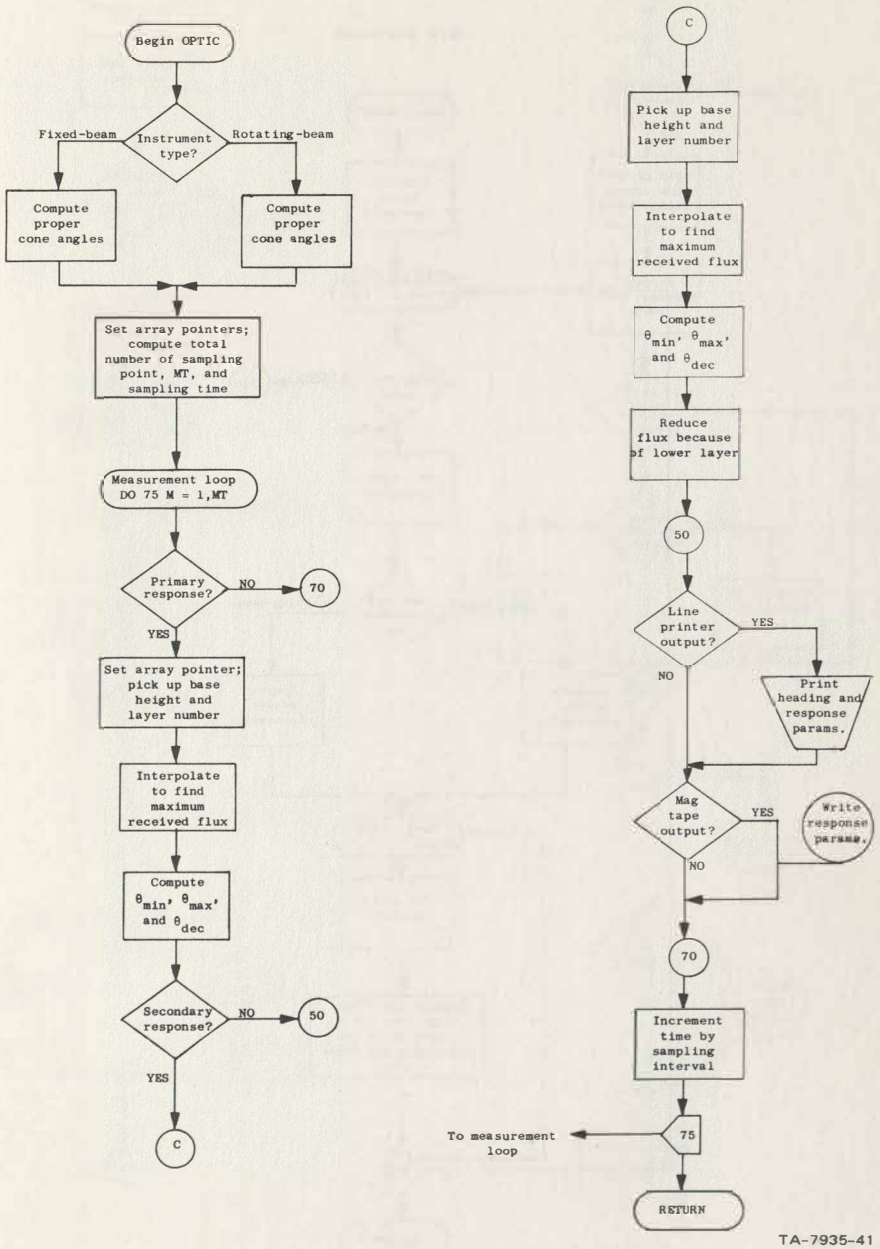

APPENDIX D PROGRAM FLOW CHARTS continued

OPTIC (Continued)

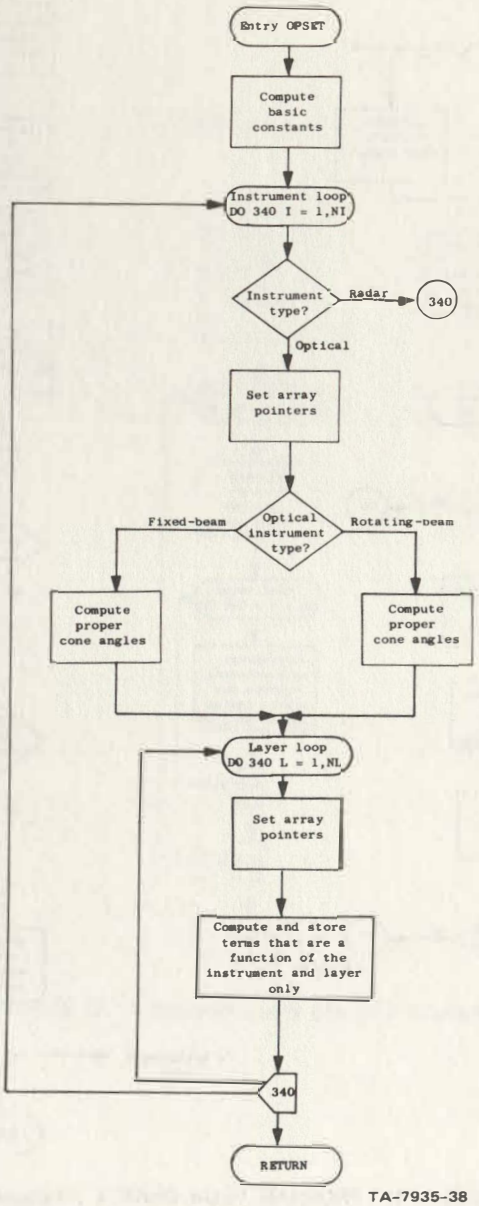

TA-7935-38

APPENDIX D PROGRAM FLOW CHARTS continued

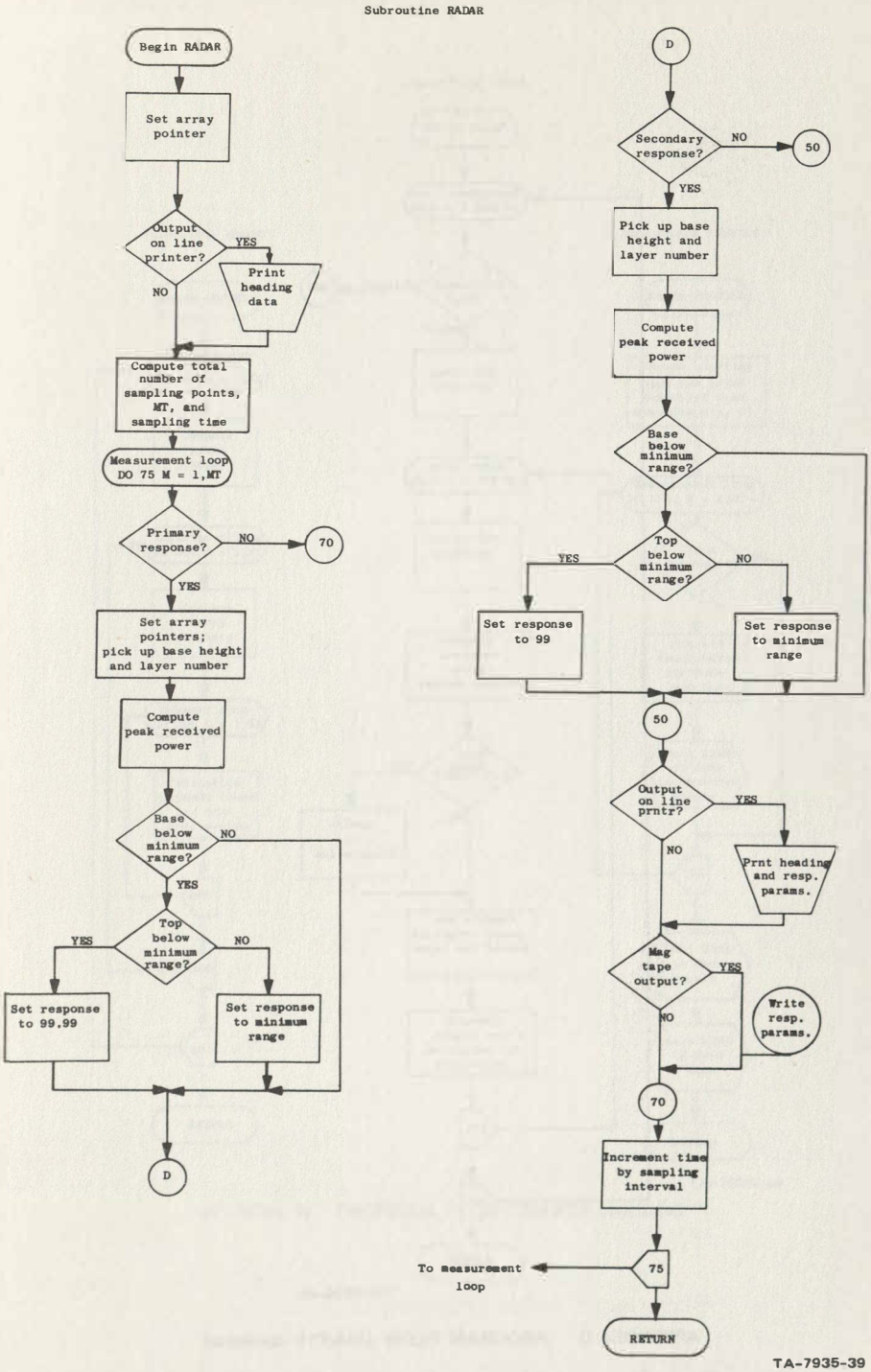

TA-7935-39

APPENDIX D PROGRAM FLOW CHARTS continued

RADAR (Continued)

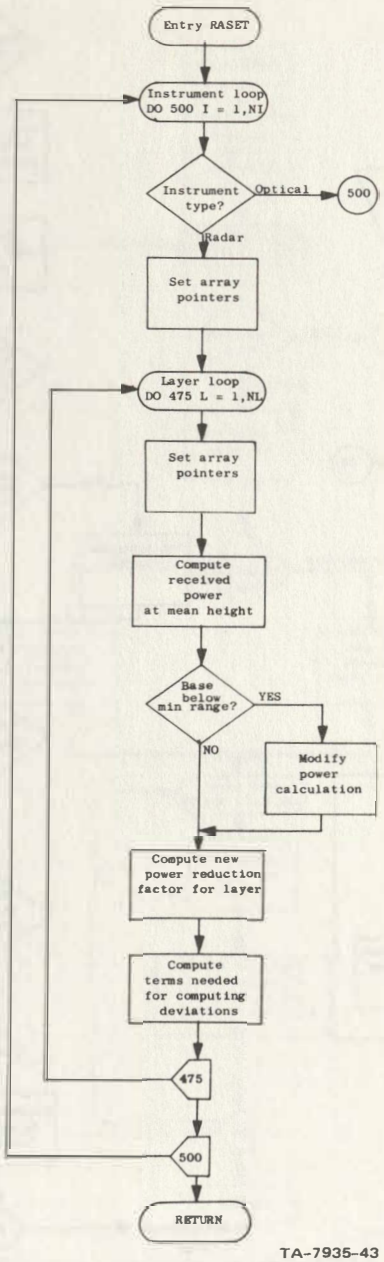

TA-7935-43

APPENDIX D PROGRAM FLOW CHARTS continued

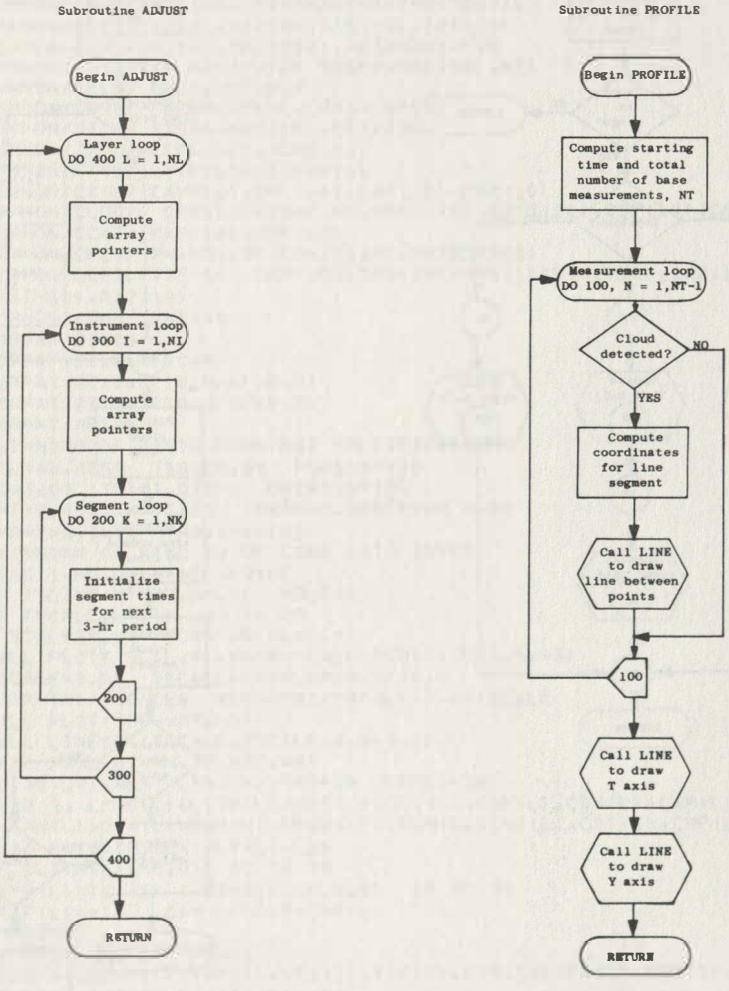

APPENDIX D PROGRAM FLOW CHARTS concluded

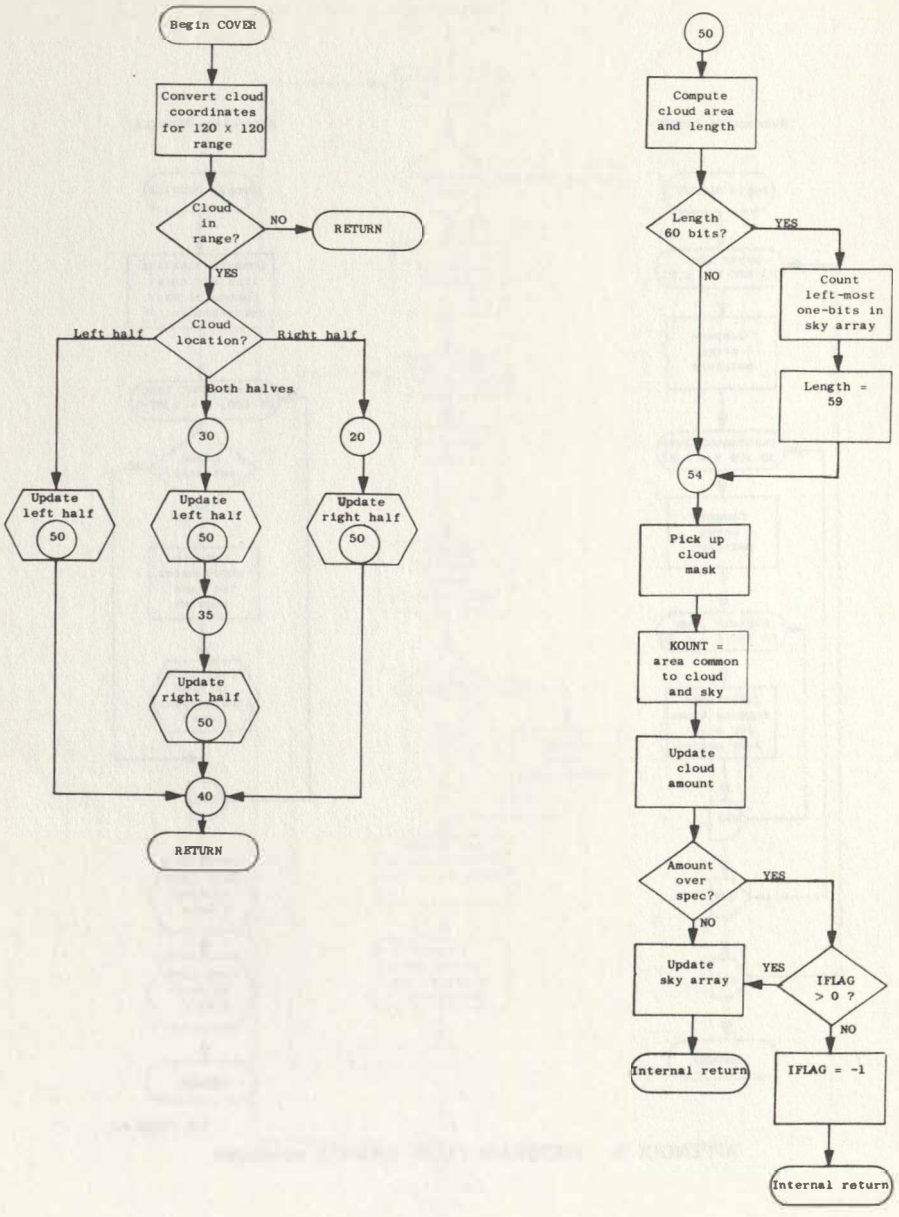

TA-7935-42

APPENDIX D PROGRAM FLOW CHARTS continued

```
      PROGRAM   CLDS(INPUT,OUTPUT,TAPE41,TAPE46)
C     THIS PROGRAM GENERATES CLOUD FIELDS,CLOUD BASE HEIGHTS AND
C        CEILOMETER RESPONSE CHARACTERISTICS OVER 3 HOUR TIME PERIODS
C        UNTIL THE TOTAL SPECIFIED TIME (TT) HAS BEEN EXCEEDED.
      COMMON/COUT/ NLINE,NTAPE,NCALC,NOUT
      COMMON/CSAL/TSCALE,YSCALE
      COMMON/CRNG/  RN,ASC,AAT
      COMMON/CTEX/ XT,T0,T9
      COMMON/CMAX/TMI,TMA,YMI,YMA,TMR,YMR,T5,T10
      COMMON/CXYI/TI(10),YI(10),XIS(10),YIS(10)
      COMMON/CXBE/KN(10),TB(2000),TE(2000),MTB
      COMMON/CX12/T1( 5000),T2( 5000),KNL(50),MT1
      COMMON/CELX/ DELX,DDT,BST
      COMMON/CBSH/ CRESP(4000),LRESP(4000)
      COMMON/CTIM/ TT,TD,CBT(10),CET(10)
      COMMON/CCOD/ LCOD(10),ICOD(10)
      COMMON/CTYP/ LTYP(10),ITYP(10)
      COMMON/CASH/ CAM(10),CML(10),CAR(10),CDR(10)
      COMMON/CLDC/  CTH(10),CBH(10),CBSD(10),CBCD(10),CSP(10),CSC(10)
      COMMON/CCAT/ CAT(10),CRF(10)
      COMMON/CFLX/ MM,NN,FON,FXH(1100),RATBS(200)
      COMMON/CCEIL/TIS(10),TFX(10),TRD(10),RAR(10),TA1(10),TA2(10),
     2 RA1(10),RA2(10)
      COMMON/CRNS/ RNS(60)
    1 FORMAT(3I10)
    2 FORMAT(2I10,4F10.5)
    3 FORMAT(2I10,6F10.5/8F10.5)
    4 FORMAT(2I10,3F10.5/7F10.5)
    5 FORMAT(8F10.5)
C     BEGINNING OF BASIC CONSTANT SPECIFICATIONS
      DELX=0.015$  T10=10.0$  T5=0.5*T10
      TD=3.0$  TDI=1.0/TD$  DDT=T10*TDI
      TMI=0.00$ TMA=T10$   YMI=-8.00$ YMA= 8.00
      TMR=TMA-TMI$  YMR=YMA-YMI
C     BEGINNING OF READ IN OF CARD DATA INPUT
      READ 1,NLINE,NTAPE,NCALC
      IF (NLINE+NTAPE.NE.0)  NOUT=1
      IF (NCALC.LT.1)  GO TO 20
        SCAL=30.0$  SCA5 =SCAL+5.0
      CALL PLOTS(SCAL,0.,46)$  CALL PLOT(1.5,1.5,-3)
      YSCALE=1.0$  TSCALE=YSCALE*10.0/16.0
      TOR=-TMI/TSCALE$  YOR=-YMI/YSCALE+7.0*YSCALE
      CALL PLOT(TOR,YOR,-3)
      CALL LINESET(TSCALE,YSCALE,0.0,0.0)
   20 READ 2,NL,NI,RN,TT,ASC,AAT
      DO 30 L=1,NL$  L1=(L-1)*40+1$  L2=L1+36
      READ 3, LCOD(L),LTYP(L),CBT(L),CET(L),CSP(L),CDR(L),CAM(L),CML(L)
     2 ,CAR(L),CTH(L),CBH(L),CBSD(L),CBCD(L),CSC(L),CAT(L),CRF(L)
      READ 5,(RATBS(LX),LX=L1,L2)
      IF (LTYP(L).NE.0)  GO TO 30
      LTYP(L)=1$  IF ( CAM(L).LE.0.5)  GO TO 30
      LTYP(L)=-1$   CAM(L)=1.0-CAM(L)
   30 CONTINUE
      ISYP=0$  DO 35 I=1,NI
      READ 4,ICOD(I),ITYP(I),XIS(I),YIS(I),TIS(I),TFX(I),TRD(I),RAR(I),
     2 RA1(I),RA2(I),TA1(I),TA2(I)
      IF (ITYP(I).GT.2)  ISYP=ISYP+1
```

APPENDIX E PROGRAM LISTINGS

```
   35 CONTINUE
      CALL TYPE1(NL,NI,IRR)
      IF (IRR.NE.0)  GO TO 888
      NR=XNR=TT/TD+1$IF (XNR.GT.NR) NR=NR+1$ NR1=NR+1
      CALL BASET(NL,NI,0)
      IF (NOUT.EQ.1.AND.ISYP.LT.NI)  CALL FLUX(NL,NI)
      IF (NOUT.EQ.1.AND.ISYP.LT.NI)  CALL OPSET(NL,NI,0)
      IF (NOUT.EQ.1.AND.ISYP.GT.0)   CALL RASET(NL,NI,0)
C     BEGINNING OF 3 HOUR TIME STEP LOOP.
   50 DO 200 N=1,NR $  N1=N-1
C     BEGINNING OF LOOP  FOR GENERATING CLOUD LAYERS.
      MTB=2000/NI$  MT1=5000/(NI*NL)
      DO 100 L=1,NL
      XNB=CBT(L)*TDI+0.5$  XNE=CET(L)*TDI+0.5
      T0=(XNB-N1 )*T10$  T9=(XNE-N1 )*T10
      IF (T0.GE.T10.OR.T9.LE.0.0) GO TO 100
      SSP=CSP(L)$  SDR=CDR(L)$  XT=DDT/SSP
      CALL ORIENT(SDR,NI)
      CALL CLOUDS(CAC,NI,N,L,IRR)
      IF (NCALC.GT.1) CALL REEL(SCA5,0.,999)
      IF (IRR.NE.0)  GO TO 888
      CALL ORDER(L,NI,IRR)
      IF (IRR.NE.0)  GO TO 888
  100 CONTINUE
      IF (N.EQ.1) GO TO 150
C     BEGINNING OF LOOP FOR GENERATING CLOUD BASE HEIGHTS AND CEILOMETER
C       CHARACTERISTICS.
      N3= 1$      DO 125 I=1,NI
      CALL BASE(NL,NI,I)
      IF (NOUT.EQ.1.AND.ITYP(I).LT.3)  CALL OPTIC(NL,NI,N,I)
      IF (NOUT.EQ.1.AND.ITYP(I).EQ.3)  CALL RADAR(NL,NI,N,I)
      IF (NCALC.LT.1)  GO TO 125
      CALL PROFIL(NI,I,N,N3)
      IF (N3.LT.3.AND.I.NE.NI)  GO TO 123
      N3=0
      CALL REEL(SCA5,0.,999)
  123 N3=N3+1
  125 CONTINUE
  150 CONTINUE
      CALL ADJUS(NL,NI)
  200 CONTINUE
      GO TO 999
  800 FORMAT (2X,*ERROR STOP, NO OF ERRORS =*,I3)
  888 PRINT 800,IRR
  999 CONTINUE
      STOP
      END
```

APPENDIX E PROGRAM LISTINGS continued

```
      SUBROUTINE TYPE1(NL,NI,IRR)
C     THIS SUBROUTINE CHECKS AND PRINTSOUT INPUT DATA.
      DIMENSION RNR(300)
      COMMON/CRNS/ RNS(60)
      COMMON/COUT/ NLINE,NTAPE,NCALC,NOUT
      COMMON/CRNG/  RN,ASC,AAT
      COMMON/CXYT/TI(10),YI(10),XIS(10),YIS(10)
      COMMON/CTIM/ TT,TD,CBT(10),CET(10)
      COMMON/CCOD/ LCOD(10),ICOD(10)
      COMMON/CTYP/ LTYP(10),ITYP(10)
      COMMON/CLDC/  CTH(10),CBH(10),CBSD(10),CBCD(10),CSP(10),CSC(10)
      COMMON/CASH/ CAM(10),CML(10),CAR(10),CDR(10)
      COMMON/CCAT/ CAT(10),CRF(10)
      COMMON/CFLX/ MM,NN,FON,FXH(1100),RATBS(200)
      COMMON/CCEIL/TIS(10),TFX(10),TRD(10),RAR(10),TA1(10),TA2(10),
     2 RA1(10),RA2(10)
    1 FORMAT(1H1)
    2 FORMAT(1H0,46X,26HCLOUD LAYER CHARATERISTICS/)
    3 FORMAT(1H0,46X,25HCEILOMETER CHARATERISTICS/)
    4 FORMAT(1H0,52X, 5HUNITS//45X,17HDISTANCE IN KM   /45X,
     2 13HTIME IN HOURS/ 45X,23HSPEED IN METERS PER SEC/45X,
     3 16HANGLE IN DEGREES/45X,25HCLOUD AMOUNT IN FRACTIONS)
    5 FORMAT(1H0,30X,*BASE RANDOM NO       SCAT COEF-AIR       ATTEN RATE-
     2AIR*,/31X,3(F10.3,10X))
    8 FORMAT(45X,*TIME INTERVAL = *,F7.2)
    9 FORMAT(45X,*TOTAL TIME = *,F7.2)
   10 FORMAT(1H0)
   11 FORMAT           (119H  CODE  TYPE  AMOUNT    LENGTH    ASP RATIO T
     2HICKNESS BASE HT   BASE SD   COR DIST  SPEED     DIR        T BEG
     3   T END)
   12 FORMAT(2X,I3,3X,I3,11F10.3)
   13 FORMAT           (110H  CODE  TYPE    X LOC    Y LOC   T INT(MIN)
     2FLX INT  T-R DIST  REC DIAM(M)   TRANS ANGLES          REC ANGLES )
   14 FORMAT           (73H  CODE  TYPE    X LOC    Y LOC   T INT(MIN)
     2RAD CON   MIN RG   REC ANGLE)
   15 FORMAT(1H0,40X,33HSIMULATED CEILOMETER MEASUREMENTS/)
   16 FORMAT(50X,*TYPE 1 = FIXED BEAM*,/50X,*TYPE 2 = ROTATING BEAM*,/
     2 50X,*TYPE 3 = RADAR*)
   17 FORMAT(50X,*TYPE  1 = CLOUDS*,/50X,*TYPE -1 = HOLES*)
   22 FORMAT(2X,I3,3X,I3,3F10.3,3X,E9.2,F8.3,5F10.3)
   23 FORMAT(1H0,3X,
     1           *SCAT C    ATTEN R   REFL(X10**6) RATIO-BETA/SIGMA*,/1X,
     2 3F10.3,8F10.5,/(31X,8F10.5))
   30 FORMAT(2X,*LAYER OR CEILOMETER CODE NO GREATER THEN 15*)
   31 FORMAT(2X,*NO. OF CEILOMETERS GREATER THEN 10*)
   32 FORMAT(2X,*NO. OF LAYERS GREATER THEN 5*)
   33 FORMAT(2X,*RECEIVER OR TRANSMITTER ANGLE GREATER 10 DEG*)
   35 FORMAT(2X,*LAYERS NOT IN ORDER OF INCREASING CLOUD BASE HEIGHT*)
   36 FORMAT(2X,*CLOUD OR HOLE AMOUNT GREATER THEN 0.8*)
   37 FORMAT(2X,*CLOUD SPEED LESS THEN 2.5 MPS OR GREATER THEN 25 MPS*)
   38 FORMAT(2X,*MEAN CLOUD BASE HEIGHT GREATER THEN 1.5 KM*)
   39 FORMAT(2X,*S D OF CLOUD BASE HEIGHT GREATER THEN 0.5 KM*)
   40 FORMAT(2X,*CEILOMETER SAMPLING TIME LESS THEN 6 SEC*)
  701 FORMAT(2I10,4F10.5)
  702 FORMAT(2I10,6F10.5/8F10.5)
  703 FORMAT(2I10,6F10.5/4F10.5)
  704 FORMAT(8F10.5)
      DTA=3.1415927*0.25*0.001*0.001
```

APPENDIX E PROGRAM LISTINGS continued

```
    RM=RN$       IF (RN.LE.0.0)  RM=1
    R0=2**18+3$  R2=2**32
    DO 43 I=1,300$  R1=RM*R0$  RM=AMOD(R1,R2)
    IXN=-ALOG10(RM)$ RM=0.1*RM*(10.0**IXN)
 43 RNB(I)=RM
    DO 45 L=1,NL$ LC=LCOD(L)$  RNS(L)=RNB(LC)
    DO 45 I=1,NI$  IC=ICOD(I)
    ILNA=NL*I+L$  ILCD=15*IC+LC$  RNS(ILNA)=RNB(ILCD)
 45 CONTINUE
    PRINT 1$  PRINT 10$  PRINT 10
    PRINT 15
    PRINT 10$  PRINT 10
    PRINT 4
    PRINT 10$  PRINT 10$  PRINT 9,TT$  PRINT 10$  PRINT 8,TD
    PRINT 10$ PRINT 5,RN,ASC,AAT
    PRINT 1$  PRINT 10$  PRINT 10
    PRINT 2
    PRINT 10$  PRINT 17
    PRINT 10$  PRINT 10
    DO 100 L=1,NL$  L1=(L-1)*40+1$  L2=L1+36$  PRINT 11
    PRINT 12,LCOD(L),LTYP(L),CAM(L),CML(L),CAR(L),CTH(L),CBH(L),
   2  CBSD(L),CBCD(L),       CSP(L),CDR(L),CBT(L),CET(L)
    PRINT 23,CSC(L),CAT(L),CRF(L),(RATBS(LX),LX=L1,L2)
100 PRINT 10
    PRINT 1$  PRINT 10$  PRINT 10
    PRINT 3
    PRINT 10$  PRINT 16
    PRINT 10$  PRINT 10
    DO 200 I=1,NI
    IF (ITYP(I).GT.2) GO TO 195
    PRINT 13
    PRINT 22,ICOD(I),ITYP(I),XIS(I),YIS(I),TIS(I),TFX(I),TRD(I),RAR(I)
   2,TA1(I),TA2(I),RA1(I),RA2(I)
    GO TO 200
195 PRINT 14
    PRINT 22,ICOD(I),ITYP(I),XIS(I),YIS(I),TIS(I),TFX(I),TRD(I),RA1(I)
200 PRINT 10
    IF (NI.LT.11) GO TO 52
    PRINT 31$IRR=IRR+1
 52 IF (NL.LT.6) GO TO 54
    PRINT 32$ IRR=IRR+1
 54 CONTINUE
    DO 70 L=1,NL
    CRF(L)=1.0E-6*CRF(L)
    IF (LCOD(L).LE.15) GO TO 62
    PRINT 30$  IRR=IRR+1
 62 IF (L.EQ.1) GO TO 64$  IF (CBH(L).GT.CBH(L-1)) GO TO 64
    PRINT 35$  IRR=IRR+1
 64 IF (CAM(L).LT.0.8)  GO TO 66
    PRINT 36$ IRR=IRR+1
 66 IF (CSP(L).GE.2.5.AND.CSP(L).LE.25.0)  GO TO 68
    PRINT 37$ IRR=IRR+1
 68 CSP(L)=3.6*CSP(L)
    IF (CBH(L).LE.1.5)      GO TO 69
    PRINT 38$  IRR=IRR+1
 69 IF (CBSD(L).LE.0.5)   GO TO 70
    PRINT 39$  IRR=IRR+1
 70 CONTINUE
    DO 80 I=1,NI
    RAR(I)=DTA*RAR(I)*RAR(I)
    IF (RA1(I).LE.10.0.AND.TA1(I).LE.10.0)  GO TO 76
    PRINT 33$  IRR=IRR+1
```

```
 76 IF (ICOD(I).LE.15) GO TO 78
    PRINT 30$  IRR=IRR+1
 78 IF (TIS(I).GE.0.1)  GO TO 80


    PRINT 40$  IRR=IRR+1
 80 TIS(I)=TIS(I)/60.0
    IF (NTAPE.NE.1)  GO TO 300
    WRITE (41,701) NL,NT,RN,TT,ASC,AAT
    DO 220 L=1,NL$  L1=(L-1)*40+1$  L2=L1+36
    WRITE (41,702)
   2        LCOD(L),LTYP(L),CRT(L),CET(L),CSP(L),CDR(L),CAM(L),CML(L)
   2 ,CAR(L),CTH(L),CBH(L),CBSD(L),CBCD(L),CSC(L),CAT(L),CRF(L)
    WRITE (41,704) (RATRS(LX),LX=L1,L2)
220 CONTINUE
    DO 230 I=1,NI
230 WRITE (41,703)
   2       ICOD(I),ITYP(I),XIS(I),YIS(I),TIS(I),TFX(I),TRD(I),RAR(I),
   2 RA1(I),RA2(I),TA1(I),TA2(I)
300 CONTINUE
    RETURN
    END
```

```
      SUBROUTINE FLUX(NL,NI)
C     THIS SUBROUTINE COMPUTES AND STORES VALUES OF THE MAXIMUN RECEIVED
C        FLUX AS A FUNCTION OF CEILOMETER AND LAYER CHARACTERISTICS
C        AND CLOUD BASE HEIGHT(BASED ON EQ B-24).
      COMMON/CRNG/  RN,ASC,AAT
      COMMON/CFLX/ MM,NN,FON,FXH(1100),RATBS(200)
      COMMON/CTYP/ LTYP(10),ITYP(10)
      COMMON/CLDC/  CTH(10),CBH(10),CHSD(10),CBCD(10),CSP(10),CSC(10)
      COMMON/CCEIL/TIS(10),TFX(10),TRD(10),RAR(10),TA1(10),TA2(10),
     2 RA1(10),RA2(10)
      MM=20$  NN=100$  FON=1.0
      ACR=0.0174533$      RCA=1.0/ACR$  MM1=MM+1
      DO 400 I=1,NI$ IF (ITYP(I).GT.2) GO TO 400$ J=(I-1)*NL*MM1+1
      D=TRD(I)$ DI=1.0/D$ D2=D*D
      IF (ITYP(I).GT.1) GO TO 30
      A1=TA1(I)*ACR$ A2=TA2(I)*ACR$ B1=RA1(I)*ACR$ B2=RA2(I)*ACR
      TTA=A1*A2$  GO TO 35
   30 A1=RA1(I)*ACR$ A2=RA2(I)*ACR$ B1=TA1(I)*ACR$ B2=TA2(I)*ACR
      TTA=B1*B2
   35 BIA=B2/A2$ A12=A1*A2
      FLX=0.25*TFX(I)*RAR(I)*FON/TTA
      DO 300 L=1,NL$  CSCL=CSC(L)$   H6=4.0/CSCL$  CTHL=CTH(L)
      BH0=CBH(L)-2*CHSD(L)
      BH9=CBH(L)+2*CBSD(L)$ BHD=(BH9-BH0)/MM$ Z0=BH0
      DO 200 M=1,MM1$ H0=Z0$ IF (H0.LE.0.0) H0=0.001
                      DIH=D/H0$  ASH0=ASC*H0$ H02=H0*H0
      H1 = 2.0*H02*DI$ H2=(H1+D+D)*B1+H0$ H1=H1*A1$H4=H3=H1+H2$H1=H0+H1
      A0=ATAN(H0*DI)$ SA0I =(H02+D2)/H02$   DXH=DIH-2.0*(A1+B1*SA0I)
      AM=A0+A1/SA0I+B1$ IAM=(AM*RCA+90.0)*0.2+1.49$ SAR=SIN(AM)
      IAM=IAM+(L-1)*40
      CON=RATBS(IAM)*CSCL*FLX
      CWH=A2+A2$ IF (SAR.GT.BIA) CWH=CWH*BIA/SAR
      CXH=A1+A1$ IF (H2.GT.H1) GO TO 40
      HT=H1$ H1=H2$ H2=HT$  CXH=(B1+B1)*SA0I
   40 CONTINUE
      H5=H0+H6$      IF (H5.LT.H4) H4=H5
      H5=CBH(L)+CTHL$ IF (H5.LT.H4)  H4=H5
      IF (H4.LE.H0) GO TO 150
      DH=(H4-H0)/NN
      HT=H0+0.5*DH$  SDF=0.0
      DO 100 N=1,NN$     HT2=HT*HT$ HTD2=HT2+D2
      GH = (ASH0+CSCL*(HT-H0))*(1.0+SQRT(HTD2)/HT)
      IF (HT.GT.H1) GO TO 60$ XH=(HT-H0)*DIH$  GO TO 70
   60 IF (HT.GT.H2) GO TO 65$ XH=CXH*HT$ GO TO 70
   65 XH=D-DXH*HT
   70 SDF=SDF +      EXP(-GH)*XH/(HT*HTD2)
  100 HT=HT+DH
          FXH(J)=CON*SDF*CWH*DH
  150 J=J+1
  200 Z0=Z0+BHD
  300 CONTINUE
  400 CONTINUE
      RETURN
      END
```

APPENDIX E PROGRAM LISTINGS continued

```
      SUBROUTINE ORIENT(WD,NI)
C     THIS SUBROUTINE ROTATES COORDINATE SYSTEM SO THAT THE Y AXIS IS
C        PERPENDICULAR AND THE X AXIS IS PARALLEL TO THE CLOUD-MOTION
C        DIRECTION--THE X AXIS IS CONVERTED TO A TIME AXIS(T=X/V).
      COMMON/CTEX/ XT,T0,T9
      COMMON/CMAX/TMI,TMA,YMI,YMA,TMR,YMR,T5,T10
      COMMON/CXYI/TI(10),YI(10),XIS(10),YIS(10)
      ACR=0.0174533*WR=ACR*(WD-90.0)
      COD=COS(WR)$  SID=SIN(WR)
      DO 100 I=1,NI
      TI(I)=(XIS(I)*COD-YIS(I)*SID)*XT+T5
  100 YI(I)=XIS(I)*SID+YIS(I)*COD
      RETURN
      END
```

```
      SUBROUTINE CLOUDS(CFA,NI,N,L,IRR)
C     THIS SUBROUTINE GENERATES RECTANGULAR CLOUDS (OR HOLES) OVER A
C        15 KM WIDE AND 3 HR (3/V KM) LONG REGION CENTERED ABOUT THE
C        AIRPORT.  BEGINING AND ENDING TMES OF CLOUDS AS VIEWED BY EACH
C        CEILOMETER ARE STORED.  CALCOMP PLOTOUT OF PLAN  VIEW OF CLOUD
C        FIELD IS GENERATED IF REQUESTED(IF NCALC=2)
      DIMENSION LSKY(5,240)
      COMMON/CSKY/ ISKY(240)
      COMMON/KSKY/ JSKY(240)
      COMMON/COUT/ NLINE,NTAPE,NCALC,NOUT
      COMMON/CSAL/XSCALE,YSCALE
      COMMON/CTEX/ XT,T0,T9
      COMMON/CMAX/TMI,TMA,YMI,YMA,TMR,YMR,T5,T10
      COMMON/CXYI/TI(10),YI(10),XIS(10),YIS(10)
      COMMON/CXBE/KN(10),TB(2000),TE(2000),MTB
      COMMON/CCOD/ LCOD(10),ICOD(10)
      COMMON/CTYP/ LTYP(10),ITYP(10)
      COMMON/CASH/ CAM(10),CML(10),CAR(10),CDR(10)
      COMMON/CRNS/ RNS(60)
      ECM=10.0/16.0$  IT0=0.0-T0$  IT9=T9-T10
      CFS=CAM(L)$  SML=CML(L)$  SAR=CAR(L)$ LC=       L$ ICT=LTYP(L)
      CF=0.0$  CFT=2.0$  IFLAG=2$   DO 8 I=1,240
      ISKY(I)=LSKY(L,I)
    8 JSKY(I)=0
      NN=N-2*(N/2)$  RNR=RANF(RNS(LC))
      M=0
   10 T=TMR*RANF(0)+TMI$  Y=YMR*RANF(0)+YMI
      DXR=RANF(0)$    DX= -SML*ALOG(DXR)$  DY=SAR*DX
      DCY=DY*RANF(0)$  DT=DX*XT
      T1=T$     T2=T1+DT$ Y1=Y-DCY$ Y2=Y1+DY
      IF (Y2.GT.YMA) Y2=YMA$  IF (Y1.LT.YMI) Y1=YMI
      Y3=Y1*ECM$  Y4=Y2*ECM
      CALL COVER(T1,T2,Y3,Y4,CFT,CF,IFLAG)
      IF  (CF.GT.CFS.AND.NN.EQ.0)  GO TO 200
      IF (T2.GT.T10)  CALL KOVER(T1-T10,T2-T10,Y3,Y4,CFT,KF,IFLAG)
      IF (T2.LT.T0.OR.T1.GT.T9)  GO TO 198
      IF (T1.LT.T0) T1=T0$  IF (T2.GT.T9) T2=T9
   20 M=M+1$  IF (M.GT.MTB)  GO TO 320
      IF (NCALC.GT.1)  CALL BOX(T1,T2,Y1,Y2)
      DO 100 I=1,NI$  IF (YI(I).LT.Y1) GO TO 100
      IF (YI(I).GT.Y2) GOTTO 100
      K=KN(I)+1$ KN(I)=K$ IK=(I-1)*MTB+K
      TB(IK)=T1-TI(I)+T10$   TE(IK)=T2-TI(I)+T10
  100 CONTINUE
      CFA=CF
  198 IF (CF.LT.CFS)  GO TO 10
  200 CONTINUE
      IF (LTYP(L).GT.0)  GO TO 210
      IF (IT0.GT.0)  GO TO 205
         IT0=1$ T1=0.0$ T2=T0$ Y1=YMI$ Y2=YMA$ GO TO 20
  205 IF (IT9.GT.0)  GO TO 210
         IT9=1$ T1=T9$ T2=T10$ Y1=YMI$ Y2=YMA$ GO TO 20
  210 CONTINUE
      DO 308 I=1,240
  308 LSKY(L,I)=JSKY(I)
      RNS(LC)=RANF(-3.0)
      IF (NCALC.LT.2)  GO TO 330
      CALL BOX(TMI,TMA,YMI,YMA)
```

```
      DO 300 I=1,NI$  Z=ICOD(I)
      T1=0.0$     IF (T1.LT.T0)  T1=T0
      T2=T10$     IF (T2.GT.T9)  T2=T9


      CALL LINE(T1,YI(I),T2,YI(I))
      TII=TI(I)/TSCALE$  YII=YI(I)/YSCALE
      CALL SYMBOL(TII-.06,YII-.105,0.21,1HX,0.,1)
  300 CALL NUMBER(TII,  YII.  0.41,Z,0.,-1)
      TII=(TMI+T5-1.0)/TSCALE$  YII=(YMI-2.5)/YSCALE
      IF (ICT.LT.0) CALL SYMBOL(TII,      YII,    0.41,6H HOLES,0.,6)
      IF (ICT.GT.0) CALL SYMBOL(TII,      YII,    0.41,6HCLOUDS,0.,6)
      TII=(TMI+T5-3.0)/TSCALE$  YII=(YMI-3.5)/YSCALE
      CALL SYMBOL(TII,YII,0.41,5HLAYER,0.,5)
      TIF=TII+3.0/TSCALE
      CALL SYMBOL(TIF,YII,0.41,5H HOUR,0.,5)
      TII=TII+2.0/TSCALE$  TIF=TIF+2.0/TSCALE$  Z=LCOD(L)$  W=(N-1)*3.0
      CALL NUMBER(TII,YII,0.41,Z,0.,-1)
      CALL NUMBER(TIF,YII,0.41,W,0.,-1)
      GO TO 330
  320 IRR=IRR+1
      PRINT 800
  800 FORMAT (51H ERROR. REDUCE NO. OF CEILOMETERS,LAYERS OR CLOUDS )
  330 CONTINUE
      RETURN
      END
```

```
      SUBROUTINE ORDER(L,NI,IRR)
C     THIS SUBROUTINE PLACES THE BEGINNING AND ENDING TIMES OF CLOUD
C        BASES FOR EACH CEILOMETER IN PROPER TIME ORDER.  BEGINNING AND
C        AND ENDING TIMES THAT OVERLAP ARE ELIMINATED.
      COMMON/CMAX/TMI,TMA,YMI,YMA,TMR,YMR,T5,T10
      COMMON/CXRE/KN(10),TB(2000),TE(2000),MTB
      COMMON/CX12/T1( 5000),T2( 5000),KNL(50),MT1
      LIK=(L-1)*NI*MT1$  LI=(L-1)*NI
      DO 200 I=1,NI$  NK=KN(I)
      IKT=(I-1)*MTB$  KTT=(I-1)*MT1+LIK$ KNK=0
      T1T=T2T=0.0$  IF (KNL(LI+I).EQ.0)  GO TO 50
      KNK=KNL(LI+I)$  KTT=KTT+KNK
      T1T=T1(KTT)$  T2T=T2(KTT)
   50 CONTINUE
      IF (NK.LT.1)  GO TO 200
      DO 100 KT=1,NK$  TMIN=1.0E20
      DO 75 K=1,NK$  IF (TB(K+IKT).GT.TMIN)  GO TO 75
      KM=K+IKT$  TMIN=TB(KM)
   75 CONTINUE
      TB(KM)=1.0E25
                     IF (TMIN.GT.T2T) GO TO 80
      IF (T2T.GT.TE(KM))  GO TO 100
      T2(    KTT)=T2T=TE(KM)$  GO TO 100
   80 KTT=KTT+1$ KNK=KNK+1$  IF (KNK.GT.MT1)  GO TO 220
                T1(    KTT)=    TMIN$   T2(    KTT)=T2T=TE(KM)
  100 CONTINUE
      DO 150  K =1,NK
      TB(IKT+K)=TE(IKT+K)=0.0
  150 CONTINUE
      KNL(LI+I)=KNK$  KN(I)=0
  200 CONTINUE
      GO TO 230
  220 IRR=IRR+1
      PRINT 800
  800 FORMAT (51H ERROR. REDUCE NO. OF CEILOMETERS,LAYERS OR CLOUDS )
  230 CONTINUE
      RETURN
      END
```

```
      SUBROUTINE BASE(NL,NI,I)
C     THIS SUBROUTINE GENERATES CLOUD BASE HEIGHT PROFILE FOR A 3 HR
C        TIME SPAN.
      DIMENSION HS(1500),HAS(100),NS(100)
      COMMON/CRNG/  RN,ASC,AAT
      COMMON/CTEX/ XT,T0,T9
      COMMON/CMAX/TMI,TMA,YMI,YMA,TMR,YMR,T5,T10
      COMMON/CELX/ DELX,DDT,BST
      COMMON/CX12/T1( 5000),T2( 5000),KNL(50),MT1
      COMMON/CBSH/ CBESP(4000),LBESP(4000)
      COMMON/CCOD/ LCOD(10),ICOD(10)
      COMMON/CTYP/ LTYP(10),ITYP(10)
      COMMON/CLDC/  CTH(10),CBH(10),CBSD(10),CBCD(10),CSP(10),CSC(10)
      COMMON/CCEIL/TIS(10),TFX(10),TRD(10),BAR(10),TA1(10),TA2(10),
     2 RA1(10),RA2(10)
      COMMON/CRNS/ RNS(60)
      LNM=(I-1)*NL*NMX2
                           LMT=1$ IC=I$      IL=(I-1)*MT1
      ST=TIS(I)*DDT
      A1=RA1(I)$ IF (ITYP(I).EQ.1) A1=TA1(I)$ TWST=SIN(ACR*A1)
      MT=T10/ST$       MTT=2*MT
      DO 25 M=1,MTT
   25 CBESP(M)=99.9999
      BH8=0.0
                        DO 300 L=1,NL$ LI=(L-1)*NI$ LIK=LI*MT1
      IF (T0.GE.T10.OR.T9.LE.0.0)  GO TO 300
      CBSDL=CBSD(L)$ CBHL=CBH(L)$ CSPL=CSP(L)$CBCDL=CBCD(L)$ CTHL=CTH(L)
      BHT=CBHL+CTHL
          BH1=CBHL  -2.0*CBSDL$    IF (BH1.LT.BH8) BH1=BH8
          BH8=CBHL  +2.0*CBSDL$    IF (BH8.GT.BHT) BH8=BHT
      LC=       L$  RNB=RANF(RNS(NL*IC+LC))
      NK=KNL(LI+I)
      INL=(I-1)*NL+L
      KTT=IL+LIK$ LMT=1$      ICL=LTYP(L)
      XT=DDT/CSPL$     DT=DELX*XT$  TWS=TWST*XT
      NM=IFIX((TWS*CBHL  )/DT)$  NMS=2*NM+1$ VNM=1.0/NMS$ TW=NM*DT
      COR=EXP(-DELX/CBCDL)$    COR1=1.0-COR
      COV=  CBSDL*SQRT(1.0-COR*COR)$ CBCR=CBHL*COR1
      HA=HAS(INL)$  N=NS(INL)
      N1=N-1$  IF (N1.EQ.0)  N1=NMS
      H1=HS(LNM+N1)
      T=0.0$  TS=0.5*ST
      K=1$ T1T=T1(KTT+K)$ T2T=T2(KTT+K)
      IF (K.GT.NK)  T1T=T2T=2.0*T10
   50 T=T+DT$ IF (T.GT.T10) GO TO 100$  TMP=T-TW
      RN=RNR*RANF(0)-RNM$ H2=H1*COR+CBCR+COV*RN
      NSS=N$            N=N+1$ IF (N.GT.NMS) N=1
      HA=HA+(H2-HS(LNM+N))*VNM$  HS(LNM+NSS)=H1=H2
      IF (TMP.LT.TS) GO TO 50
      LMX=LMT$      IF (CBESP(LMX).GT.99.)  GO TO 78
      LMX=LMT+MT$  IF (CBESP(LMX).LT.99.)  GO TO 76
   78 IF  (TMP.LT.T2T)  GO TO 80
      K=K+1$ KTK=KTT+K$ T1T=T1(KTK)$ T2T=T2(KTK)
      IF (K.GT.NK)  T1T=T2T=2.0*T10$  GO TO 78
   80 IF (TMP.LT.T1T)   GO TO 72
      IF (ICL.GT.0) 74,76
   72 IF (ICL.GT.0) GO TO 76
   74 HB=HA
```

APPENDIX E PROGRAM LISTINGS continued

```
      IF (HB.LT.BH1) HB=BH1$  IF (HB.GT.BH8) HB=BH8
      CRESP(LMX  )=HB$  LRESP(LMX)=L
   76                   LMT=LMT+1$  TS=TS+ST
      GO TO 50
  100 CONTINUE
      LNM=LNM+NMS$ HAS(INL)=HA$ NS(INL)=N
      RNS(NL*IC+LC)=RANF(-3.0)
      BHB=BHT
  300 CONTINUE
      RETURN
      ENTRY BASFT
      ACR=0.0174533$  RCA=1.0/ACR$  MM1=MM+1
      NMX2=1500/(NL*NI)$  NMX=(NMX2-1)/2
      RNM=SQRT(3.0)$  RNR=2.0*RNM
      DO 540 I=1,NT$  LNM=(I-1)*NL*NMX2
      A1=RA1(I)$ IF (ITYP(I).EQ.1) A1=TA1(I)$ TWST=SIN(ACR*A1)
      DO 530 L=1,NL$ INL=(I-1)*NL+L
      CBHL=CBH(L)$ HAS(INL)=CBHL$ NS(INL)=1
      XT=DDT/CSP(L)$  DT=DELX*XT$  TWS=TWST*XT
      NM=IFIX((TWS*CBHL)/DT)$    NMS=2*NM+1
      DO 520 N=1,NMS
  520 HS(LNM+N)=CBHL
  530 LNM=LNM+NMS
  540 CONTINUE
      RETURN
      END
```

```
      SUBROUTINE OPTIC(NL,NI,N,I)
C     THIS SUBROUTINE COMPUTES THE CEILOMETERS PRIMARY AND SECONDARY
C        RESPONSE CHARACTERISTICS (MAX RECEIVED FLUX, MAX ANGLE, MIN
C        ANGLE AND DECAY ANGLE) BASED ON EQS B-17,B-18,B-19 AND STORED
C        VALUES OF SUBR FLUX.  THE RESULTS ARE PRINTED OUT
C        BY LINE PRINTER(IF NLINE=1) AND MAG TAPE(IF NTAPE=1).
      DIMENSION REDC(50),CMI(50),AMI(50)
      COMMON/COUT/ NLINE,NTAPE,NCALC,NOUT
      COMMON/CRNG/  RN,ASC,AAT
      COMMON/CMAX/TMI,TMA,YMI,YMA,TMR,YMR,T5,T10
      COMMON/CELX/ DELX,DDT,RST
      COMMON/CFLX/ MM,NN,FON,FXH(1100),RATBS(200)
      COMMON/CBSH/ CRESP(4000),LRESP(4000)
      COMMON/CCOD/ LCOD(10),ICOD(10)
      COMMON/CTYP/ LTYP(10),ITYP(10)
      COMMON/CLDC/  CTH(10),CBH(10),CBSO(10),CRCD(10),CSP(10),CSC(10)
      COMMON/CCFIL/TIS(10),TFX(10),TRD(10),RAR(10),TA1(10),TA2(10),
     2 RA1(10),RA2(10)
    1FORMAT(2X,F10.3,2X,F10.3,E11.3,3F10.2,4X,F10.3,E11.3,3F10.2)
    3 FORMAT    (11E12.4)
   20 FORMAT(1H1,45X,*SIMULATED CEILOMETER MEASUREMENTS*/)
   21 FORMAT (32X,*PRIMARY RESPONSE*,38X,*SECONDARY RESPONSE*,//
     2  8X,*TIME       HT MAX     FLX MAX    ANG MAX    ANG MIN    ANG DEC
     3      HT MAX     FLX MAX    ANG MAX    ANG MIN    ANG DEC*,/)
   22 FORMAT(50X,*CEILOMETER NO*,I3,/)
      LIS=NL*(I-1)
      TRDI=TRD(I)$ IF (ITYP(I).GT.1)  GO TO 120
      A1=TA1(I)$ B1=RA1(I)$  GO TO 122
  120 A1=RA1(I)$  B1=TA1(I)
  122 BH=TRDI*B1*ACR$    AH=(A1+B1)*ACR/TRDI
      TRDI2=TRDI*TRDI$ TRCSI=RCA/TRDI
      ST=DDT*TIS(I)$  MT=T10/ST$ RST=TIS(I)$ TIM=0.5*RST+(N-2)*3.0
      DO  75 M=1,MT$ M2=M+MT
      RES0=RES2=RES3=RES4=RES5=RES9=RES7=RES8=99.99$ RES1=RES6=99.999
      IF (CRESP(M).GT.90.0) GO TO 50
      L=LRESP(M)$  LI=LIS+L$  HA=CRESP(M)
      RES1=HA*HA*AH+BH+HA
      MHT=CHT=HA*CMI(LI)+AMI(LI)$  DHT=CHT-MHT
      RES2         =FXH(MHT)+(FXH(MHT+1)-FXH(MHT))*DHT
      SAO2=HA*HA/(HA*HA+TRDI2)$      SAO=SQRT(SAO2)$  AO=ASIN(SAO)*RCA
      AT=  A1*SAO2+B1$              RES3=AO+AT$           RES4=AO-AT
           RES5=SAO*(1.0-SAO)*TRCSI/CSC(L)
      IF (CRESP(M2).GT.90.0)  GO TO 50
      L2=LRESP(M2)$ LI2=LIS+L2$ HB=CRESP(M2)
      RES6=HB*HB*AH+BH+HB
      MHT=CHT=HB*CMI(LI2)+AMI(LI2)$  DHT=CHT-MHT
      RES7   =     (FXH(MHT)+(FXH(MHT+1)-FXH(MHT))*DHT)*REDC(LI)
      SAO2=HB*HB/(HB*HB+TRDI2)$      SAO=SQRT(SAO2)$  AO=ASIN(SAO)*RCA
      AT=  A1*SAO2+B1$              RES8=AO+AT$           RES9=AO-AT
           RES0=SAO*(1.0-SAO)*TRCSI/CSC(L2)
   50 IF (NLINE.NE.1)   GO TO 55
      IF (M.NE.1)  GO TO 53
      PRINT 20$  PRINT 22,ICOD(I)$  PRINT 21
   53 PRINT 1, TIM,RES1,RES2,RES3,RES4,RES5,RES6,RES7,RES8,RES9,RES0
   55 IF (NTAPE.EQ.1)  WRITE (41,3)
     1          TIM,RES1,RES2,RES3,RES4,RES5,RES6,RES7,RES8,RES9,RES0
```

APPENDIX E PROGRAM LISTINGS continued

```
 75 TIM=TIM+BST
    RETURN
    ENTRY OPSFT
    ACR=0.0174533$  RCA=1.0/ACR$  MM1=MM+1
    DO 340 I=1,NI$  IF (ITYP(I).GT.2)  GO TO 340
    LIS=NL*(I-1)$  IHS=LIS*MM1+1
    TRDI=TRD(I)$ IF (ITYP(I).GT.1)  GO TO 320
    A1=TA1(I)$ B1=RA1(I)$  GO TO 322
320 A1=RA1(I)$  B1=TA1(I)
322 TRDI2=TRDI*TRDI
    DO 340 L=1,NL$  LI=LIS+L
                    IHS=(L-1)*MM1+IHS
    CBSDL=CBSD(L)$ CBHL=CBH(L)$ CSCL=CSC(L)$ CTHL=CTH(L)
    HA=CBHL
    SA02=HA*HA/(HA*HA+TRDI2)$      SA0=SQRT(SA02)$  A0=ASIN(SA0)*RCA
    AT= (A1*SA02+B1)$   SAMI=1.0/SIN((A0+AT)*ACR)+1.0
    REDC(LI)=EXP((-CSCL+ASC)*CTHL*SAMI)
        BH0=CBHL  -2.0*CBSDL
        BH9=CBHL  +2.0*CBSDL
    CMI(LI)=MM/(BH9-BH0)$  AMI(LI)=LHS-BH0*CMI(LI)
340 CONTINUE
    RETURN
    END
```

```
      SUBROUTINE RADAR(NL,NI,N,I)
C     THIS SUBROUTINE COMPUTES THE RADAR CEILOMETER RESPONSE
C        CHARACTERISTICS (POWER AND RANGE OF THE PRIMARY AND SECONDARY
C        PEAK RESPONSES).      THE RESULTS ARE PRINTED OUT
C        BY LINE PRINTER(IF NLINE=1) AND MAG TAPE(IF NTAPE=1).
      DIMENSION P1(50),P2(50),PW1(50),PW2(50),PW3(50)
      COMMON/COUT/ NLINE,NTAPE,NCALC,NOUT
      COMMON/CRNG/  RN,ASC,AAT
      COMMON/CMAX/TMI,TMA,YMI,YMA,TMR,YMR,T5,T10
      COMMON/CFLX/ DFLX,ODT,HST
      COMMON/CHSH/ CRESP(4000),LRESP(4000)
      COMMON/CCOD/ LCOD(10),ICOD(10)
      COMMON/CTYP/ LTYP(10),ITYP(10)
      COMMON/CLOC/  CTH(10),CBH(10),CBSD(10),CBCD(10),CSP(10),CSC(10)
      COMMON/CCAT/ CAT(10),CRF(10)
      COMMON/CCEIL/TIS(10),TFX(10),TRD(10),RAR(10),TA1(10),TA2(10),
     2 RA1(10),RA2(10)
    1 FORMAT(2X,F10.3,2X,F11.3,3F10.3,14X,E11.3,3F10.3)
    3 FORMAT     (9E12.4)
   20 FORMAT(1H1,45X,*SIMULATED CEILOMETER MEASUREMENTS*/)
   21 FORMAT (32X,*PRIMARY RESPONSE*,38X,*SECONDARY RESPONSE*,//
     2  8X,*TIME       POWER1     RANGE1     RANGE2     ATT RATE
     3     POWER1     RANGE1     RANGE2     ATT RATE*,/)
   22 FORMAT(50X,*CEILOMETER NO*,I3,/)
      LIS=NL*(I-1)$  TRDI=TRD(I)
      ST=ODT*TIS(I)$  MT=T10/ST$ BST=TIS(I)$ TIM=0.5*HST+(N-2)*3.0
      DO  75 M=1,MT$ M2=M+MT
           RES2=RES3=RES4=RES5=RES6=RES7=99.999$  RES1=RES5=99.99
      IF (CRESP(M).GT.90.0) GO TO 50
      L=LRESP(M)$  LI=LIS+L$  HA=HC=CRESP(M)
      IF (TRDI.LT.HC)  GO TO 40
      IF (TRDI.GT.CBH(L)+CTH(L))  GO TO 42$  HC=TRDI
   40 RES2=HC$ RES1=P1(LI)*(1.0+(HA-CBH(L))*PW1(LI))
      RES3=CBH(L)+CTH(L)$  RES4=CAT(L)
   42 IF (CRESP(M2).GT.90.0)  GO TO 50
      L2=LRESP(M2)$ LI2=LIS+L2$ HB=HC=CRESP(M2)
      IF (TRDI.LT.HC)  GO TO 48
      IF (TRDI.GT.CBH(L2)+CTH(L2))  GO TO 50$  HC=TRDI
   48 RES6=HC$  RES7=CBH(L2)+CTH(L2)$  RES8=CAT(L2)
      RES5=((HB-CBH(L2))*PW2(LI2)+(HA-CBH(L))*PW3(LI)+1)*P2(LI)*P1(LI2)
   50 IF (NLINE.NE.1)   GO TO 55
      IF (M.NE.1)  GO TO 53
      PRINT 20$  PRINT 22,ICOD(I)$  PRINT 21
   53 PRINT 1, TIM,RES1,RES2,RES3,RES4,RES5,RES6,RES7,RES8
   55 IF (NTAPE.EQ.1)
     2 WRITE (41,3)  TIM,RES1,RES2,RES3,RES4,RES5,RES6,RES7,RES8
   75 TIM=TIM+HST
      RETURN
      ENTRY RASET
      DO 500 I=1,NI$  IF (ITYP(I).NE.3)  GO TO 500
      LIS=(I-1)*NL$  TRDI=TRD(I)
      DO 475 L=1,NL$ LI=LIS+L$  CBHL=CBH(L)$  UAT=-1.0/CBHL
      P1(LI)=TFX(I)*CRF(L)*EXP(-2.0*AAT*CBHL)/(CBHL*CBHL)
      IF (TRDI.LE.CBHL)  GO TO 450
      UAT=CAT(L)$ RA=CBHL/TRDI$ CBHT=CBHL+CTH(L)
      P1(LI)=P1(LI)*RA*RA*EXP(-2.0*UAT*(TRDI-CBHL))
      IF (TRDI.GT.CBHT)  P1(LI)=0.0
  450 PW1(LI)=2.0*(UAT-AAT)$ P2(LI)=EXP(-2.0*CTH(L)*(CAT(L)-AAT))
```

```
      PW2(LI)=2.0*(UAT-AAT)$  PW3(LI)=2.0*(CAT(L)-AAT)
475 CONTINUE
500 CONTINUE
      RETURN
      END
```

APPENDIX E PROGRAM LISTINGS continued

```
      SUBROUTINE AOJUS(NL,NI)
C     THIS SUBROUTINE ADJUST THE ARRAYS IN WHICH THE CLOUD BASE BEGINING
C        AND ENDING TIMES ARE STORED FOR THE NEXT 3 HR TIME SPAN.
      COMMON/CMAX/TMI,TMA,YMI,YMA,TMR,YMR,T5,T10
      COMMON/CX12/T1( 5000),T2( 5000),KNL(50),MT1
      DO 400 L=1,NL$  LI=(L-1)*NI$  LIK=LI*MT1
      DO 300 I=1,NI$  KTT=     (I-1)*MT1+LIK$  NK=KNL(LI+I)$ KT=0
      DO 200 K=1,NK$ KTK=KTT+K$ T1T=T1(KTK)-T10$ T2T=T2(KTK)-T10
      T1(KTK)=T2(KTK)=0.0
      IF (T2T.LT.0)   GO TO 200
      KT=KT+1$  KTN=KTT+KT$ IF (T1T.LT.0)   T1T=0.0
      T1(KTN)=T1T$  T2(KTN)=T2T
  200 KNL(LI+I)=KT
  300 CONTINUE
  400 CONTINUE
      RETURN
      END
```

```
      SUBROUTINE PROFIL(NT,I,N,N3)
C     THIS SUBROUTINE  PLOTSOUT CEILOMETER RESPONSE CHARACTERISTICS
C        BY CALCOMP PLOTTER(IF NCALC=1 OR 2).
      COMMON/CMAX/TMI,TMA,YMI,YMA,TMR,YMR,T5,T10
      COMMON/CELX/ DELX,DDT,BST
      COMMON/CBSH/ CRESP(4000),LRESP(4000)
      COMMON/CCEIL/TIS(10),TFX(10),TRD(10),RAR(10),TA1(10),TA2(10),
     2 RA1(10),RA2(10)
      ST=TIS(I)*DDT$  NT=  T10/ST$  NT1=NT-1
      T27=0.5*ST$  X6=6.0
      Y26= (N3-1)*X6*1.5-12.0
      DO 100   JN=1,NT1$    LMT=JN
      IF (CRESP(LMT)+CRESP(LMT+1).GT.99.)  GO TO 100
      Y27=Y26+CRESP(LMT)*X6$  Y28=Y26+CRESP(LMT+1)*X6
      T28=T27+ ST
      CALL LINE(T27,Y27,T28,Y28)
  100 T27=T27+ ST
      CALL LINE(0.0,Y26,T10,Y26)
      Y28=Y26+1.0*X6$  CALL LINE(0.0,Y26,0.0,Y28)
      RETURN
      END
```

APPENDIX E PROGRAM LISTINGS continued

```
      SUBROUTINE COVER(X1,X2,Y1,Y2,CSPEC,CACTUAL,IFLAG)
C     THIS SUBROUTINE TAKES A NEW PLAN-VIEW CLOUD AND UPDATES A
C        120 BY 120 BINARY ARRAY TO COMPUTE THE NEW CLOUD AMOUNT.
C        MXIFT AND ONEBIT ARE ASSEMBLY-LANGUAGE ROUTINES TO SHIFT
C        A WORD AND TO COUNT THE ONE-BITS IN A WORD.
      DIMENSION          MASKS(60)
      COMMON/CSKY/ ISKY(240)
C     QUANTIZE, CHECK AND TRUNCATE COORDINATES
C
C
      SCALE = 60./5.
          NX1 = SCALE*X1
          NX2 = SCALE*X2
          NY1 = SCALE*Y1 + 61.0
          NY2 = SCALE*Y2 + 61.0
      IF (NX1.GT.120) RETURN
      IF (NY1.GT.120) RETURN
      IF (NX2.LT.1) RETURN
      IF (NY2.LT.1) RETURN
      IF (NX1.GT.NX2) RETURN
      IF (NY1.GT.NY2) RETURN
      IF (NX1.LT.1) NX1 = 1
      IF (NY1.LT.1) NY1 = 1
      IF (NX2.GT.120) NX2 = 120
      IF (NY2.GT.120) NY2 = 120
C
C     LOCATE CLOUD IN ARRAY AND SETUP ARGS
C
      CTEMP=CACTUAL
      IF (NX1.GT.60) GO TO 20
      IF (NX2.GT.60) GO TO 30
      ASSIGN 40 TO LABEL
      GO TO 50
   20 NX1 = NX1 - 60
      NX2 = NX2 - 60
      NY1 = NY1 + 120
      NY2 = NY2 + 120
      ASSIGN 40 TO LABEL
      GO TO 50
   30 NTEMP = NX2
      NX2 = 60
      ASSIGN 35 TO LABEL
      GO TO 50
   35 NX1 = 1
      NX2 = NTEMP - 60
      NY1 = NY1 + 120
      NY2 = NY2 + 120
      ASSIGN 40 TO LABEL
      GO TO 50
   40 RETURN
C
C     COMPUTE NEW FRACTIONAL CLOUD COVER
C
   50 LENGTH = NX2 - NX1 + 1
      KAREA = LENGTH*(NY2 - NY1 + 1)
      KOUNT = 0
      IF (LENGTH.LT.60) GO TO 54
      DO 52  I = NY1, NY2
```

```
      IWORD=ISKY(I).AND.(-1)
      IF  (IWORD.LT.0) KOUNT = KOUNT + 1
   52 CONTINUE
      NX1 = NX1 + 1
      LENGTH = LENGTH - 1
   54 MASK = MXIFT (MASKS(LENGTH), 60 - NX2)
      DO 60  I = NY1, NY2
      ICOM = MASK .AND.ISKY (I)
      IF (ICOM.EQ.0) GO TO 60
      CALL ONEBIT(ICOM,KANT)$ KOUNT=KOUNT+KANT
   60 CONTINUE
      CNEW = (KAREA - KOUNT)/14400.
C
C     CHECK TERM CONDS AND UPDATE
C
      IF ((CACTUAL+CNEW).LE.CSPEC) GO TO 70
      IF (IFLAG.GT.0) GO TO 70
      CACTUAL=CTEMP
      IFLAG=-1
      GO TO LABEL, (35,40)
   70 CACTUAL = CACTUAL + CNEW
      DO 75  I = NY1, NY2
   75 ISKY(I)=ISKY(I).OR.MASK
      GO TO LABEL, (35,40)
C
C     MASKS
C
      DATA (MASKS =       1B,                    3B,                   7B,
     1                   17B,                   37B,                  77B,
     1                  177B,                  377B,                 777B,
     1                 1777B,                 3777B,                7777B,
     1                17777B,                37777B,               77777B,
     1               177777B,               377777B,              777777B,
     1              1777777B,              3777777B,             7777777B,
     1             17777777B,             37777777B,            77777777B,
     1            177777777B,            377777777B,           777777777B,
     1           1777777777B,           3777777777B,          7777777777B,
     1          17777777777B,          37777777777B,         77777777777B,
     1         177777777777B,         377777777777B,        777777777777B,
     1        1777777777777B,        3777777777777B,       7777777777777B,
     1       17777777777777B,       37777777777777B,      77777777777777B,
     1      177777777777777B,      377777777777777B,     777777777777777B,
     1     1777777777777777B,     3777777777777777B,    7777777777777777B,
     1    17777777777777777B,    37777777777777777B,   77777777777777777B,
     1   177777777777777777B,   377777777777777777B,  777777777777777777B,
     1  1777777777777777777B,  3777777777777777777B, 7777777777777777777B,
     1 17777777777777777777B, 37777777777777777777B,77777777777777777777B,
     1177777777777777777777B,377777777777777777777B,777777777777777777778)
      END
```

APPENDIX E PROGRAM LISTINGS continued

```
      SUBROUTINE BOX(X1,X2,Y1,Y2)
C     THIS SUBROUTINE DRAWS A RECTANGLE DEFINED BY THE POINTS (X1,Y1),
C          (X1,Y2),(X2,Y1) AND (X2,Y2).
      CALL LINE(X1,Y1,X1,Y2)
      CALL LINE(X1,Y1,X2,Y1)
      CALL LINE(X2,Y2,X2,Y1)
      CALL LINE(X2,Y2,X1,Y2)
      RETURN
      END
```

```
      SUBROUTINE LINE(X1,Y1,X2,Y2)
C     THIS SUBROUTINE DRAWS THE SEGMENT OF THE LINE DEFINED BY THE POINTS
C          (X1,Y1) AND (X2,Y2).
      XS=X1*XGRID$    YS=Y1*YGRID
      XE=X2*XGRID$    YE=Y2*YGRID
      CALL PLOT(XS,YS,3)$  CALL PLOT(XE,YE,2)
      RETURN
      ENTRY LINESET
      XGRID = 1./X1
      YGRID = 1./Y1
      RETURN
      END
```

(V)

```
      SUBROUTINE REEL(X,Y,I)
      CALL PLOT(X,Y,-3)
      RETURN
      END
```

```
          IDENT  ONEBIT
*      THIS ROUTINE RETURNS THE NUMBER OF ONE BITS IN A WORD.
          ENTRY  ONEBIT
+         VFD    42/0HONEBIT,18/2
ONEBIT    BSS    1
          SA1    B1
          SA2    B2
          CX2    X1
          SX6    X2
          SA6    B2
          JP     ONEBIT
          END
```

```
          IDENT  MXIFT                                                    RM     MXIFT
*         ASCENT INTEGER FUNCTION                                          RM     MXIFT
*                                                                          RM     MXIFT
*         K=MXIFT(A,ISH)                                                   RM     MXIFT
*                                                                          RM     MXIFT
*         A-VARIABLE                                                       RM     MXIFT
*         ISH-SHIFT                                                        RM     MXIFT
*                                                                          RM     MXIFT
          ENTRY     MXIFT                                                   RM    MXIFT
          EXT       SYSTEM                                                  RM    MXIFT
 +        VFD       42/0HMXIFT,18/2                                         RM    MXIFT
 MXIFT    DATA      0                                                        RM    MXIFT
          SA1   B1            VARIABLE X1                                  RM    MXIFT
          SA2   B2            SHIFT X2                                     RM    MXIFT
          SB2   X2            SHIFT B2                                     RM    MXIFT
          LX6   B2,X1         SHIFT                                        RM    MXIFT
          JP        MXIFT                                                   RM    MXIFT
          END                                                                     MXIFT
```

```
          IDENT  MXGET                                                    RM     MXGET
          ENTRY  MXGET                                                           MXGET
 +        VFD       42/0HMXGET,18/3                                         RM    MXGET
 MXGET    DATA      0                                                        RM    MXGET
*         FUNCTION   Y=MXGET(X,A,N)                                              MXGET
*                     X=VARIABLE                                                 MXGET
*                     A=FIRST CHARACTER                                          MXGET
*                     N=NUMBER CHARACTERS(TO RIGHT)                              MXGET
*                                                                                MXGET
*-------------------------------------------------------------------------RM    MXGET
          SA1   B2            X1=START CHAR                                      MXGET
          SA2   B3            X2=NCHAR                                           MXGET
          SB3   X2                                                               MXGET
          IX1   X1+X2         X1=NSHIFTS                                         MXGET
          SB4   X1-1          B4=N                                               MXGET
          SB5   B4+B4         B5=2N                                              MXGET
          SB4   B5+B5         B4=4N                                              MXGET
          SB5   B4+B5         B5=6N                                              MXGET
          SA3   B1            X3=ARGUMENT                                        MXGET
          LX6   B5,X3                                                            MXGET
```

```
          SA4   B3+MASK                                          MXGET
          BX6   X6*X4           X6=RESULT                       MXGET
          JP      MXGET                                   RM    MXGET


MASK      DATA  0000000000000000000B       .N=0                  MXGET
          DATA  0000000000000000077B       .N=1                  MXGET
          DATA  0000000000000007777B       .N=2                  MXGET
          DATA  0000000000000777777B       .N=3                  MXGET
          DATA  0000000000077777777B       .N=4                  MXGET
          DATA  0000000007777777777B       .N=5                  MXGET
          DATA  0000000777777777777B       .N=6                  MXGET
          DATA  0000077777777777777B       .N=7                  MXGET
          DATA  0007777777777777777B       .N=8                  MXGET
          DATA  0077777777777777777B       .N=9                  MXGET
          DATA  7777777777777777777B       .N=10                 MXGET
          DATA  0000000000000000000B                             MXGET
A         PS                                                     MXGET
          END                                                    MXGET
```

APPENDIX E PROGRAM LISTINGS concluded

SIMULATED CEILOMETER MEASUREMENTS

UNITS

DISTANCE IN KM
TIME IN HOURS
SPEED IN METERS PER SEC
ANGLE IN DEGREES
CLOUD AMOUNT IN FRACTIONS

TOTAL TIME = 6.00

TIME INTERVAL = 3.00

BASE RANDOM NO	SCAT COEF-AIR	ATTEN RATE-AIR
3.000	.100	.040

APPENDIX F SAMPLE PRINTOUT

CLOUD LAYER CHARATERISTICS

TYPE 1 = CLOUDS
TYPE -1 = HOLES

CODE	TYPE	AMOUNT	LENGTH	ASP RATIO	THICKNESS	BASE HT	BASE SD	COR DIST	SPEED	DIR	T BEG	T END
1	1	.400	1.500	1.500	.030	.100	.015	2.500	3.000	90.000	-3.000	9.000
SCAT C		ATTEN R	REFL(X10+6)	RATIO-BETA/SIGMA								
30.000		.060	1.000	2.00000	1.70000	1.30000	1.00000	.65000	.50000	.35000	.30000	
				.18000	.13000	.08600	.05500	.04000	.03000	.01700	.01100	
				.00800	.00500	.00500	.00400	.00380	.00380	.00420	.00590	
				.00690	.00850	.02000	.03700	.02700	.02300	.01900	.01700	
				.01600	.01500	.01500	.01400	.01300				

CODE	TYPE	AMOUNT	LENGTH	ASP RATIO	THICKNESS	BASE HT	BASE SD	COR DIST	SPEED	DIR	T BEG	T END
2	-1	.200	1.000	1.000	.300	.200	.030	10.000	8.000	180.000	-3.000	9.000
SCAT C		ATTEN R	REFL(X10+6)	RATIO-BETA/SIGMA								
75.000		.100	2.000	2.00000	1.70000	1.30000	1.00000	.65000	.50000	.35000	.30000	
				.18000	.13000	.08600	.05500	.04000	.03000	.01700	.01100	
				.00800	.00500	.00500	.00400	.00380	.00380	.00420	.00590	
				.00690	.00850	.02000	.03700	.02700	.02300	.01900	.01700	
				.01600	.01500	.01500	.01400	.01300				

APPENDIX F SAMPLE PRINTOUT continued

CEILOMETER CHARATERISTICS

TYPE 1 = FIXED BEAM
TYPE 2 = ROTATING BEAM
TYPE 3 = RADAR

CODE	TYPE	X LOC	Y LOC	T INT(MIN)	FLX INT	T-R DIST	REC DIAM(M)	TRANS ANGLES		REC ANGLES	
1	1	-4.500	-4.500	6.000	1.00E+03	.100	.500	.400	.400	4.000	4.000

CODE	TYPE	X LOC	Y LOC	T INT(MIN)	FLX INT	T-R DIST	REC DIAM(M)	TRANS ANGLES		REC ANGLES	
2	2	4.500	4.500	1.000	1.00E+03	.100	.500	.400	.400	4.000	4.000

CODE	TYPE	X LOC	Y LOC	T INT(MIN)	RAD CON	MIN RG	REC ANGLE
3	3	0.000	0.000	1.000	1.00E-03	.050	4.000

APPENDIX F SAMPLE PRINTOUT continued

SIMULATED CEILOMETER MEASUREMENTS

CEILOMETER NO 1

	PRIMARY RESPONSE					SECONDARY RESPONSE				
TIME	HT MAX	FLX MAX	ANG MAX	ANG MIN	ANG DEC	HT MAX	FLX MAX	ANG MAX	ANG MIN	ANG DEC
.050	.236	1.829E-05	67.58	58.94	.73	99.999	9.999E+01	99.99	99.99	99.99
.150	99.999	9.999E+01	99.99	99.99	99.99	99.999	9.999E+01	99.99	99.99	99.99
.250	.215	2.287E-05	65.62	57.01	.82	99.999	9.999E+01	99.99	99.99	99.99
.350	99.999	9.999E+01	99.99	99.99	99.99	99.999	9.999E+01	99.99	99.99	99.99
.450	.249	1.599E-05	68.74	60.09	.68	99.999	9.999E+01	99.99	99.99	99.99
.550	.253	1.548E-05	69.03	60.38	.66	99.999	9.999E+01	99.99	99.99	99.99
.650	.219	2.219E-05	65.97	57.35	.81	99.999	9.999E+01	99.99	99.99	99.99
.750	.081	7.816E-05	39.31	31.04	4.66	.186	4.045E-06	62.23	53.65	.99
.850	.203	2.552E-05	64.31	55.71	.89	99.999	9.999E+01	99.99	99.99	99.99
.950	.093	1.168E-04	43.18	34.86	4.45	99.999	9.999E+01	99.99	99.99	99.99
1.050	.101	1.300E-04	45.64	37.29	4.27	.200	3.283E-06	63.90	55.31	.91
1.150	.110	9.759E-05	48.12	39.74	4.06	.229	2.535E-06	66.93	58.30	.76
1.250	.088	7.649E-05	41.72	33.43	4.54	.219	2.759E-06	66.00	57.38	.80
1.350	.104	1.274E-04	46.49	38.12	4.20	.221	2.725E-06	66.14	57.52	.80
1.450	.092	9.917E-05	42.88	34.56	4.47	.205	3.122E-06	64.54	55.94	.87
1.550	.122	7.172E-05	51.05	42.63	3.77	99.999	9.999E+01	99.99	99.99	99.99
1.650	.118	8.004E-05	49.90	41.49	3.89	.192	3.527E-06	62.96	54.37	.95
1.750	.115	8.711E-05	49.26	40.86	3.95	.257	1.861E-06	69.38	60.72	.65
1.850	.270	1.341E-05	70.31	61.64	.60	99.999	9.999E+01	99.99	99.99	99.99
1.950	.283	1.204E-05	71.20	62.53	.56	99.999	9.999E+01	99.99	99.99	99.99
2.050	.288	1.153E-05	71.55	62.87	.55	99.999	9.999E+01	99.99	99.99	99.99
2.150	.230	2.010E-05	67.04	58.41	.75	99.999	9.999E+01	99.99	99.99	99.99
2.250	.212	2.353E-05	65.29	56.68	.84	99.999	9.999E+01	99.99	99.99	99.99
2.350	.180	3.540E-05	61.37	52.81	1.03	99.999	9.999E+01	99.99	99.99	99.99
2.450	.167	3.999E-05	59.48	50.94	1.12	99.999	9.999E+01	99.99	99.99	99.99
2.550	99.999	9.999E+01	99.99	99.99	99.99	99.999	9.999E+01	99.99	99.99	99.99
2.650	.170	3.868E-05	60.01	51.47	1.10	99.999	9.999E+01	99.99	99.99	99.99
2.750	.192	2.424E-05	62.98	54.40	.95	99.999	9.999E+01	99.99	99.99	99.99
2.850	.227	2.057E-05	66.81	58.18	.77	99.999	9.999E+01	99.99	99.99	99.99
2.950	.227	2.072E-05	66.73	58.10	.77	99.999	9.999E+01	99.99	99.99	99.99

APPENDIX F SAMPLE PRINTOUT continued

SIMULATED CEILOMETER MEASUREMENTS

CEILOMETER NO 2

	PRIMARY RESPONSE					SECONDARY RESPONSE				
TIME	HT MAX	FLX MAX	ANG MAX	ANG MIN	ANG DEC	HT MAX	FLX MAX	ANG MAX	ANG MIN	ANG DEC
.008	.104	2.453E-04	46.34	41.68	4.05	.228	2.900E-06	66.70	59.53	.74
.025	.107	2.370E-04	47.11	42.35	3.98	99.999	9.999E+01	99.99	99.99	99.99
.042	.105	2.438E-04	46.47	41.79	4.04	99.999	9.999E+01	99.99	99.99	99.99
.058	99.999	9.999E+01	99.99	99.99	99.99	99.999	9.999E+01	99.99	99.99	99.99
.075	99.999	9.999E+01	99.99	99.99	99.99	99.999	9.999E+01	99.99	99.99	99.99
.092	99.999	9.999E+01	99.99	99.99	99.99	99.999	9.999E+01	99.99	99.99	99.99
.108	.225	2.482E-05	66.42	59.28	.75	99.999	9.999E+01	99.99	99.99	99.99
.125	.222	2.552E-05	66.17	59.07	.76	99.999	9.999E+01	99.99	99.99	99.99
.142	.199	3.346E-05	63.65	56.82	.88	99.999	9.999E+01	99.99	99.99	99.99
.158	.204	3.152E-05	64.23	57.33	.85	99.999	9.999E+01	99.99	99.99	99.99
.175	.219	2.638E-05	65.88	58.80	.77	99.999	9.999E+01	99.99	99.99	99.99
.192	.217	2.711E-05	65.62	58.57	.78	99.999	9.999E+01	99.99	99.99	99.99
.208	.198	3.387E-05	63.53	56.72	.88	99.999	9.999E+01	99.99	99.99	99.99
.225	.193	3.632E-05	62.87	56.13	.91	99.999	9.999E+01	99.99	99.99	99.99
.242	.193	3.601E-05	62.92	56.17	.91	99.999	9.999E+01	99.99	99.99	99.99
.258	.201	3.252E-05	63.92	57.06	.86	99.999	9.999E+01	99.99	99.99	99.99
.275	.225	2.488E-05	66.40	59.27	.75	99.999	9.999E+01	99.99	99.99	99.99
.292	.228	2.413E-05	66.67	59.51	.74	99.999	9.999E+01	99.99	99.99	99.99
.308	.112	1.627E-04	48.37	43.44	3.87	.206	3.698E-06	64.48	57.56	.84
.325	.109	2.198E-04	47.58	42.76	3.94	.216	3.305E-06	65.51	58.48	.79
.342	.105	2.442E-04	46.43	41.76	4.04	.225	3.004E-06	66.38	59.25	.75
.358	.097	2.687E-04	44.30	39.90	4.22	.237	2.538E-06	67.50	60.25	.70
.375	.092	1.781E-04	42.63	38.45	4.35	.235	2.612E-06	67.36	60.13	.71
.392	.091	1.617E-04	42.48	38.32	4.36	.235	2.634E-06	67.32	60.09	.71
.408	.081	1.798E-04	39.22	35.48	4.56	.242	2.356E-06	67.94	60.64	.68
.425	.091	1.579E-04	42.34	38.20	4.37	.249	2.182E-06	68.57	61.21	.65
.442	.094	2.519E-04	43.26	39.00	4.30	.240	2.397E-06	67.79	60.51	.69
.458	.098	2.663E-04	44.50	40.08	4.20	.249	2.188E-06	68.54	61.19	.65
.475	.106	2.408E-04	46.75	42.04	4.01	.250	2.163E-06	68.64	61.27	.65
.492	.104	2.467E-04	46.23	41.58	4.06	.260	1.954E-06	69.43	61.98	.62
.508	.111	1.882E-04	47.99	43.11	3.90	99.999	9.999E+01	99.99	99.99	99.99
.525	.117	1.529E-04	49.70	44.60	3.74	.266	1.837E-06	69.90	62.41	.60
.542	.257	1.664E-05	69.23	61.80	.63	99.999	9.999E+01	99.99	99.99	99.99
.558	99.999	9.999E+01	99.99	99.99	99.99	99.999	9.999E+01	99.99	99.99	99.99
.575	.240	1.980E-05	67.82	60.54	.69	99.999	9.999E+01	99.99	99.99	99.99
.592	.249	1.813E-05	68.55	61.20	.65	99.999	9.999E+01	99.99	99.99	99.99
.608	.231	2.331E-05	66.96	59.77	.72	99.999	9.999E+01	99.99	99.99	99.99
.625	.241	1.962E-05	67.90	60.61	.68	99.999	9.999E+01	99.99	99.99	99.99
.642	.257	1.675E-05	69.18	61.75	.63	99.999	9.999E+01	99.99	99.99	99.99
.658	.251	1.769E-05	68.75	61.37	.65	99.999	9.999E+01	99.99	99.99	99.99
.675	.263	1.569E-05	69.67	62.20	.61	99.999	9.999E+01	99.99	99.99	99.99
.692	.260	1.623E-05	69.42	61.98	.62	99.999	9.999E+01	99.99	99.99	99.99
.708	.271	1.450E-05	70.28	62.75	.58	99.999	9.999E+01	99.99	99.99	99.99
.725	.295	1.161E-05	71.84	64.16	.52	99.999	9.999E+01	99.99	99.99	99.99
.742	.286	1.261E-05	71.28	63.65	.54	99.999	9.999E+01	99.99	99.99	99.99
.758	.275	1.405E-05	70.51	62.96	.57	99.999	9.999E+01	99.99	99.99	99.99
.775	.287	1.256E-05	71.30	63.67	.54	99.999	9.999E+01	99.99	99.99	99.99
.792	.265	1.536E-05	69.84	62.36	.60	99.999	9.999E+01	99.99	99.99	99.99
.808	.259	1.631E-05	69.39	61.94	.62	99.999	9.999E+01	99.99	99.99	99.99
.825	.256	1.679E-05	69.16	61.74	.63	99.999	9.999E+01	99.99	99.99	99.99
.842	.249	1.806E-05	68.58	61.22	.65	99.999	9.999E+01	99.99	99.99	99.99
.858	.248	1.834E-05	68.46	61.11	.66	99.999	9.999E+01	99.99	99.99	99.99
.875	.260	1.619E-05	69.44	61.99	.62	99.999	9.999E+01	99.99	99.99	99.99
.892	.268	1.500E-05	70.02	62.52	.59	99.999	9.999E+01	99.99	99.99	99.99

APPENDIX F SAMPLE PRINTOUT continued

.908	.282	1.310E-05	71.01	63.41	.55	99.999	9.999E+01	99.99	99.99	99.99
.925	.276	1.391E-05	70.59	63.03	.57	99.999	9.999E+01	99.99	99.99	99.99
.942	.291	1.208E-05	71.57	63.92	.53	99.999	9.999E+01	99.99	99.99	99.99
.958	.279	1.350E-05	70.80	63.22	.56	99.999	9.999E+01	99.99	99.99	99.99
.975	.253	1.736E-05	68.90	61.51	.64	99.999	9.999E+01	99.99	99.99	99.99
.992	.243	1.915E-05	68.11	60.79	.67	99.999	9.999E+01	99.99	99.99	99.99
1.008	.265	1.540E-05	69.82	62.34	.60	99.999	9.999E+01	99.99	99.99	99.99
1.025	.269	1.486E-05	70.10	62.59	.59	99.999	9.999E+01	99.99	99.99	99.99
1.042	.243	1.933E-05	68.03	60.72	.68	99.999	9.999E+01	99.99	99.99	99.99
1.058	.225	2.473E-05	66.45	59.31	.75	99.999	9.999E+01	99.99	99.99	99.99
1.075	.229	2.378E-05	66.79	59.62	.73	99.999	9.999E+01	99.99	99.99	99.99
1.092	.247	1.946E-05	68.40	61.06	.66	99.999	9.999E+01	99.99	99.99	99.99
1.108	.232	2.272E-05	67.12	59.91	.72	99.999	9.999E+01	99.99	99.99	99.99
1.125	.240	1.97ME-05	67.83	60.55	.69	99.999	9.999E+01	99.99	99.99	99.99
1.142	.228	2.397E-05	66.73	59.56	.74	99.999	9.999E+01	99.99	99.99	99.99
1.158	.226	2.451E-05	66.53	59.38	.74	99.999	9.999E+01	99.99	99.99	99.99
1.175	.214	2.811E-05	65.29	58.28	.80	99.999	9.999E+01	99.99	99.99	99.99
1.192	.225	2.472E-05	66.45	59.32	.75	99.999	9.999E+01	99.99	99.99	99.99
1.208	.218	2.685E-05	65.71	58.65	.78	99.999	9.999E+01	99.99	99.99	99.99
1.225	.224	2.394E-05	66.74	59.57	.73	99.999	9.999E+01	99.99	99.99	99.99
1.242	.223	2.541E-05	66.21	59.10	.76	99.999	9.999E+01	99.99	99.99	99.99
1.258	.249	1.804E-05	68.59	61.23	.65	99.999	9.999E+01	99.99	99.99	99.99
1.275	.259	1.636E-05	69.36	61.92	.62	99.999	9.999E+01	99.99	99.99	99.99
1.292	.250	1.792E-05	68.65	61.28	.65	99.999	9.999E+01	99.99	99.99	99.99
1.308	.253	1.729E-05	68.93	61.53	.64	99.999	9.999E+01	99.99	99.99	99.99
1.325	.247	1.847E-05	68.40	61.06	.66	99.999	9.999E+01	99.99	99.99	99.99
1.342	.250	1.786E-05	68.67	61.30	.65	99.999	9.999E+01	99.99	99.99	99.99
1.358	.249	1.803E-05	68.60	61.23	.65	99.999	9.999E+01	99.99	99.99	99.99
1.375	.265	1.547E-05	69.79	62.31	.60	99.999	9.999E+01	99.99	99.99	99.99
1.392	.255	1.71ME-05	69.01	61.61	.63	99.999	9.999E+01	99.99	99.99	99.99
1.408	.241	1.966E-05	67.88	60.59	.68	99.999	9.999E+01	99.99	99.99	99.99
1.425	.222	2.558E-05	66.15	59.05	.76	99.999	9.999E+01	99.99	99.99	99.99
1.442	.253	1.745E-05	68.86	61.47	.64	99.999	9.999E+01	99.99	99.99	99.99
1.458	.244	1.908E-05	68.14	60.82	.67	99.999	9.999E+01	99.99	99.99	99.99
1.475	.229	2.386E-05	66.76	59.59	.73	99.999	9.999E+01	99.99	99.99	99.99
1.492	.256	1.693E-05	69.09	61.68	.63	99.999	9.999E+01	99.99	99.99	99.99
1.508	.253	1.732E-05	68.92	61.52	.64	99.999	9.999E+01	99.99	99.99	99.99
1.525	.241	1.955E-05	67.93	60.64	.68	99.999	9.999E+01	99.99	99.99	99.99
1.542	99.999	9.999E+01	99.99	99.99	99.99	99.999	9.999E+01	99.99	99.99	99.99
1.558	99.999	9.999E+01	99.99	99.99	99.99	99.999	9.999E+01	99.99	99.99	99.99
1.575	99.999	9.999E+01	99.99	99.99	99.99	99.999	9.999E+01	99.99	99.99	99.99
1.592	99.999	9.999E+01	99.99	99.99	99.99	99.999	9.999E+01	99.99	99.99	99.99
1.608	99.999	9.999E+01	99.99	99.99	99.99	99.999	9.999E+01	99.99	99.99	99.99
1.625	99.999	9.999E+01	99.99	99.99	99.99	99.999	9.999E+01	99.99	99.99	99.99
1.642	99.999	9.999E+01	99.99	99.99	99.99	99.999	9.999E+01	99.99	99.99	99.99
1.658	99.999	9.999E+01	99.99	99.99	99.99	99.999	9.999E+01	99.99	99.99	99.99
1.675	99.999	9.999E+01	99.99	99.99	99.99	99.999	9.999E+01	99.99	99.99	99.99
1.692	.218	2.671E-05	65.76	58.70	.78	99.999	9.999E+01	99.99	99.99	99.99
1.708	.236	2.145E-05	67.41	60.17	.70	99.999	9.999E+01	99.99	99.99	99.99
1.725	.252	1.753E-05	68.82	61.44	.64	99.999	9.999E+01	99.99	99.99	99.99
1.742	.280	1.342E-05	70.83	63.25	.56	99.999	9.999E+01	99.99	99.99	99.99
1.758	.284	1.293E-05	71.10	63.50	.55	99.999	9.999E+01	99.99	99.99	99.99
1.775	.266	1.529E-05	69.88	62.39	.60	99.999	9.999E+01	99.99	99.99	99.99
1.792	.277	1.382E-05	70.63	63.07	.57	99.999	9.999E+01	99.99	99.99	99.99
1.808	.254	1.718E-05	68.98	61.58	.64	99.999	9.999E+01	99.99	99.99	99.99
1.825	.267	1.519E-05	69.93	62.43	.60	99.999	9.999E+01	99.99	99.99	99.99
1.842	99.999	9.999E+01	99.99	99.99	99.99	99.999	9.999E+01	99.99	99.99	99.99
1.858	99.999	9.999E+01	99.99	99.99	99.99	99.999	9.999E+01	99.99	99.99	99.99
1.875	.260	1.614E-05	69.46	62.02	.62	99.999	9.999E+01	99.99	99.99	99.99
1.892	.262	1.584E-05	69.60	62.14	.61	99.999	9.999E+01	99.99	99.99	99.99
1.908	.257	1.664E-05	69.23	61.80	.63	99.999	9.999E+01	99.99	99.99	99.99
1.925	.246	1.874E-05	68.28	60.95	.67	99.999	9.999E+01	99.99	99.99	99.99
1.942	.239	2.020E-05	67.69	60.42	.69	99.999	9.999E+01	99.99	99.99	99.99
1.958	.238	2.052E-05	67.62	60.36	.70	99.999	9.999E+01	99.99	99.99	99.99
1.975	.233	2.260E-05	67.15	59.94	.72	99.999	9.999E+01	99.99	99.99	99.99
1.992	.239	1.996E-05	67.75	60.48	.69	99.999	9.999E+01	99.99	99.99	99.99

2.008	.259	1.639E-05	69.35	61.91	.62	99.999	9.999E+01	99.99	99.99	99.99
2.025	.244	1.910E-05	68.13	60.82	.67	99.999	9.999E+01	99.99	99.99	99.99
2.042	.246	1.861E-05	68.34	61.00	.66	99.999	9.999E+01	99.99	99.99	99.99
2.058	.244	1.900E-05	68.17	60.85	.67	99.999	9.999E+01	99.99	99.99	99.99
2.075	.233	2.263E-05	67.14	59.93	.72	99.999	9.999E+01	99.99	99.99	99.99
2.092	.232	2.277E-05	67.11	59.90	.72	99.999	9.999E+01	99.99	99.99	99.99
2.108	.249	1.814E-05	68.55	61.19	.65	99.999	9.999E+01	99.99	99.99	99.99
2.125	.234	2.214E-05	67.26	60.03	.71	99.999	9.999E+01	99.99	99.99	99.99
2.142	.226	2.441E-05	66.57	59.42	.74	99.999	9.999E+01	99.99	99.99	99.99
2.158	.111	1.751E-04	48.15	43.26	3.89	.225	3.003E-06	66.39	59.25	.75
2.175	.104	2.457E-04	46.31	41.65	4.05	.247	2.224E-06	68.41	61.07	.66
2.192	.103	2.517E-04	45.80	41.21	4.10	.220	3.144E-06	65.98	58.89	.77
2.208	.109	2.170E-04	47.62	42.79	3.94	.220	3.162E-06	65.93	58.85	.77
2.225	.110	2.065E-04	47.75	42.91	3.92	.206	3.703E-06	64.47	57.55	.84
2.242	.097	2.690E-04	44.28	39.88	4.22	.192	4.523E-06	62.74	56.01	.92
2.258	.091	1.585E-04	42.26	38.13	4.37	.188	4.954E-06	62.32	55.65	.94
2.275	.099	2.637E-04	44.74	40.28	4.18	.204	3.802E-06	64.22	57.33	.85
2.292	.092	2.019E-04	42.83	38.63	4.33	.210	3.536E-06	64.90	57.93	.82
2.308	.095	2.738E-04	43.45	39.17	4.28	.214	3.362E-06	65.16	58.14	.80
2.325	.090	1.606E-04	41.95	37.86	4.39	.223	3.051E-06	66.24	59.13	.76
2.342	.094	2.693E-04	43.41	39.13	4.29	.205	3.736E-06	64.39	57.47	.84
2.358	.085	1.707E-04	40.52	36.61	4.48	.200	3.979E-06	63.77	56.93	.87
2.375	.091	1.576E-04	42.39	38.24	4.36	.220	3.160E-06	65.93	58.85	.77
2.392	.099	2.646E-04	44.65	40.21	4.19	.219	3.183E-06	65.87	58.80	.77
2.408	.097	2.681E-04	44.35	39.95	4.22	.236	2.565E-06	67.45	60.21	.70
2.425	.103	2.510E-04	45.86	41.26	4.09	.248	2.210E-06	68.46	61.11	.66
2.442	.110	2.102E-04	47.71	42.87	3.93	.246	2.249E-06	68.32	60.99	.66
2.458	.109	2.143E-04	47.65	42.82	3.93	.250	2.169E-06	68.61	61.25	.65
2.475	.100	2.605E-04	45.02	40.53	4.16	.256	2.031E-06	69.13	61.71	.63
2.492	.094	2.438E-04	43.20	38.94	4.30	.234	2.675E-06	67.24	60.02	.71
2.508	.101	2.577E-04	45.28	40.75	4.14	.235	2.590E-06	67.40	60.17	.70
2.525	.112	1.627E-04	48.38	43.45	3.86	.256	2.027E-06	69.15	61.73	.63
2.542	.217	2.712E-05	65.62	58.57	.79	99.999	9.999E+01	99.99	99.99	99.99
2.558	.216	2.741E-05	65.52	58.48	.79	99.999	9.999E+01	99.99	99.99	99.99
2.575	.210	2.937E-05	64.89	57.92	.82	99.999	9.999E+01	99.99	99.99	99.99
2.592	.206	3.064E-05	64.49	57.57	.84	99.999	9.999E+01	99.99	99.99	99.99
2.608	.195	3.514E-05	63.17	56.40	.90	99.999	9.999E+01	99.99	99.99	99.99
2.625	.196	3.466E-05	63.31	56.52	.89	99.999	9.999E+01	99.99	99.99	99.99
2.642	.191	3.793E-05	62.69	55.97	.92	99.999	9.999E+01	99.99	99.99	99.99
2.658	.195	3.529E-05	63.13	56.36	.90	99.999	9.999E+01	99.99	99.99	99.99
2.675	.204	3.145E-05	64.25	57.35	.85	99.999	9.999E+01	99.99	99.99	99.99
2.692	.193	3.584E-05	62.96	56.21	.91	99.999	9.999E+01	99.99	99.99	99.99
2.708	.188	4.125E-05	62.31	55.63	.94	99.999	9.999E+01	99.99	99.99	99.99
2.725	.189	3.979E-05	62.48	55.78	.93	99.999	9.999E+01	99.99	99.99	99.99
2.742	.174	5.189E-05	60.31	53.87	1.03	99.999	9.999E+01	99.99	99.99	99.99
2.758	.191	3.855E-05	62.62	55.91	.92	99.999	9.999E+01	99.99	99.99	99.99
2.775	.187	4.229E-05	62.18	55.52	.94	99.999	9.999E+01	99.99	99.99	99.99
2.792	.192	4.613E-05	61.55	54.96	.97	99.999	9.999E+01	99.99	99.99	99.99
2.808	.114	1.586E-04	48.93	43.93	3.81	.168	6.709E-06	59.55	53.20	1.06
2.825	.112	1.635E-04	48.30	43.38	3.87	.167	6.819E-06	59.38	53.05	1.07
2.842	.111	1.874E-04	48.00	43.12	3.90	.172	6.361E-06	60.13	53.71	1.04
2.858	.107	2.367E-04	47.14	42.38	3.98	.171	6.434E-06	60.00	53.60	1.04
2.875	.104	2.476E-04	46.20	41.56	4.06	.170	6.522E-06	59.84	53.46	1.05
2.892	.105	2.444E-04	46.42	41.75	4.04	.195	4.225E-06	63.20	56.42	.90
2.908	.098	2.650E-04	44.61	40.18	4.19	.205	3.775E-06	64.29	57.39	.85
2.925	.096	2.725E-04	43.99	39.64	4.24	.211	3.491E-06	65.02	58.04	.81
2.942	.102	2.543E-04	45.58	41.02	4.12	.197	4.141E-06	63.39	56.59	.89
2.958	.102	2.527E-04	45.71	41.13	4.10	.185	5.399E-06	61.85	55.22	.96
2.975	.106	2.413E-04	46.71	42.00	4.02	.191	4.659E-06	62.61	55.90	.92
2.992	.108	2.355E-04	47.25	42.47	3.97	.188	4.963E-06	62.32	55.64	.94

APPENDIX F SAMPLE PRINTOUT continued

SIMULATED CEILOMETER MEASUREMENTS

CEILOMETER NO 3

	PRIMARY RESPONSE				SECONDARY RESPONSE			
TIME	POWER1	RANGE1	RANGE2	ATT RATE	POWER1	RANGE1	RANGE2	ATT RATE
.008	5.041E-08	.198	.500	.100	9.999E+01	99.999	99.999	99.999
.025	5.452E-08	.189	.500	.100	9.999E+01	99.999	99.999	99.999
.042	5.278E-08	.193	.500	.100	9.999E+01	99.999	99.999	99.999
.058	5.057E-08	.185	.500	.100	9.999E+01	99.999	99.999	99.999
.075	4.975E-08	.199	.500	.100	9.999E+01	99.999	99.999	99.999
.092	5.159E-08	.195	.500	.100	9.999E+01	99.999	99.999	99.999
.108	5.052E-08	.197	.500	.100	9.999E+01	99.999	99.999	99.999
.125	4.276E-08	.213	.500	.100	9.999E+01	99.999	99.999	99.999
.142	3.719E-08	.224	.500	.100	9.999E+01	99.999	999999	99.999
.158	4.036E-08	.218	.500	.100	9.999E+01	99.999	99.999	99.999
.175	3.999E-08	.219	.500	.100	9.999E+01	99.999	99.999	99.999
.192	3.943E-08	.220	.500	.100	9.999E+01	99.999	99.999	99.999
.208	3.801E-08	.227	.500	.100	9.999E+01	99.999	99.999	99.999
.225	4.033E-08	.218	.500	.100	9.999E+01	99.999	99.999	99.999
.242	4.246E-08	.214	.500	.100	9.999E+01	99.999	99.999	99.999
.258	4.487E-08	.209	.500	.100	9.999E+01	99.999	99.999	99.999
.275	4.075E-08	.217	.500	.100	9.999E+01	99.999	99.999	99.999
.292	4.283E-08	.213	.500	.100	9.999E+01	99.999	99.999	99.999
.308	4.961E-08	.199	.500	.100	9.999E+01	99.999	99.999	99.999
.325	5.853E-08	.181	.500	.100	9.999E+01	99.999	99.999	99.999
.342	6.023E-08	.178	.500	.100	9.999E+01	99.999	99.999	99.999
.358	6.134E-08	.176	.500	.100	9.999E+01	99.999	99.999	99.999
.375	6.550E-08	.167	.500	.100	9.999E+01	99.999	99.999	99.999
.392	6.468E-08	.169	.500	.100	9.999E+01	99.999	99.999	99.999
.408	7.220E-08	.154	.500	.100	9.999E+01	99.999	99.999	99.999
.425	6.812E-08	.172	.500	.100	9.999E+01	99.999	99.999	99.999
.442	6.185E-08	.175	.500	.100	9.999E+01	99.999	99.999	99.999
.458	5.772E-08	.183	.500	.100	9.999E+01	99.999	99.999	99.999
.475	5.334E-08	.191	.500	.100	9.999E+01	99.999	99.999	99.999
.492	4.750E-08	.203	.500	.100	9.999E+01	99.999	99.999	99.999
.508	4.855E-08	.201	.500	.100	9.999E+01	99.999	99.999	99.999
.525	5.459E-08	.189	.500	.100	9.999E+01	99.999	99.999	99.999
.542	9.999E+01	99.999	99.999	99.999	9.999E+01	99.999	99.999	99.999
.558	1.071E-07	.096	.130	.060	6.079E-08	.176	.500	.100
.575	1.134E-07	.093	.130	.060	6.655E-08	.165	.500	.100
.592	1.204E-07	.089	.130	.060	7.209E-08	.154	.500	.100
.608	1.013E-07	.099	.130	.060	7.422E-08	.149	.500	.100
.625	8.599E-08	.107	.130	.060	6.326E-08	.172	.500	.100
.642	7.855E-08	.110	.130	.060	7.232E-08	.153	.500	.100
.658	9.106E-08	.104	.130	.060	6.884E-08	.160	.500	.100
.675	7.407E-08	.113	.130	.060	6.838E-08	.161	.500	.100
.692	7.116E-08	.114	.130	.060	7.225E-08	.153	.500	.100
.708	6.933E-08	.115	.130	.060	7.304E-08	.152	.500	.100
.725	6.934E-08	.115	.130	.060	7.891E-08	.140	.500	.100
.742	5.890E-08	.120	.130	.060	7.823E-08	.141	.500	.100
.758	4.551E-08	.127	.130	.060	9.999E+01	99.999	99.999	99.999
.775	7.897E-08	.140	.500	.100	9.999E+01	99.999	99.999	99.999
.792	7.884E-08	.141	.500	.100	9.999E+01	99.999	99.999	99.999
.808	7.738E-08	.143	.500	.100	9.999E+01	99.999	99.999	99.999
.825	7.897E-08	.140	.500	.100	9.999E+01	99.999	99.999	99.999
.842	7.807E-08	.146	.500	.100	9.999E+01	99.999	99.999	99.999
.858	7.897E-08	.140	.500	.100	9.999E+01	99.999	99.999	99.999
.875	7.897E-08	.140	.500	.100	9.999E+01	99.999	99.999	99.999
.892	7.897E-08	.140	.500	.100	9.999E+01	99.999	99.999	99.999

APPENDIX F SAMPLE PRINTOUT continued

.908	7.897E-08	.140	.500	.100	9.999E+01	99.999	99.999	99.999
.925	7.897E-08	.140	.500	.100	9.999E+01	99.999	99.999	99.999
.942	7.897E-08	.140	.500	.100	9.999E+01	99.999	99.999	99.999
.958	7.897E-08	.140	.500	.100	9.999E+01	99.999	99.999	99.999
.975	7.284E-08	.152	.500	.100	9.999E+01	99.999	99.999	99.999
.992	6.973E-08	.159	.500	.100	9.999E+01	99.999	99.999	99.999
1.008	7.368E-08	.151	.500	.100	9.999E+01	99.999	99.999	99.999
1.025	7.373E-08	.151	.500	.100	9.999E+01	99.999	99.999	99.999
1.042	7.430E-08	.149	.500	.100	9.999E+01	99.999	99.999	99.999
1.058	7.175E-08	.155	.500	.100	9.999E+01	99.999	99.999	99.999
1.075	6.929E-08	.160	.500	.100	9.999E+01	99.999	99.999	99.999
1.092	6.888E-08	.170	.500	.100	9.999E+01	99.999	99.999	99.999
1.108	5.790E-08	.182	.500	.100	9.999E+01	99.999	99.999	99.999
1.125	6.359E-08	.171	.500	.100	9.999E+01	99.999	99.999	99.999
1.142	5.803E-08	.182	.500	.100	9.999E+01	99.999	99.999	99.999
1.158	5.783E-08	.183	.500	.100	9.999E+01	99.999	99.999	99.999
1.175	5.908E-08	.180	.500	.100	9.999E+01	99.999	99.999	99.999
1.192	9.999E+01	99.999	99.999	99.999	9.999E+01	99.999	99.999	99.999
1.208	1.160E-07	.092	.130	.060	9.999E+01	99.999	99.999	99.999
1.225	1.293E-07	.085	.130	.060	9.999E+01	99.999	99.999	99.999
1.242	1.478E-07	.076	.130	.060	9.999E+01	99.999	99.999	99.999
1.258	1.437E-07	.078	.130	.060	4.894E-08	.200	.500	.100
1.275	1.582E-07	.070	.130	.060	3.954E-08	.219	.500	.100
1.292	1.493E-07	.075	.130	.060	3.572E-08	.227	.500	.100
1.308	1.473E-07	.076	.130	.060	2.951E-08	.240	.500	.100
1.325	1.405E-07	.075	.130	.060	3.251E-08	.233	.500	.100
1.342	1.387E-07	.080	.130	.060	2.578E-08	.247	.500	.100
1.358	2.446E-08	.250	.500	.100	9.999E+01	99.999	99.999	99.999
1.375	3.140E-08	.236	.500	.100	9.999E+01	99.999	99.999	99.999
1.392	2.571E-08	.247	.500	.100	9.999E+01	99.999	99.999	99.999
1.408	9.999E+01	99.999	99.999	99.999	9.999E+01	99.999	99.999	99.999
1.425	9.999E+01	99.999	99.999	99.999	9.999E+01	99.999	99.999	99.999
1.442	9.999E+01	99.999	99.999	99.999	9.999E+01	99.999	99.999	99.999
1.458	9.999E+01	99.999	99.999	99.999	9.999E+01	99.999	99.999	99.999
1.475	9.999E+01	99.999	99.999	99.999	9.999E+01	99.999	99.999	99.999
1.492	9.999E+01	99.999	99.999	99.999	9.999E+01	99.999	99.999	99.999
1.508	3.803E-08	.223	.500	.100	9.999E+01	99.999	99.999	99.999
1.525	4.013E-08	.218	.500	.100	9.999E+01	99.999	99.999	99.999
1.542	4.166E-08	.215	.500	.100	9.999E+01	99.999	99.999	99.999
1.558	3.998E-08	.219	.500	.100	9.999E+01	99.999	99.999	99.999
1.575	3.490E-08	.229	.500	.100	9.999E+01	99.999	99.999	99.999
1.592	3.932E-08	.220	.500	.100	9.999E+01	99.999	99.999	99.999
1.608	4.041E-08	.218	.500	.100	9.999E+01	99.999	99.999	99.999
1.625	3.991E-08	.219	.500	.100	9.999E+01	99.999	99.999	99.999
1.642	4.236E-08	.214	.500	.100	9.999E+01	99.999	99.999	99.999
1.658	4.082E-08	.217	.500	.100	9.999E+01	99.999	99.999	99.999
1.675	3.440E-08	.230	.500	.100	9.999E+01	99.999	99.999	99.999
1.692	3.566E-08	.227	.500	.100	9.999E+01	99.999	99.999	99.999
1.708	4.181E-08	.215	.500	.100	9.999E+01	99.999	99.999	99.999
1.725	4.938E-08	.200	.500	.100	9.999E+01	99.999	99.999	99.999
1.742	5.853E-08	.181	.500	.100	9.999E+01	99.999	99.999	99.999
1.758	5.586E-08	.187	.500	.100	9.999E+01	99.999	99.999	99.999
1.775	5.886E-08	.181	.500	.100	9.999E+01	99.999	99.999	99.999
1.792	5.201E-08	.194	.500	.100	9.999E+01	99.999	99.999	99.999
1.808	5.347E-08	.191	.500	.100	9.999E+01	99.999	99.999	99.999
1.825	1.040E-07	.098	.130	.060	9.999E+01	99.999	99.999	99.999
1.842	9.532E-08	.102	.130	.060	9.999E+01	99.999	99.999	99.999
1.858	1.006E-07	.099	.130	.060	9.999E+01	99.999	99.999	99.999
1.875	9.704E-08	.101	.130	.060	9.999E+01	99.999	99.999	99.999
1.892	8.305E-08	.108	.130	.060	9.999E+01	99.999	99.999	99.999
1.908	7.402E-08	.113	.130	.060	6.079E-08	.177	.500	.100
1.925	8.081E-08	.109	.130	.060	6.028E-08	.178	.500	.100
1.942	9.759E-08	.101	.130	.060	6.784E-08	.162	.500	.100
1.958	9.052E-08	.104	.130	.060	6.327E-08	.172	.500	.100
1.975	8.715E-08	.106	.130	.060	5.868E-08	.181	.500	.100
1.992	9.837E-08	.100	.130	.060	6.060E-08	.177	.500	.100

APPENDIX F SAMPLE PRINTOUT continued

2.008	1.072E-07	.096	.130	.060	7.033E-08	.157	.500	.100
2.025	1.064E-07	.095	.130	.060	6.719E-08	.164	.500	.100
2.042	1.139E-07	.093	.130	.060	6.232E-08	.173	.500	.100
2.058	1.060E-07	.097	.130	.060	6.828E-08	.161	.500	.100
2.075	1.166E-07	.091	.130	.060	7.153E-08	.155	.500	.100
2.092	9.664E-08	.101	.130	.060	6.340E-08	.171	.500	.100
2.108	9.227E-08	.103	.130	.060	6.649E-08	.165	.500	.100
2.125	8.134E-08	.109	.130	.060	6.542E-08	.167	.500	.100
2.142	8.552E-08	.107	.130	.060	6.193E-08	.174	.500	.100
2.158	8.69JE-08	.106	.130	.060	6.556E-08	.167	.500	.100
2.175	7.088E-08	.114	.130	.060	5.45UE-08	.149	.500	.100
2.192	7.213E-08	.114	.130	.060	4.995E-08	.198	.500	.100
2.208	8.760E-08	.106	.130	.060	5.271E-08	.193	.500	.100
2.225	7.908E-08	.110	.130	.060	5.996E-08	.178	.500	.100
2.242	7.93ME-08	.110	.130	.060	6.103E-08	.176	.500	.100
2.258	7.728E-08	.111	.130	.060	6.132E-08	.175	.500	.100
2.275	5.933E-08	.120	.130	.060	6.146E-08	.175	.500	.100
2.292	7.11JE-08	.114	.130	.060	6.097E-08	.176	.500	.100
2.308	7.035E-08	.113	.130	.060	5.926E-08	.180	.500	.100
2.325	7.507E-08	.112	.130	.060	6.029E-08	.178	.500	.100
2.342	9.876E-08	.100	.130	.060	5.862E-08	.181	.500	.100
2.358	1.041E-07	.098	.130	.060	5.731E-08	.184	.500	.100
2.375	1.126E-07	.093	.130	.060	6.915E-08	.160	.500	.100
2.392	8.824E-08	.106	.130	.060	6.340E-08	.171	.500	.100
2.408	7.826E-08	.111	.130	.060	6.449E-08	.169	.500	.100
2.425	6.312E-08	.172	.500	.100	9.999E+01	99.999	99.999	99.999
2.442	6.086E-08	.177	.500	.100	9.999E+01	99.999	99.999	99.999
2.458	6.432E-08	.170	.500	.100	9.999E+01	99.999	99.999	99.999
2.475	6.391E-08	.170	.500	.100	9.999E+01	99.999	99.999	99.999
2.492	6.398E-08	.170	.500	.100	9.999E+01	99.999	99.999	99.999
2.508	6.778E-08	.163	.500	.100	9.999E+01	99.999	99.999	99.999
2.525	6.792E-08	.162	.500	.100	9.999E+01	99.999	99.999	99.999
2.542	6.815E-08	.166	.500	.100	9.999E+01	99.999	99.999	99.999
2.558	6.805E-08	.166	.500	.100	9.999E+01	99.999	99.999	99.999
2.575	5.795E-08	.182	.500	.100	9.999E+01	99.999	99.999	99.999
2.592	6.242E-08	.173	.500	.100	9.999E+01	99.999	99.999	99.999
2.608	6.201E-08	.174	.500	.100	9.999E+01	99.999	99.999	99.999
2.625	6.360E-08	.171	.500	.100	9.999E+01	99.999	99.999	99.999
2.642	7.003E-08	.158	.500	.100	9.999E+01	99.999	99.999	99.999
2.658	6.056E-08	.177	.500	.100	9.999E+01	99.999	99.999	99.999
2.675	6.244E-08	.173	.500	.100	9.999E+01	99.999	99.999	99.999
2.692	6.084E-08	.164	.500	.100	9.999E+01	99.999	99.999	99.999
2.708	6.212E-08	.174	.500	.100	9.999E+01	99.999	99.999	99.999
2.725	5.791E-08	.182	.500	.100	9.999E+01	99.999	99.999	99.999
2.742	4.812E-08	.202	.500	.100	9.999E+01	99.999	99.999	99.999
2.758	4.646E-08	.206	.500	.100	9.999E+01	99.999	99.999	99.999
2.775	3.058E-08	.225	.500	.100	9.999E+01	99.999	99.999	99.999
2.792	3.177E-08	.235	.500	.100	9.999E+01	99.999	99.999	99.999
2.808	9.999E+01	99.999	99.999	99.999	9.999E+01	99.999	99.999	99.999
2.825	9.999E+01	99.999	99.999	99.999	9.999E+01	99.999	99.999	99.999
2.842	9.999E+01	99.999	99.999	99.999	9.999E+01	99.999	99.999	99.999
2.858	9.999E+01	99.999	99.999	99.999	9.999E+01	99.999	99.999	99.999
2.875	9.999E+01	99.999	99.999	99.999	9.999E+01	99.999	99.999	99.999
2.892	9.999E+01	99.999	99.999	99.999	9.999E+01	99.999	99.999	99.999
2.908	9.999E+01	99.999	99.999	99.999	9.999E+01	99.999	99.999	99.999
2.925	9.999E+01	99.999	99.999	99.999	9.999E+01	99.999	99.999	99.999
2.942	9.999E+01	99.999	99.999	99.999	9.999E+01	99.999	99.999	99.999
2.958	1.061E-07	.097	.130	.060	9.999E+01	99.999	99.999	99.999
2.975	8.474E-08	.107	.130	.060	4.602E-08	.206	.500	.100
2.992	8.222E-08	.109	.130	.060	4.885E-08	.201	.500	.100

APPENDIX F SAMPLE PRINTOUT concluded

REFERENCES

H. J. aufm Kampe, 1950, "Visibility and Liquid Water Content in Clouds in the Free Atmosphere," J. Appl. Meteor., Vol. 7, No. 1, pp. 54-57.

P. M. Austin, 1947, "Note on Comparison of Ranges of Radio Set SCR-615-B and Radar Set An/TPS-10A for Storm Detection," Technical Report 5, Weather Radar Research, Mass. Inst. Tech., Cambridge, Massachusetts.

O. D. Barteneva and E. A. Polyakova, 1965, "A Study of Attenuation and Scattering of Light in a Natural Fog due to its Microphysical Properties," Izvestiya, Atm. and Oceanic Phys., Vol. 1, No. 2, pp. 193-207.

L. J. Battan, 1959, Radar Meteorology (University of Chicago Press, Chicago).

R. H. Blackmer, Jr., 1962, "Statistical Distribution of Cumulus Clouds from U-2 Photographs," Technical Report 1, Contract A3(653)-3892, Stanford Research Institute, Menlo Park, California.

R. H. Blackmer and S. M. Serebreny, 1962, "Dimensions and Distributions of Cumulus Clouds as Shown by U-2 Photographs," Scientific Report 4, Contract AF 19(604)-7312, Stanford Research Institute, Menlo Park, California.

A. M. Borovikov et al., 1961, Cloud Physics (Leningrad). Translated from Russian Israel Program for Scientific Translations (Jerusalem, 1963), 392 pp.

J. V. Dave, 1968, "Subroutines for Computing the Parameters of the Electro-magnetic Radiation Scattered by a Sphere," IBM Report No. 320-3237, Palo Alto, California.

N. E. Davis, 1969, "The Variation of Very Low Cloud Base with Time and Distance and with Height," Meteorological Magazine, Vol. 98, pp. 351-356.

D. Deirmendjian, 1969, Electromagnetic Scattering on Spherical Polydispersions (American Elsevier, New York).

A. S. Dennis and F. G. Fernald, 1963, "Frequency Distribution of Shower Sizes," J. Appl. Meteor., Vol. 2, No. 6, pp. 767-769.

R. F. Hansford, Ed., 1960, Radio Aids to Civil Aviation (Heywood and Co. Ltd., London).

G. W. Kattawar and G. N. Plass, 1967, "Electromagnetic Scattering from Absorbing Spheres," Applied Optics, Vol. 6, No. 7, pp. 1377-1382.

K. Naito and D. Atlas, 1966, "On Microwave Scatter by Partially Coherent Clouds," Proc. 12th Conf. on Radar Meteorology, pp. 7-12.

W. von Olbers, 1955, "Basic Principles Underlying the Objective Measurement of Cloud Heights," Technische Mitteilungen des Instrumentenvesens des deutschen Wetterdienstes, Neue Folge Nr. 1, pp. 3-18 (Hamburg).

V. G. Plank, 1969, "The Size Distribution of Cumulus Clouds in Representative Florida Populations," J. Appl. Meteor., Vol. 8, No. 1, pp. 46-67.

L. N. Ridenour, 1947, Radar System Engineering (McGraw-Hill, New York).

K. S. Shifrin and E. A. Chayanova, 1967, "Theory of a Nephelometric Method of Measuring the Transparency and Structure of an Atmospheric Aerosol," Izvestiya, Atm. and Oceanic Phys., Vol. 3, No. 3, pp. 274-283.

H. C. van de Hulst, 1957, Light Scattering by Small Particles (Wiley, New York).

K. E. Wilk, 1958, "Evaluation of the AN/APQ-39(XA-3) Cloud Detection Radar," Final Report, Contract No. AF19(604)-1395.